Investigating the feasibility of light (in)dependent continuous cultivation of an Extremophilic Algae, *Galdieria* sp. RTK37.1

A thesis submitted in fulfilment of the requirements for Masters of Engineering in Chemical and Process Engineering at the University of Canterbury

Emma Buckeridge

2022

UNIVERSITY OF CANTERBURY
Te Whare Wānanga o Waitaha
CHRISTCHURCH NEW ZEALAND

Abstract

The extremophilic nature and metabolic flexibility of *Galdieria* spp. have major potential in several biotechnological applications[1]. However, limiting research into successful large scale continuous cultivation of *Galdieria sulphuraria* has restricted industrial application of the species[1]. This research focused on investigating the feasibility of light dependant and independent continuous cultivation of *Galdieria* sp. RTK37.1 in various trophic and light conditions. Stable growth of *Galdieria* sp. RTK37.1 was achieved during photoautotrophic, mixotrophic and heterotrophic conditions, highlighting the ability to achieve submaximal specific growth while continuous collecting biomass for product retrieval. These results have potential industrial ramifications as they demonstrate that the growth of *Galdieria* sp. RTK37.1 can be manipulated to obtain desired biomass and product yields over long cultivation periods.

Continuous cultivation of *Galdieria* sp. RTK37.1 under various light intensities highlighted that operating chemostats under non-optimal light conditions not only affect the growth of *Galdieria* sp. RTK37.1 but also the ability to control and achieve desired stable growth. Light intensities greater than ~ 101 μmol m^{-2} s^{-1} increased wall adhesion and decreased overall photosynthesis rates in photoautotrophically grown *Galdieria* sp. RTK37.1. Although biomass production increased during cultivation under warm white LED lighting at 191.3 μmol m^{-2} s^{-1}, the presence of immobilised cells is not desired during chemostat cultivation as can lead to non-optimal operation and the inability to obtain steady state growth.

Mixotrophic growth is defined as the ability for a cell to combine the mechanisms of photoautotrophic and heterotrophic growth, utilising both inorganic carbons through photosynthesis and organic carbon through respiration simultaneously[6]. Mixotrophic cultivation of *Galdieria* sp. RTK37.1 was shown to be an ideal growth condition for obtaining greater biomass production compared to photoautotrophically and heterotrophically grown *Galdieria* sp. RTK37.1. During steady state mixotrophic growth, *Galdieria* sp. RTK37.1 achieved a biomass concentration of 1.43 (± 0.12) g L^{-1}, significantly greater than biomass concentrations during photoautotrophic and heterotrophic growth, which were only 0.93 (± 0.01) g L^{-1} and 0.63 (± 0.02) g L^{-1} respectively (t-test: p-value < 0.0001). The increased biomass production, along with the decreased net specific oxygen evolution rates and crude protein percentage (which indicated a decrease in photosynthesis compared with photoautotrophy) lead to the conclusion that *Galdieria* sp. RTK37.1 is a true mixotroph. The results demonstrated a synergistic effect between photosynthesis and aerobic respiration during mixotrophy,

indicating both metabolism methods being utilised simultaneously in mixotrophic *Galdieria* sp. RTK37.1.

This research demonstrated that *Galdieria* sp. RTK37.1 is a promising strain for larger scale production, with evidence towards its ability to be used for large scale continuous cultivation in a range of applications such as phycocyanin production. Biomass production and growth of *Galdieria* sp. RTK37.1 can be controlled during continuous cultivation by limiting nutrients such as carbon or ammonia, or through various light intensity and wavelength conditions. Additionally, this research highlighted the ability for *Galdieria* sp. RTK37.1 to adapt to a wide range of conditions, achieving stable growth even under multiply limiting factors.

Acknowledgements

The completion of this research would not have been possible without the help, guidance and support of many people. An enormous thank you to my supervisor Carlo Carere for your encouragement, teaching and support throughout my years at the University of Canterbury. I am truly grateful to have been able to work with such an inspiring dedicated supervisor like yourself. Thank you for sparking my interest in bioprocess research and extremophilic microalgae species. I look forward to working with you in the future.

Thank you to my co-supervisor, Matthew Stott, for providing guidance and support for my biological requirements, and teaching me so much within the microbiological field. Special thanks and gratitude to the other bioprocess students, Harry Grant, Flynn Adcock and Fletcher Gilbertson for all the advice, encouragement and laboratory assistance through the past year. Additionally, I would like to thank all the technical staff within the chemical and process department at the University of Canterbury, particularly Stephen Beuzenberg, Leigh Richardson, and Graham Mitchell. Thank you also Rayleen Fredericks and Michael Sandridge for your endless help in the lab and making sure I was safe throughout my research and, thanks to Glenn Wilson for ordering all my required equipment and chemicals. A special thanks to the financial support from Marsden and CAPE, which without I would not have been able to undertake this research.

And last but not least, a special thanks to all my friends, my partner and of course my family. Thank you for your encouragement, support and for allowing me to endlessly discuss my research with you all. This support encouraged me to pursue this research to the best of my ability.

Thank you, everyone.

Table of Contents

Table of Figures

Table of Tables

1 Chapter 1: Research Introduction

Anthropogenic activity including rice paddles, domesticated animals, landfills, fossil fuel acquisition, and agriculture all account for increasing greenhouse gas emissions[7]. Currently, 50 billion tonnes of greenhouse gases (carbon dioxide equivalents) are being emitted into the atmosphere, concentrations 40% greater than in 1990[8]. Greenhouse gases, including water vapour, carbon dioxide (CO_2), methane (CH_4), nitrous oxide and ozone, trap heat increasing the temperature within the atmosphere[9,10]. This increasing temperature is resulting in unpredictable weather patterns, increased natural disaster occurrence, sea level rising and an increase in droughts and heatwaves[11]. CH_4 and CO_2 are major greenhouse gases produced predominantly as by-products associated with hydrocarbon fuel production and use, geothermal power generation, animal farming and other agriculture[12]. CH_4 is approximately 200 times less concentrated in the atmosphere than CO_2, although CH_4 is 25% more potent in terms of heat holding capacity[7]. Gas streams produced by geothermal power generation, oil and gas production are often too dilute for traditional pollution mitigation devices such as dry scrubbers and electrostatic precipitators, therefore are released into the environment through ventilation systems[7].

The agricultural industry is the greatest contributor to greenhouse gas emissions. This is largely due to methane emissions from livestock, nitrous oxide from fertilisation and limiting CO_2 reduction by photosynthesis due to land clearing for crop and livestock yielding[13]. Agriculture is the third largest user of fresh water, a major polluter, and accelerates the loss of biodiversity driving wildlife extinction[13]. Although the agricultural industry has significant negative effects on the environment there is a major conflict as the industry provides 34% of protein and 16% of the energy required in human diets[14]. With the human population estimated to reach 9 billion people in 2024 the requirement for a wider range of nutritional food across developing countries is increasing. As a result, the requirement for crops and livestock production is estimated to double by 2050[15]. The availability for a regular supply of safe, cost effective animal feed is required in order to meet the demands of this 'livestock revolution' currently occurring[14].

Galdieria spp. is an extremophilic microalgae which due to its growth versatility and ability to adapt to a range of environmental conditions, poses a possible solution for the greenhouse effect and Livestock Revolution. *Galdieria* spp. can metabolise CO_2 and generate high density biomass that has the possibility to be converted into a high protein content

feedstock. *Galdieria* spp. is a thermoacidophilic unicellular microalgae that thrives in acidic conditions, hot temperatures and can survive under pure concentrations of CO_2[16,17]. Studies on the industrial application of *Galdieria* spp. are increasing but lacks research supporting successful large scale continuous cultivation. This research aims to investigate the growth of *Galdieria* sp. RTK37.1 during continuous cultivation in different trophic (photoautotrophy, mixotrophy and heterotrophy) and light conditions. This will provide evidence around the suitability for this strain to be continuously cultivated in larger volumes for commercial biotechnical use of this extremophilic species.

1.1 Statement of Research Aims and Objectives

The overall objective of this research is to investigate the feasibility of light (in)dependent continuous cultivation of an extremophilic algae species, *Galdieria* sp. RTK37.1. This objective will be achieved by investigating the following hypotheses:

1. *Galdieria* sp. RTK37.1 is a true mixotroph.

Galdieria sp. RTK37.1 will be grown mixotrophically, in both batch and continuous cultivation to determine if *Galdieria* sp. RTK37.1 is a true mixotroph. Mixotrophic growth is the ability of a cell to combine the mechanisms of photoautotrophic and heterotrophic growth, utilising both inorganic carbons through photosynthesis and organic carbon through respiration simultaneously[6]. True mixotrophy will be concluded based on steady state biomass production, nutritional compositions and net specific oxygen evolution rates. Although it has been concluded that some strains of *G. sulphuraria* are capable of mixotrophy, it has not been concluded whether *Galdieria* sp. RTK37.1 is a mixotroph.

2. Stable continuous cultivation of *Galdieria* sp. RTK37.1 is achievable during photoautotrophic, mixotrophic and heterotrophic growth conditions.

Galdieria sp. RTK37.1 will be grown in continuous chemostats to achieve steady state growth in different trophic growth conditions including photoautotrophic, mixotrophic and heterotrophic. Biomass will be collected over the duration of steady state growth to investigate growth yields, nutritional composition and phycocyanin production. Providing evidence in the successful stable growth of *Galdieria* sp. RTK37.1 in chemostats shows scale up potentially for numerous biotechnical applications.

3. The growth and pigment production of *Galdieria* sp. RTK37.1 depends on the light intensity and wavelength condition during continuous cultivation

During continuous photoautotrophic cultivation of *Galdieria* sp. RTK37.1, the effect of varying light intensity and wavelength has on the overall growth and pigment production of *Galdieria* sp. RTK37.1 will be investigated. The light dependence of *Galdieria* sp. RTK37.1 photosynthesis rates will also be investigated through oxygen evolution experiments.

2 Chapter 2: Microalgae - Literature Background

2.1 The Ecology and Taxonomic Classification of Algae

Algae are defined as a heterogeneous group of photosynthetic, oxygen-producing eukaryotic organisms present in diverse habitats throughout the world[18]. Algae have been found growing in both aquatic and terrestrial environments, and can also grow as an epiphyte (ability to grow on another plant species), endophyte (ability to grow inside another plant species) and in extreme conditions[19]. Aquatic algae are found in both fresh and saline water, with ranging conditions in pH, temperature, turbidity, O_2 and CO_2 concentrations[18]. Terrestrial algae can survive in habitats such as rocks, soil and other dry environments, forming stable relationships with fungi and other organisms[18]. Algae aid in oxygen and complex nutrient supply to these organisms in return for protection and simple nutrients[18].

Taxonomic classification of algae species is based on a number of factors including morphology, physiology, biochemical factors and more recently molecular characteristics[19]. The hierarchy for the classification of algae follows that of plants, including division, class, order, family, genus, and species. Current algae classification was proposed in 1935 by Fritsch[20], which groups different algae species into 11 classes based on the occurrence of the species in specific environments (e.g. Aquatic, Terrestrial etc.), photosynthetic pigments produced, reserved food material, cell structure, presence of flagella and reproductive method[19,20].

2.1.1 Extremophilic Microalgae

Extremophiles are those organisms that thrive in conditions beyond that considered to be "normal" from an anthropocentric perspective[21,22]. Environmental conditions considered "normal" include temperatures between 4-40 °C, pH conditions between 5-8.5 and saturated salinity concentrations[21,22].

Cyanidiaceae

The Cyanidiaceae (within the order Cyandiales) are a class of thermoacidophilic unicellular algae, which grow in volcanic and thermal environments in acidic pH (0.05 – 5) and hot temperature (35 – 56˚C) conditions[1,16,23]. The first isolation of Cyanidiaceae (1933) led to a large investigation into the taxonomic position to which Cyanidiaceae belong[1,16]. This is due to the simple morphology and pigment colour resulting in the Cyanidiaceae class being

placed in various taxon groups, including cyanobacteria (blue-green algae)[1,16,24], Chlorophyta[1,25], Cryptophyta[1,26] and Glaucophyta[1,278]. The Cyanidiaceae were officially recognised within the phylum Rhodophyta in 1958[1,16,17], due to the presence of several characteristics of Rhodophyceae[28]. These features include lack of flagella, production of phycobiliprotein pigments, unstacked thylakoids and chloroplasts lacking an external endoplasmic reticulum[28,29].

Phylogenetic analysis of Cyanidiaceace (including *Galdieria* spp., *Cyanidium* spp. and *Cyandioschyzon* spp.) supported the division into four distinct lineages, as described in Merola *et al*, 1981[28,30,31]. The first lineage is the *Galdieria* lineage, which is divided into clades A and B[28]. *Galdieria* A clade contains *Galdieria sulphuraria*, while *Galdieria* B clade contains *Galdieria phlegrea*. *G. phlegrea* was described by Pinto *et al.* in 2007 and differs from *G. sulphuraria* due to the relative number of substitutions in the plasmid encoded *rbcL* (subunit of ribulose 1, 5 bisphosphate carboxylase) gene[28 32]. *Galdieria* A clade contains strains that are globally distributed, whereas *Galdieria* B clade has only been isolated from endolithic habitats exclusively in Italy[28]. The *Galdieria* clades do not differ in morphological features but differ in terms of ecophysiology as *Galdieria* clade B has an optimal growth temperature at 25˚C compared with *Galdieria* clade A (Optimal growth temperature at 45˚C)[28,32]. This is likely an adaptation for endolithic environments[28,32]. The second lineage within the class Cyanidiaceae is *Cyanidium caldarium* followed alongside mesophilic *Cyanidium spp.* Mesophilic *Cyanidium spp.* are isolated from nonacidic, nonthermal caves within Italy. The fourth lineage includes *Cyandioschyzon merolae* and *Galdieria maxima. Cyandioschyzon merolae* is physiologically distinct due to the absence of a cell wall, division through binary fission and lack of vacuole.

The phylogenetic relationship between the four lineages was determined through *16s rRNA* and three plasmid genes (*rbcL*, *psaA* and *psbA*)[28], revealing that the *Galdieria* lineage diverged initially followed by mesophilic *Cyanidium spp.*, then *Cyandioschyzon merolae* and *Galdieria maxima* and the finally diverged was the *Cyanidium caldarium* lineage[28,30]. The relationships are outlined in the schematic drawing in Figure 1.

The three genera within the Cyanidiaceae class (*Galdieria, Cyanidium* and *Cyanidioschyzon*) have well defined ecophysiological, morphological and biochemical differences[16,28]. The genus *Cyanidium*, which contains mesophilic *Cyanidium* spp. and *Cyanidium caldarium*, has spherical shaped cells, reproduces through endospores and has an average cell size of 1 µm[16,28]. The genus *Cyanidioschyzon*, which contains the species

Cyandioschyzon merolae and *Galdieria maxima*, has oval club shaped cells, reproduces through binary fission and has an average cell size of 3 µm[16,28]. Both *Cyanidium* spp. and *Cyanidioschyzon* spp. can utilise both nitrate and ammonium as nitrogen sources[28]. *Galdieria* is the largest of the three genera in terms of cell size, with spherical cells averaging around 6 µm[16]. *Galdieria* spp. reproduce through endospores and is only able to grow on ammonium and not nitrate[28]. *Galdieria* spp. possess the greatest metabolic flexibility, with the ability to grow photoautotrophically and heterotrophically, whereas *Cyanidium* spp. and *Cyanidioschyzon* spp. are only reported to grow photoautotrophically[16,33]. The major differences between the three genera are summarised in Table 1.

Table 1: General morphological and physiological characteristics of genera within the class Cyandiales[28].

	***Galdieria* spp.**	***Cyanidium* spp.**	***Cyanidioschyzon* spp.**
Cell Shape	Spherical	Spherical	Oval, club shapes cells
Cell Size	6 µm[16]	1 µm[16]	3 µm[16]
Reproduction Method	Endospores	Endospores	Binary Fission
Vacuole	Yes	No	No
Cell Wall	Yes	Yes	No
Facultative Heterotrophy	Yes	No	No
Nitrogen Source	Ammonia only	Ammonia and Nitrate	Ammonia and Nitrate

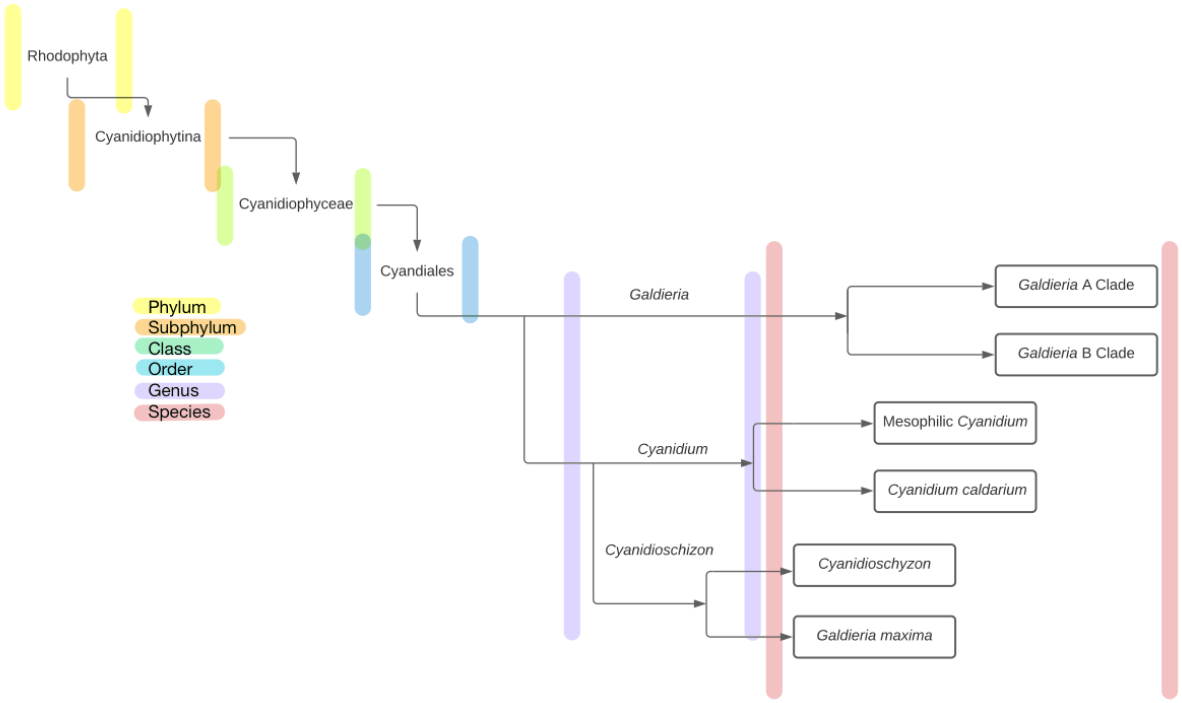

Figure 1: Schematic representation of the Cyanidiophyceae lineage. Based off the schematic representation in Reeb *et al.*[1].

2.2 The genus *Galdieria*

Galdieria spp. possess the greatest metabolic flexibility compared to the other genera of Cyandiales, leading to an increase in biotechnical research surrounding the species. As mentioned previously, the *Galdieria* genus contains two described species, *Galdieria* A clade which has a worldwide distribution, including locations in Italy, the United States, Mexico, Indonesia, Russia and New Zealand, and *Galdieria* B clade which is restricted to Italy[30].

The *Galdieria* A clade was originally defined as containing four species by Sentsova *et al* in 1991 after isolations were obtained from acid-thermal springs in Russia[34-36]. These species included *Galdieria sulphuraria*, *Galdieria maxima*, *Galdieria partitia* and *Galdieria daedala*[34,35]. The four species of *Galdieria* were not easily distinguishable due to very small variations in critical morphological features used for the identification of microalgae[34,35]. Therefore, Sentsova used the form and number of chloroplasts to distinguish between the four species of the *Galdieria* Clade A[34,36]. These results were then contradicted by Cozzolino *et al.* in 2000[36], who assessed the phylogenic relationship for *Galdieria* spp. based on geographical distribution[36]. A selected region of *rbcL* was sequenced from *Galdieria* spp. collected from various locations[36]. This region was chosen as it contained the greatest level of sequence divergence between the four genera after alignment of the *rbcL* units published in the literature.

Cozzolino *et al.* found that the spacers between *Galdieria maxima*, *Galdieria partitia* and *Galdieria daedala* were identical, and shared the same deletion of the 5' 10 bp as other strains of *G. sulphuraria* isolated from California (USA), Yellowstone (USA) and Naples (Italy) [36]. It was concluded that *Galdieria maxima*, *Galdieria partitia* and *Galdieria daedala* were strains of *G. sulphuraria.* This resulted in the genus *Galdieria* being defined as monospecific[36], containing only the species *G. sulphuraria*. The phylogenetic results obtained from Cozzolino *et al.* showed a pattern that aligned with the geographical distribution of *Galdieria* spp. and showed a distinct latitudinal gradient[36].

2.2.1 Introduction to *Galdieria sulphuraria* (*G. sulphuraria*)

G. sulphuraria is a unicellular, spherical species of extremophilic algae within the genus *Galdieria*, Clade A[16]. *G. sulphuraria* lives predominantly in sulphuric acidic hot springs or anthropogenic hostile environments, in temperatures ranging from 35-56°C and pH conditions ranging from 0.05-2[1]. Growth of *G. sulphuraria,* although slow, has been reported at temperatures as cold as 20°C[1]. *G. sulphuraria* displays high salt and metal tolerance, along with extensive metabolic flexibility. Due to the growth versatility of *G. sulphuraria* and the ability to grow and adapt to a range of extreme environmental conditions, the species is becoming more heavily studied[4].

Genomic sequencing of *G. sulphuraria* was first completed in 2013 by Schonknecht *et al*[37]. Originally, the only other member within Cyanidiaceae to be genome sequenced was *Cyanidioschzon merolae*, which is estimated to have diverged from *G. sulphuraria* lineage over a billion years ago[37]. Genome sequencing of *G. sulphuraria* revealed that the metabolic versatility and tolerance to extreme conditions was facilitated by horizontal gene transfer from several critical genes within extremophilic proteobacteria[37,38]. These bacteria are believed to include *Leptospirillm ferriphilum*, *Thiomonas*, and *Acidthiobacillus*, as they live in the same environment as isolated *G. sulphuraria*.

2.3 Metabolic Flexibility of *G. sulphuraria*

G. sulphuraria has been reported to grow photoautotrophically, heterotrophically and mixotrophically[39-42], with each trophic condition affecting the overall growth, biomass yield, and biochemical products[39-43].

2.3.1 Photoautotrophy

Photoautotrophic growth necessitates the use of solar radiation to generate adenosine triphosphate (ATP) and nicotinamide adenine dinucleotide phosphate (NADPH) for the reduction of inorganic carbon (CO_2) into biomass[3]. In Eukaryotes, photosynthesis occurs in the chloroplast. Photosynthesis is operated by a series of light-dependent and light-independent reactions, which can occur simultaneously in the presence of light[3]. The relationship between electron transportation and carbon fixation in the production of energy was first suggested by studies completed by Robert Hill[44,45]. An overview of photosynthesis is shown in Figure 2[3].

In the light-dependent reactions, two membrane protein complexes, known as photosystem I (PSI) and photosystem II (PSII), catalyse the conversion of light energy into chemical energy[46,47]. Initially, photons of light are absorbed by pigments within PSII, which results in the formation of high energy electrons[46]. These energised electrons are transferred by electron carriers in an electron transport chain to PSI[46]. The energised electrons that were transferred are then replaced by oxygen and protons via hydrolysis[46]. The protons are released to the lumen (interior) side within the thylakoid membrane and the oxygen ions combine to form O_2 which gets released into the atmosphere or utilised in respiration[46]. High concentrations of protons inside the lumen causes the flow of protons across the photosynthetic membrane (proton motive force), providing the energy required to drive the synthesis of ATP[3,48]. Within PSI, light energy is used to catalyses the electron transfer from electron carrier complexes on the lumen side of the thylakoid membrane, to ferredoxin complexes at the stromal (exterior) side[47]. The reduced ferredoxin then reduces NADP+ to NADPH. This reducing power and ATP is used by the cell to fuel the light-independent reactions[3,48].

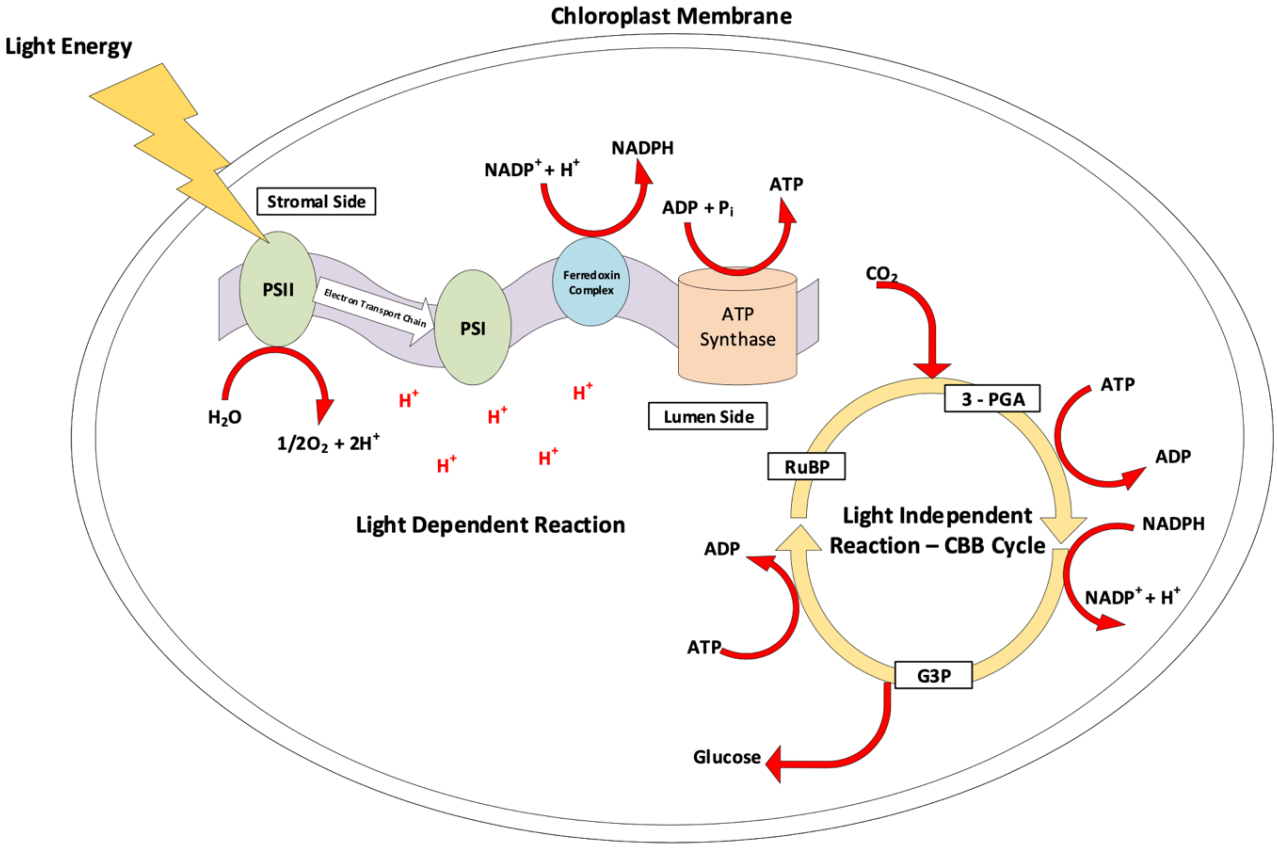

Figure 2: An overview of photosynthesis illustrating the light-dependent and light-independent reactions which occur in the chloroplasts typically found in Cyandiales[3].

The light-independent reactions are described by the Calvin-Bassham-Benson (CBB) cycle[44,49]. The light-independent reaction occurs in the stroma of the chloroplast, where CO_2 fixation occurs producing glucose[3]. The glucose produced in the CBB cycle is then used as the main energy source for growth[50] and in algae, is directly converted to glycogen without conversion to GAP (Glyceraldehyde phosphate)[48].

The basic overall photoautotrophic metabolic reaction is described below[51].

$$6H_2O + 6CO_2 \xrightarrow{h\nu} C_6H_{12}O_6 + 6O_2 \quad (1)$$

Equation 1: Overall photoautotrophic metabolic reaction.

Photoautotrophic growth is limited by the external light supply available[3]. Light cannot be homogeneously distributed through microalgae cultures and therefore the light energy is absorbed within a narrow photic zone[3,52]. The light intensity is the greatest within the photic zone, increasing photosynthesis rates within that region[3,52]. This results in lower photosynthetic efficiencies in the overall culture[52]. Therefore, for photoautotrophic cultures to be successful

the biomass concentration must remain low, which results in lower overall biomass production[52].

There is limited knowledge on the photosystems of *G. sulphuraria* although studies completed by Vanselow *et al.* concluded that the photosystem of *G. sulphuraria* has a common ancestor with cyanobacteria, green algae and plants[47,53]. This is further confirmed by analysis completed on other Cyanidiaceaes, which found that the photosynthesis apparatus appeared as an intermediate between plants and cyanobacteria[47]. Growth rates for photoautotrophic *G. sulphuraria* have been reported to reach 0.16 day^{-1}, achieving biomass dry weights up to 1.1 g L^{-1} (dependant on the illumination intensity provided, further discussed in Section 2.4.4)[54,55].

2.3.2 Heterotrophy

Heterotrophic growth involves harnessing organic carbon dissolved within the external environment in the absence of light[56]. Heterotrophs will derive the energy required for growth and maintenance through the oxidation of organic compounds during respiration, resulting in the formation of CO_2[38,57,59].

For the cell to utilise organic carbon substrates it requires numerous enzymatic systems to aid with transportation, activation through phosphorylation, and the ability to generate energy through respiration[58,59]. To introduce organic carbons into the central respiratory metabolism system, a range of sugar kinases are required within the cell[38,59]. Kinases play a role in sugar sensing and direct phosphorylation of sugars[60]. The organic carbons are then metabolised by glycolysis (also known as the Embden-Meyerhof-Parnas pathway)[59]. The process of glycolysis involves glucose being broken down into pyruvate. The initial stage of glycolysis involves preparatory reactions beginning with the phosphorylation of glucose which requires ATP[59]. The second stage of glycolysis involves the production of NADH, ATP and pyruvate through redox reactions. The energy released from the redox reactions is conserved within the cell as phosphate compounds[59]. Glycolysis requires two ATP molecules but generates four ATP molecules providing an overall yield of 2 ATP molecules. The process of glycolysis is outlined in Figure 3.

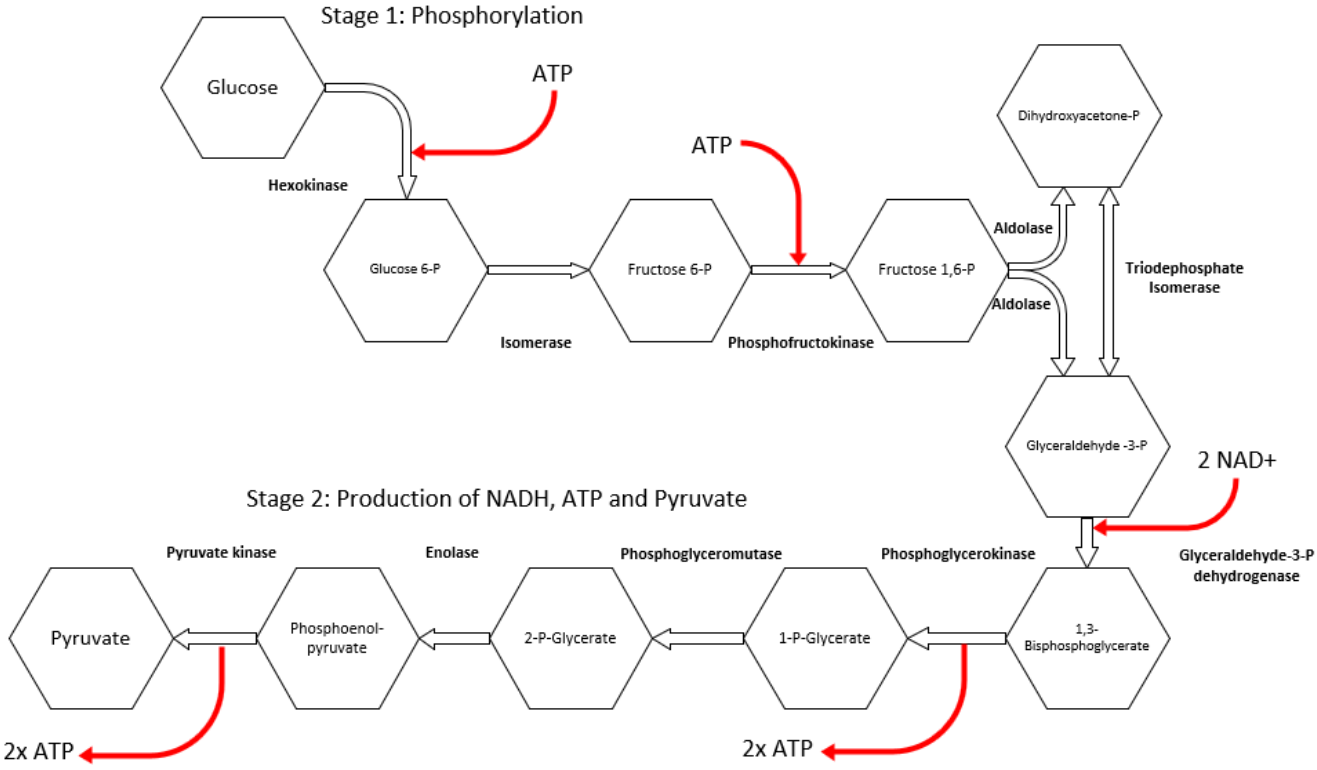

Figure 3: Process outline for glycolysis, the process where glucose is broken down to form Pyruvate. Glycolysis has two main stages, the first stage involves preliminary reactions where glucose is phosphorylated by ATP, producing the molecule glucose 6-phosphate[59]. Glucose 6-phosphate is then isomerized, forming fructose 6-phosphate which is phosphorylated to produce fructose 1,6-bisphosphate[59]. The enzyme aldolase splits fructose 1, 6-bisphosphate into two 3 carbon molecules called glyceraldehyde 3-phosphate and the isomer, dihydroxyacetone phosphate, which is converted to glyceraldehyde 3-phosphate[59]. The second stage of glycolysis includes the production of NADH, ATP and Pyruvate. Glyceraldehyde 3-phosphate is oxidised to 1,3-bishosphglyceric acid, the first redox reaction to occur during Glycolysis. During this reaction, the enzyme glyceraldehyde 3-phosphate dehydrogenase reduces the coenzyme NAD+ to NADH[59]. This occurs twice, generating ATP as 1,3-bishosphglyceric acid is an energy-rich molecule[59]. ATP is synthesised when 1,3-bishosphglyceric acid is converted to 3-phosphoglyceric acid and when phosphoenolpyruvate is converted to pyruvate. Figure based on information sourced from Madigan *et al*.[59].

Aerobic cellular respiration follows glycolysis, producing a high yield of energy through the complete oxidation of glucose to CO_2. Cellular respiration involves the TCA cycle, which is outlined in Figure 4. The electrons released during the oxidation of intermediates within the TCA cycle are used to reduce NAD+ to form NADH or FAD to $FADH_2$[61]. An electrochemical potential is generated across the membrane during electron transfer, as protons are extruded to the outer surface of the membrane. The charge and polarity of the hydroxyl proton limits diffusion through the membrane[61]. This electrochemical potential and difference in pH (called the proton motive force) results in the membrane being energised[61]. The combined reactions of the TCA cycle and the proton motive force allows for the complete

oxidation of glucose. The entire process of aerobic respiration results in a total of 38 ATP being produced by the cell[61].

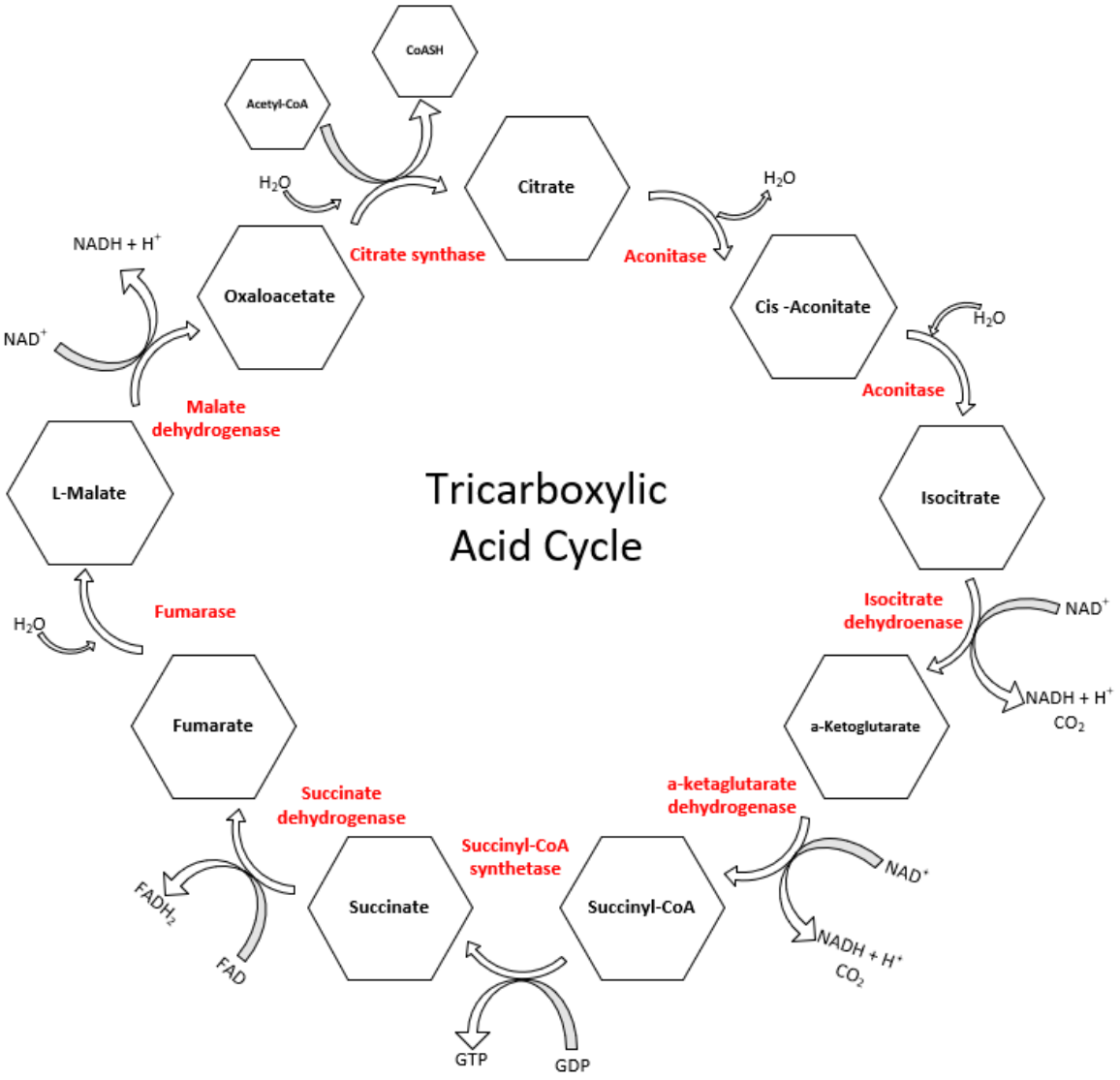

Figure 4: Process outline of the Tricarboxylic Acid Cycle (TCA), also known as the Citric acid cycle. In the TCA cycle, pyruvate is first decarboxylated forming CO_2, NADH and the energy rich substance acetyl-CoA. The acetyl group of acetyl-CoA combines with oxaloacetate forming the citric acid. A series of reactions follow, where two additional CO_2 molecules, three more NADH molecules and one FADH molecule are formed. Oxaloacetate is regenerated as an acetyl acceptor, completing the cycle[61].

Heterotrophic growth does not require light, therefore the growth is not limited by light distribution[56]. Due to the ability to achieve high density cultures, heterotrophic applications are becoming more common commercially for microalgae cultivation[48,62]. Heterotrophic conditions provide a cheaper method for algae cultivation as there is no requirement for artificial or natural lighting[63]. Heterotrophic growth has several advantages including higher ATP production, increased growth rates and overall increased quality of biomass compared to photoautotrophic growth[48,62].

Galdieria is the only genus within the Cyanidiaceae family that is capable of heterotrophic growth[39]. *Galdieria* spp. are often found colonised in endolithic habitats, for example within pumice rock, where light availability is limited[4,40,41,64]. The ability for *Galdieria* spp. to grow heterotrophically is critical for survival within these environments[4,40,41,64]. The *G. sulphuraria* genome encodes for a range of kinases including gluco- , galacto-, fructo- , glycerol- , xylulo- , and ribokinase[39]. *G. sulphuraria* also encodes several polyol dehydrogenases required to introduce sugar alcohols into heterotrophic metabolism[39]. In heterotrophic growth, the sugar and polyols uptake in *G. sulphuraria* is achieved by 14 different transporters, which are induced by only small concentrations of the organic substances[4,65,66]. Heterotrophic growth of *G. sulphuraria* results in growth rates 85% higher than *G. sulphuraria* grown in photoautotrophic conditions[55,67]. Heterotrophic growth of *G. sulphuraria* has been reported on several different carbon substrates as shown in Table 2[39,54].

Table 2: Carbon substrates reported to support heterotrophic growth of *G. sulphuraria*, supplied with 25 mM concentrations of the carbon substrate. *G. sulphuraria* was grown at 45˚C, 100RPM[39,54.]

Chemical Subcategory	Chemical
Hexoses	D-glucose
	D-galactose
	D-fructose
	D-arabinose
	D-mannose
	L-arabinose
	D-fucose
Pentoses	D-ribose
	D-xylose
Disaccharides	Saccharose
	Lactose
	Maltose
Organic Acids	Citrate
	S-malate
	Succinate
Amino acids	L-glutamate
	L-alanine
	L-aspartate
	Glycine
Polyols	D-xylitol
	D-sorbitol
	D-mannitol
	Glycerol
	Ethylene glycol

2.3.3 Mixotrophy

Mixotrophic growth is the ability for a cell to combine the mechanisms of photoautotrophic and heterotrophic growth, utilising both inorganic carbons through photosynthesis and organic carbon through respiration simultaneously[6]. Mixotrophic growth has major advantages including the ability to achieve faster growth rates as it utilises both heterotrophic and phototrophic metabolic pathways[68]. For an organism to be defined as a true mixotroph, it must invest in the growth and maintenance of both the photosynthesis apparatus and uptake machinery of organic carbons simultaneously[4].

Initially mixotrophic was considered a simple combination of photoautotrophic and heterotrophic growth rates. However, in some microalgae species such as *Chlorella sorokiniana*[69], the maximum dry biomass weight in mixotrophic conditions is higher than the sum of photoautotrophic and heterotrophic biomass weights[69,70]. This indicates the synergistic effects of photosynthesis and aerobic respiration within the cell during mixotrophic growth[70,71].

It was previously unclear whether *Galdieria* spp. were true mixotrophs until Curien *et al.* (2021) investigated the mixotrophic growth of *G. sulphuraria* by transferring mixotrophically grown cells into heterotrophic conditions and observing the effect the absence of light had on the growth rate and biomass yield[4,40,54]. It was concluded, based on the observed reduced biomass yield in cells transferred from mixotrophic conditions to heterotrophic conditions, that mixotrophic growth promotes synergistic interactions between light and dark energy metabolites[54]. Greater biomass concentrations after 9 days of batch growth were obtained in mixotrophic conditions (dry weight 2 g L^{-1}) compared to heterotrophic (dry weight 1.4 g L^{-1}) and photoautotrophic (dry weight 0.18 g L^{-1}) conditions[54].

In the natural environment, there is little dissolved inorganic carbon which limits the CBB cycle and production of glucose. The ability for an organism to grow mixotrophically decreases this limitation as it provides supplemented CO_2 via respiration to enhance photosynthesis[54]. The ability for *Galdieria* spp. to grow mixotrophically ensures all energy resources available are exploited for growth[54]. Due to the interaction between the photosynthesis and respiration system, *G. sulphuraria* can overcome the limitation of CO_2 in the natural environment to complete the CBB cycle[54].

2.3.4 Protein Regulation in Different Trophic Conditions

Curien *et al.* (2021) completed a complete survey of the metabolic changes, using proteomic and metabolic profiling, in *G. sulphuraria* grown in different trophic conditions (mixotrophic, photoautotrophic and heterotrophic)[54]. It was observed that during mixotrophic growth, the photosynthetic proteins, which are complexes of the electron transport chain and enzymes of the CBB cycle, were downregulated compared to photoautotrophic conditions[54]. This downregulation of the photosynthetic proteins during mixotrophic growth further concluded that respiration provides the CO_2 to help supplement the CBB cycle during photosynthesis. The respiratory proteins of *G. sulphuraria* remained constant throughout photoautotrophic, mixotrophic and heterotrophic conditions[54].

There has been no known reported transcriptome analysis for *Galdieria* spp. grown in different trophic conditions, mixotrophic, photoautotrophic and heterotrophic.

2.4 *G. sulphuraria* Growth Factors

Many factors contribute to microalgae growth and biomass production, including nutrients, pH, temperature and light energy[68].

2.4.1 General Organic Nutrient Requirements in Algae

Nitrogen, phosphorous and carbon are the major macronutrients required for microalgae growth[68], where cultures often require a minimum 10^{-4} molarity concentration[72]. Nitrogen and phosphorus account for 10-20% of the total algae biomass[68,73] and consumption is directly proportional to cell growth[68]. Carbon is added to microalgae cultures in either organic or inorganic forms depending on the metabolic condition[68]. Nitrogen, phosphorous and carbon are building materials for the cell[72] and therefore low concentrations of these major macronutrients can lead to decreased growth rates and biomass productivity[68,74]. Other growth nutrients are only required in trace amounts (required concentrations $10^{—5}$ M or less[72]) including macronutrients; sodium, magnesium, calcium and potassium and micronutrients; molybdenum, manganese, boron, cobalt, iron and zinc[68]. The requirements for particular nutrients are species-specific, other than the major macronutrients like nitrogen, phosphorous and carbon, which are required for all microalgae species[68].

Cyanidium caldarium has been reported to accumulate glycogen under conditions that are growth-limiting, such as macronutrient limitation[75,76]. Glycogen is a glucose polysaccharide that serves as an energy source of which the cell can break down to gain glucose when required[77]. *Galdieria* spp. have been reported to accumulate glycogen at early stages of growth, accumulating the polymer up to 50% of dry cell weight[75,76]. A study completed by Sakurai *et al.* investigated the lipid and glycogen accumulation of *G. sulphuraria* cells grown under different growth conditions[76,78]. It was observed that during exponential growth of *G. sulphuraria* during mixotrophic, heterotrophic (cells were provided with 25 mM Glucose) and photoautotrophic growth, glycogen and lipid content of the cell was similar[78]. During stationary growth, the maximum glycogen content per volume measured during mixotrophic growth was reported to be 10- and 2- folds greater than photoautotrophically and heterotrophically grown *G. sulphuraria* cells respectively[78]. The highest amount of lipid per volume was observed in the heterotrophic cultures, where the lipid content was 3- and 2- folds greater than photoautotrophic and mixotrophic cultures of *G. sulphuraria*[78]. The study concluded that the regulation of metabolic carbon flow into glycogen and other fatty acid synthesis was largely dependent on the growth conditions of *G. sulphuraria*[78].

2.4.2 Acidophily in Algae

pH is a critical growth condition of microalgae as it impacts the solubility, CO_2 availability and metabolism rate[79]. Each microalgae species has an optimal pH, and when the pH is at an extreme, the growth rate rapidly decreases and ultimately leads to cell death[79]. Optimal pH is strain specific and can be a relatively narrow spectrum compared to the temperature range algae can be successfully cultivated in[79]. The optimal pH for *Galdieria* spp. is reported to be between pH 0.5-2.5[1].

During photoautotrophic cultivation, pH is a particularly important factor as it is a determinant of the relative concentration of CO_2 in solution, impacting the carbon fixation rate during photosynthesis[79,80]. The concentration of dissolved CO_2 is inversely proportional to the pH[79], therefore as pH increases the concentration of carbonate increases while the concentration of CO_2 decreases[80]. Extracellular pH also affects the electrochemical potential in the proton motive force, impacting the generation of ATP in photosynthesis[81]. Depending on the optimal pH of the microorganisms, any major shift from the reported optimal can result in a decrease of the electrochemical potential reducing the drive for protons to transport across the photosynthetic membrane[81].

Oesterhelt *et al.* (2007) investigated the effect the media pH had on the doubling rate of *G. sulphuraria* in photoautotrophic and heterotrophic conditions, as shown in Figure 5[4]. Cells grown in heterotrophic conditions exhibited growth until a pH 8, with a minimum doubling time measured a pH 2, while photoautotrophic cells exhibited no growth above a pH 7 with a minimum doubling rate within the pH range of 1 – 5[4]. Heterotrophic cells also had a higher acidification capacity, reducing the media pH from 8 to 3, whereas photoautotrophic cells were only capable of reducing the media pH from 6 to 3[4].

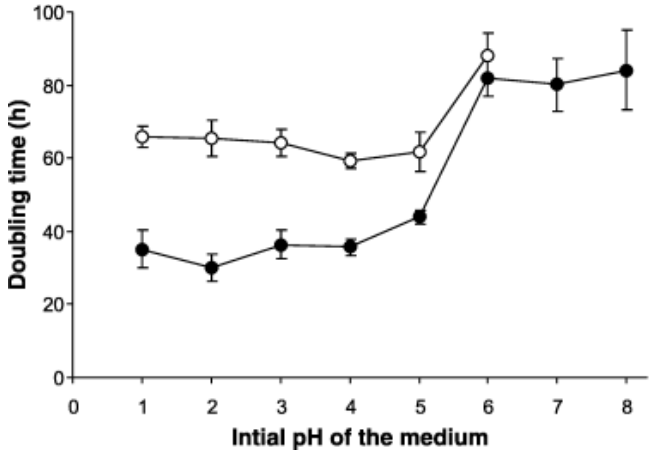

Figure 5: Doubling rate of exponentially grown *G. sulphuraria* at different initial media pH levels. Photoautotrophic cells (o) were illuminated with white incandescent light (120 µmol m^{-2} s^{-1}) and supplied with 2% (v/v) CO_2. Heterotrophic cultures (•) were supplied with 25 mM of glucose. Experiment was operated at ambient temperature, in a shaking incubator set at 120 RPM. Figure sourced from Oesterhelt *et al.*[4].

2.4.3 Thermophily in Algae

Temperature is an important growth parameter to consider when cultivating microalgae, as although many algae species can grow under a wide range of temperatures each species has an optimal temperature for growth[84]. The optimal temperature of *Galdieria* spp. is between a 45-50°C[1], with growth observed at temperatures as high as 55˚C[85].

The growth rate of microalgae as a function of the temperature is expressed as a bell curve[86]. When the temperature is significantly less than the optimal temperature, the growth rate of the microalgae declines until they reach an inactivated state[86]. When below the optimal conditions, the temperature is proportional to cell division and the photosynthesis rate due to increasing enzymatic activity[28,29]. This relationship is described by the Arrhenius function, where for every 10°C increase in temperature the rate of photosynthesis, cell division and growth are estimated to double up until the optimal temperature is reached[86,87].

When the temperature is significantly hotter than the optimal temperature of the cell, it has a more detrimental effect on the microalgae[86]. Cell growth declines rapidly due to enzyme denaturation and protein modification inhibiting photosynthesis, ultimately leading to the death of the microalgae species[86].

Rossoni *et al.* looked at changes in *G. sulphuraria* gene expression through RNA sequencing during a temperature shift, with temperatures ranging from 42°C to 28°C in 3 day time periods[85]. The experiment was conducted by following the expression of 21 highly

expressed *G. sulphuraria* genes[85]. The growth rate remained constant throughout the temperature shifts[85]. It was observed that only one gene exhibited a rapid 4.5-fold upregulation in response to the reduction in temperature, while most other transcriptome factor genes had decreased expression[85]. These results showed that in lower temperatures there was a decrease in protein biosynthesis rates and an increase in expression of ribosomal protein[85]. This showed that *G. sulphuraria* is thermophilic and not a thermotolerant organism, as the cells reacted to the reduction in temperature and reduced the protein biosynthesis rates as a stress response[85].

2.4.4 Light Requirements in Algae

Light intensity is of primary importance during photoautotrophic microalgae cultivation, as it is directly proportional to the maximum possible rate of photosynthesis and biomass production[68]. In natural habitats, light conditions are dependent on geographical location, seasonal changes and the effect of light scattering by the atmosphere[82]. Microalgae species must dynamically adapt to their environment depending on variable light conditions. In contrast, during cultivation, artificial lighting sources is often used allowing control over the productivity of biomass and pigments[82]. Light requirements vary for microalgae species, therefore the optimal light intensity and wavelength should be identified to maximise photosynthesis and biomass accumulation during cultivation[68]. At lower light intensities, there is a linear correlation between intensity and photosynthetic rates[82]. As light intensity increases, however, there is the risk of overexposing causing photoinhibition[68] where radiation damage to the photosynthesis apparatus decreases photosynthesis production rates[83]. Oesterhelt *et al.* (2007) reported that light intensities greater than 225 μE m^{-2} s^{-1} (E represents Einstein's, which is equivalent to μmol m^{-2} s^{-1}) results in a slower photosynthesis rate of oxygen production due to photoinhibition in *G. sulphuraria* (Figure 6) [4]. This maximal light intensity for *G. sulphuraria* is significantly lesser than that reported for *Chlorella spp.*, which have a maximal light intensity of 2000 μE m^{-2} s^{-1} [4].

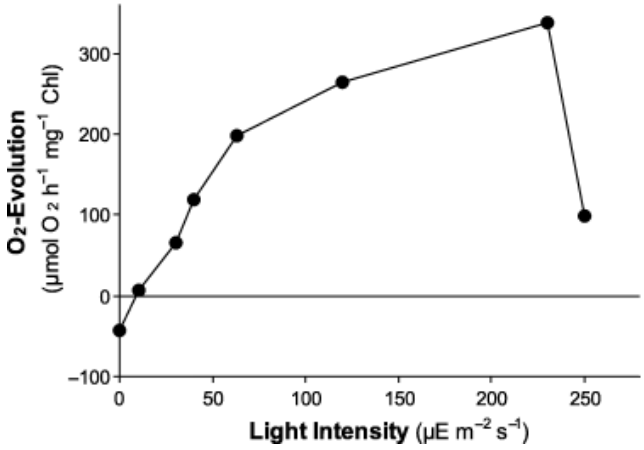

Figure 6: The light intensity dependence of photosynthesis in *G. sulphuraria.* The rate of photosynthesis was measured as oxygen evolution, where 160 μg Chl 10^9 cells^{-1}. The experiment was operated at ambient temperature, in a shaking incubator set at 120 RPM. Figure sourced from Oesterhelt *et al*[4].

The abrupt decrease in oxygen evolution rate observed in *G. sulphuraria* (Figure 6) is likely as a result of the algae often living in endolithic ecosystems where light availability is compromised[4]. Therefore, the species does not require high light intensities as it is adapted to these lower light conditions. Due to this *Galdieria* spp. often undertake heterotrophic metabolism in their natural environment[4]. Interestingly, *G. sulphuraria* have a similar observed maximum photosynthesis rate to photosynthesis rates reported for *Chlorella* spp. Maximum photosynthesis rates for *G. sulphuraria* observed were 330 µmol O^2 h^{-1} mg^{-1} Chlorophyll (Chl) (at light intensity 225 μE m^{-2} s^{-1})[4], while for *Chlorella* spp. the maximum reported photosynthesis rate was 350 µmol O^2 h^{-1} mg^{-1} Chl (at light intensity 200 μE m^{-2} s^{-1})[4]. This makes *Galdieria* spp. ideal candidates for biotechnical applications due to the lesser requirement for expensive lighting[88].

Oesterhelt *et al.* (2007) reported oxygen evolution rates ranging from 40-50 µmol O_2 h^{-1} (10^9 cells)$^{-1}$ for photoautotrophically grown *G. sulphuraria* (pH 1-6, under illumination 120 µE m^{-2} s^{-1})[4], whereas a negative oxygen production rate was observed during heterotrophic and mixotrophic conditions (i.e. O_2 consumption due to respiration) (25 mM glucose)[4]. Oesterhelt *et al.* concluded that the PSII was not active in these cells, likely the reason for the reduction in the CBB cycle enzyme RuBisCO (ribulose bisphosphate carboxylase/oxygenase) in both heterotrophic and mixotrophic grown cells[4]. RuDisCO activase is an enzyme that converts RuBisCO from an inactive state to an active state[54] during the CBB cycle, outlining why it was the prominent protein in extracts from photoautotrophic cells. Due to the decrease in RuBisCO protein and negative oxygen evolution rate measured during mixotrophic growth,

Oesterhelt *et al.* (2007) concluded that the *G.sulphuraria* 074W strain was not a true mixotroph[4]. Although, it is important to note that this experiment was conducted at ambient temperature, not the reported optimal growth temperature for *Galdieria* spp.[1,4,85].

Pigments within microalgae allow light energy to be absorbed. Once pigment molecules become excited and are converted into a higher energy state, energy is released due to photochemical transformations resulting in net ATP production[82]. Each microalgae species contains a photosystem containing a distinct light harvesting pigment which provides the cell with an absorption spectrum (Figure 7)[82]. As a result of this, not all wavelengths are absorbed by the photosynthetic apparatus and therefore cannot be used for photosynthesis. For *Galdieria* spp. the absorption peaks are at 618 nm (phycocyanin), 450 nm and 680 nm (chlorophyll-α), Chlorophyll-α and phycocyanin are the primary absorbing pigments found within *G. sulphuraria* [5].

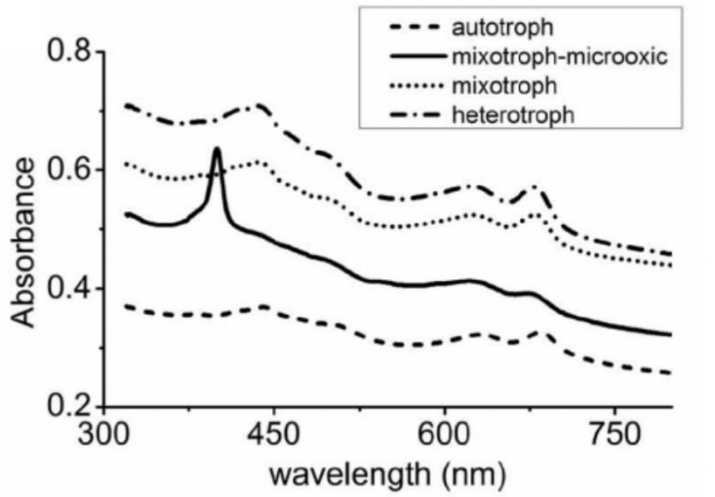

Figure 7: Absorption spectra for *G. sulphuraria* grown in various growth conditions, at pH 2.0, 40˚C. Mixotrophic and heterotrophic cells were grown with the addition of 50 mM glucose. The absorption peak at 618 nm corresponds to the phycocyanin pigment, and the absorption peaks at 450 nm and 680 nm correspond to chlorophyll-α pigment. The absorption peak at 400 nm observed in the oxygen-limited mixotrophic sample corresponds to porphyrin- like compounds. Figure sourced from Sarian *et al.*[5]

Exposure to different wavelengths impacts the biomass and pigment production in *Galdieria* spp., as investigated by Baer *et al.* (2016)[71]. It was found that the maximum biomass productivity was achieved when *G. sulphuraria* were grown under red light, while green and blue light decreased the biomass production[71].

Unfortunately, the majority of research into the effect light has on the growth and biomass yield of *G. sulphuraria* were performed in batch conditions[4,5,71] and therefore it is unknown what impact limiting nutrients during continuous cultivation has on *Galdieria* spp. under various light conditions.

2.5 Biotechnology Application of *Galdieria* spp.

Galdieria spp. offer a range of potential biotechnology applications due to their ability to grow in extreme conditions and their metabolic flexibility[1]. As *Galdieria* spp. grows under extreme conditions (pH 2.5 and 45°C[1]), this precludes contamination of non-extreme taxa[88]. Additionally, the ability to grow at hotter temperatures results in increased biomass growth rates compared to microalgae that grow in cooler temperatures (e.g. mesophiles)[86]. Hotter temperatures increase enzymatic activity leading to increased rates of photosynthesis and biomass productivity[86,88].

The metabolic versatility of *Galdieria* spp. is another advantage, as they are capable of growing heterotrophically and mixotrophically. Light requirements are a constraint for the industrial cultivation of microalgae and can contribute to increased operating costs for a process[88]. Photoautotrophic cultures are limited by exposure to ultraviolet light and the ability to obtain inorganic carbon (CO_2)[88]. Approximately 90% of photons are absorbed by the uppermost 10% of cultures, prohibiting the deeper layers from optimal photosynthesis[88]. The large surface area to volume ratio for open raceway ponds leads to unrealistic amounts of land required for photoautotrophic algae cultivation[88]. The ability to grow without the requirement of light greatly reduces cost and results in greater production rates, resulting in easier scale up in terms of reactor size, mixing, and gas transfer[89].

2.5.1 Phycocyanin Production

Phycocyanin (PC) is a blue, multi-chained light-harvesting holo-protein pigment within a group of proteins called phycobiliproteins. PC is produced solely from microalgae and cyanobacteria[90]. The major role of phycobiliproteins within cyanobacteria and Rhodophyta is photosynthetic light-harvesting and the ability to absorb light at wavelengths ranging from approximately 540-650 nm[89]. Although phycobiliproteins are highly abundant within cyanobacteria and Rhodophyta, they are not required for cell functions and therefore when the cells are starved of nitrogen, phycobiliproteins are selectively degraded[89]. PC has major industrially use as a fluorescent marker in diagnostic histochemistry and as a dye in the food and cosmetic industry[90,75.]

As PC is a photosynthetic pigment, it is largely produced under photoautotrophic conditions making it expensive to produce due to lighting requirements[90,42,91,92]. Currently, PC is commercially produced from photoautotrophic cultivation of the cyanobacteria species,

Arthrospira (Spirulina) platensis[90]. Current limitations for PC production in *Spirulina platensis* include the requirement for a light supply and the efficiency by which the light energy is utilised[89]. Open raceways, the primary process in which *Spirulina platensis* is commercially cultivated, have a limited depth to ensure that light can penetrate through the culture[89]. Cells located near the top surface are exposed to high light intensities which can result in an overload of the reaction centres and can cause photoinhibition resulting in low photosynthetic efficiency[89]. *Spirulina platensis* has been reported to grow mixotrophically, but it has not been reported as to whether this provides an advantage in PC production and growth[89]. *Spirulina platensis* can also grow heterotrophically on glucose and fructose, but PC production rates in heterotrophic conditions are not viable for commercial use[89]. In contrast, *G. sulphuraria* can produce PC under heterotrophic conditions making it an economically feasible option for PC synthesis[40,42]. *G. sulphuraria* is also able to achieve greater biomass concentrations of PC compared to *S. platensis*[42,93]. *G. sulphuraria* has been reported to produce PC in heterotrophic conditions at rates 1.7-13.6 times faster than photoautotrophic *S. platensis* PC production rates[42,90]. It has also been reported that the greatest phycocyanin production was achieved at a ratio of 60:0:40 (red; green; blue), 5.4% higher than red light alone[71].

Despite the potential for industrial PC production using *Galdieria* spp., very few studies have investigated PC production in chemostat (continuous) photobioreactors or concerning different trophic modes.

2.6 Cultivation Techniques for *Galdieria* spp.

The ability to cultivate a microalgae species in large scale cultivation methods is critical in order to utilise the species in biotechnical applications. In general, microalgae cultivation methods range from small scale laboratory techniques, such as solid media plating methods, to large scale industrial bioreactors[94].

2.6.1 Batch Cultivation

Batch cultivation is undertaken in a closed system, where required growth nutrients are provided at the beginning of the cultivation process and no additional nutrients are added throughout[94]. The main advantages of batch cultivation include short duration, less chance of contamination as no additional nutrient is added, and easier management[95]. The disadvantage of batch cultivation is that results are dependent on the time of harvest[95].

Galdieria spp. have been successfully cultivated in several different batch systems, both liquid and solid media. Solid cultivation is often used to generate axenic cultures, as it allows for the presence of bacterial contamination to be easily verified within algae cultures[96-98]. Axenic cultures of *G. sulphuraria* have been successfully generated using Luria Broth agar plates[96-98]. The most common system used to cultivate *Galdieria* spp. is a laboratory flask, often placed on a shaker set at 150 RPM[99]. Microalgae cultivation in laboratory flasks results in lower biomass growth and photosynthetic performance compared to other suspended systems but the reduced volume provides an effective cultivation technique for laboratory scale research[99]. Another common cultivation method is an airlift photobioreactor which is an enclosed glass column surrounded by a light source, where culture mixing is achieved by an aeration system[99].

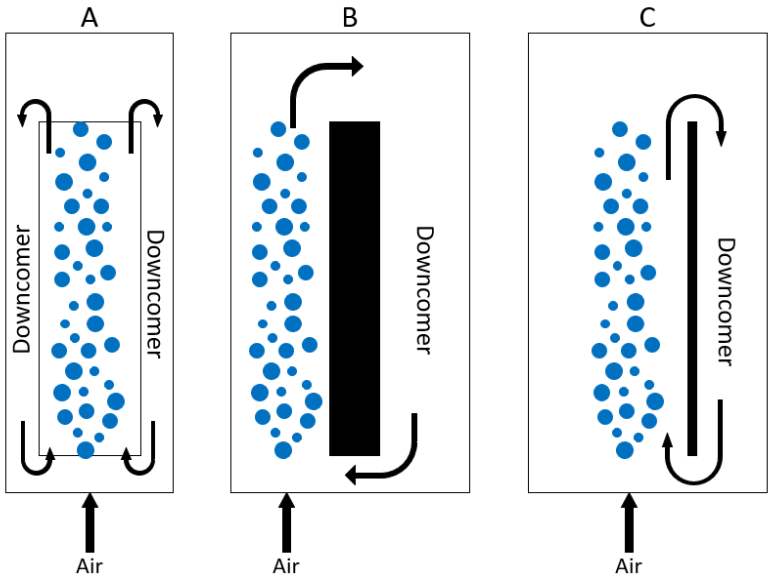

Figure 8: Example of common airlift bioreactor configurations. A is a concentric tube, B is an external draught and C is a split tube. Figure based on Christi *et al*[2].

An ultra-flat bioreactor contains panels spaced between silicone sheets, with the front panel housing the microalgae species (exposed to light) and the back panel contains a cooling jacket to control the temperature of the system[99,100].

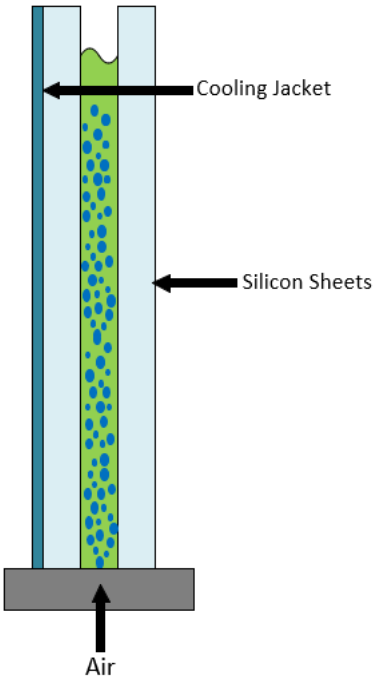

Figure 9: Ultra-flat bioreactor configuration. Figure based on Carbone *et al.* [99].

A twin-layer system consists of an immobilised photobioreactor, where the microalgae are inoculated onto a substrate layer[99]. Media containing nutrients flows past the immobilised culture, allowing nutrients to diffusion through. Twin layer systems are successful systems to cultivate *Galdieria* spp. as they mimic the natural habitat of the genus, as *Galdieria* spp. are often found living in rocks and soil[40,85,99]. Photoinhibition is reduced in twin layer systems due to mutual shading from the upper layers of culture, resulting in higher growth rates and photosynthetic performance compared to suspended systems[99]. Twin layer systems offer economic advantages due to better space utilisation, ease of harvesting biomass, and lower water consumption compared to suspended cultures [99].

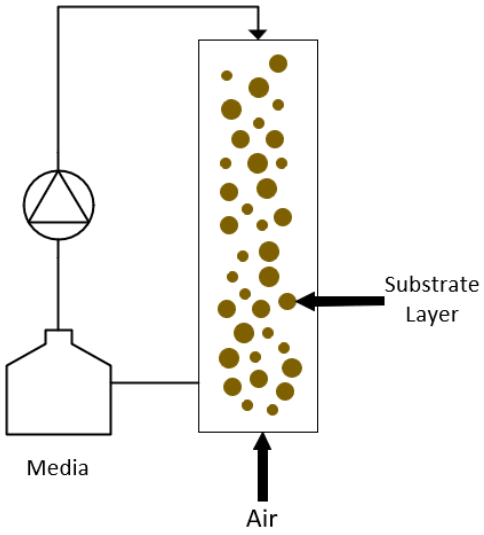

Figure 10: Twin layer photobioreactor configuration. Based on Carbone *et al.*[99].

An investigation conducted by Carbone *et al.* (2020) surrounding the growth and photosynthetic activity of *G. sulphuraria* in different culture systems concluded that the highest growth, productivity and photosynthesis performance was achieved when the microalgae species were grown in suspended systems[99]. The research investigated the use of different reactors, including suspended systems (laboratory flask, ultra-flat photobioreactor, and an airlift bioreactor) and an immobilised system (twin layer system)[99]. Among the suspended cultivation systems investigated by Carbone *et al.*, *G. sulphuraria* cultivated in the airlift bioreactor had the highest growth and photosynthetic performance[99]. The maximum growth rate was 0.119 $d^{-}1$, achieved in the airlift photobioreactor[99]. The ultra-flat bioreactor system used to cultivate *G. sulphuraria* achieved a similar growth rate but lower photosynthetic activity compared to the airlift bioreactor[99].

2.6.2 Large Scale Batch Cultivation

Due to the numerous biotechnological applications of *Galdieria* spp., large scale production is highly desired[4]. Raceway configuration serves well in cultivating large scale production of biomass, although growth is limited by light availability and gas sparging required to provide the cells with CO_2[101]. Raceway systems must be shallow enough to ensure light can penetrate through the culture, which requires a larger footprint to obtain high biomass yields[101]. Henkanatte - Gedera *et al.* investigated the potential for an enclosed 700 L photobioreactor configuration, cultivating *G. sulphuraria* in conditions that imitate raw urban primary effluent[101]. Mixotrophic conditions were used to produce high biomass yields, eliminating the limitation of light availability which photoautotrophic conditions pose[101]. *G. sulphuraria* was successfully cultivated in a large volume, removing organic carbon and nutrients from the urban wastewater[101].

2.7 Continuous Cultivation

A major drawback of batch cultures systems is that steady state cannot be achieved, therefore the results will be dependent on the time of harvest[95]. This limits the ability to obtain knowledge and information surrounding the general physiology of microorganisms[95]. Continuous culture techniques allow submaximal growth rates to be achieved in microorganism cultivation under defined, nutrient-limited conditions[95]. This allows the culture conditions to remain virtually constant, achieving a steady state which is beneficial for metabolic studies[95]. In continuous cultivation, the media reservoir contains all components required for growth in excess apart from the growth-limiting factor (s)[95]. Microorganisms will continue to grow at a maximum growth rate until this one essential substrate becomes limiting, which then results in steady state growth[95]. The observed growth rate (μ) of the microorganisms is dependent on the concentration of the growth-limiting substrate according to Monod's equation, as shown below in Equation 2[95].

$$\mu = \frac{\mu_{max} s}{K_s + s} \tag{2}$$

Equation 2: Monod's Equation, where μ is the growth rate, μ_{max} is the maximum growth rate, s is the concentration of the growth-limiting substrate and K_s is the Monod saturation concentration (which is numerically equal to the substrate concentration at ½ μ_{max})[95].

G. sulphuraria is highly suited for continuous flow cultures, achieving higher phycocyanin production rates compared to fed-batch cultivation conditions[90]. Steady state

growth of *G. sulphuraria* has been achieved in mixotrophic conditions with the carbon substrate, glucose, being the limiting nutrient in the system[102]. A dilution rate of 0.63 day^{-1} was used[102].

There is currently no known large scale continuous cultivation using *Galdieria* spp. for commercial purposes.

2.8 Literature Review Summary

Due to the extremophilic nature and metabolic flexibility, *Galdieria* spp. offer major potential in several biotechnological applications[4]. However, due to limiting research into the growth of *G. sulphuraria* within continuous cultivation systems, commercial cultivation has not been successful on a large scale[99]. As discussed in this literature review, the lighting requirements of photoautotrophic cultivation are a major constraint in the industry, contributing to increased operating costs[88]. Additionally, critical gaps in the ability to upscale and continuously cultivate *Galdieria* spp. limits industrial application. To provide insight into the ability to upscale *Galdieria* spp., this research project grow *Galdieria* sp. RTK37.1 in a continuous culture system to obtain steady state growth conditions to investigate several light (in)-dependant growth factors. This provided an understanding of the effect light has on the physiology of *Galdieria* sp. RTK37.1 and provided additional insight into the optimal growth conditions aiding in achieving large scale production of *Galdieria* sp. RTK37.1.

The specific hypothesises of this research were:

1. *Galdieria* sp. RTK37.1 is a true mixotroph.
2. Stable continuous cultivation of *Galdieria* sp. RTK37.1 is achievable during photoautotrophic, mixotrophic and heterotrophic growth conditions.
3. The growth and pigment production of *Galdieria* sp. RTK37.1 depends on the light intensity and wavelength condition during continuous cultivation

3 Chapter 3: General Method and Materials

The methods and materials presented in this chapter are general and can be applied unless otherwise stated, to forthcoming research chapters 4, 5 & 6.

3.1 Cultivation and Routine Maintenance

Xenic cultures of *Galdieria* sp. RTK37.1 were received (courtesy of Scion, Rotorua), known to be contaminated with low concentrations of an unknown bacterium. After isolation (Section 3.4), *Galdieria* sp. RTK37.1 were maintained under photoautotrophic conditions in warm white LED lights operating at 170 µmol m^{-2} s^{-1}, with a constant supply of 3% (v/v) CO_2 (unless otherwise stated).

Maintenance cells were grown in 250 mL baffled glass shake flasks (KIMAX, Kimble, USA), in V4 medium at a pH 2.5 in a shaking incubator (150 rpm, 45°C). Culture stocks were continuously inoculated (initial concentration of OD 0.1) into fresh V4 medium during the duration of the research to ensure a supply of active *Galdieria* sp. RTK37.1 cells were readily available. Culture stocks were typically discarded after four weeks of growth.

3.2 Medium Preparation

Galdieria sp. RTK37.1 cells were grown in V4 mineral salts growth medium as described by Dunfield et al[103], in Appendix C. Solid medium for plating methods was made using double concentrated V4 medium with 15 g L^{-1} Phytagel solution, as described in Appendix D. All medium used was autoclaved at 121°C and 103 kPa (15 psi) for 30 minutes.

3.3 Sterilisation and Aseptic Techniques

All glassware used during this research was autoclaved at 121°C and 103 kPa (15 psi) for 30 minutes. Spent cultures and contaminated glassware was first sterilised using 4 wt% sodium hypochlorite prior to autoclaving. Handling of cultures was completed in laminar flow biohoods to avoid contamination with any airborne microorganisms. All materials including pipettes, syringe needles and inoculation loops were flame sterilised before being utilised on cultures. Disinfection of the biohoods was completed using 70% (v/v) ethanol solution.

3.4 Isolation of *Galdieria* sp. RTK37.1

An axenic culture of *Galdieria* sp. RTK37.1 was generated by completing three rounds of dilution to extinction experiments (to 10^{-9}). The presence of bacterial contamination within samples was confirmed under a Primo Star microscope (Zeiss, Germany) at 1000x magnification.

Galdieria sp. RTK37.1 was also grown on Phytagel plates to determine the presence of bacterial contamination. Plating the samples was an effective way to confirm bacterial contamination as the bacterial species had a shorter lag time compared to *Galdieria* sp. RTK37.1 cells, appearing as large yellow colonies compared to the significantly smaller green algae growth on the plates (Figure 11). The presence of bacterial growth on the plates took 3 days, while *Galdieria* sp. RTK37.1 colonies were not typically observed until 10 days post-inoculation.

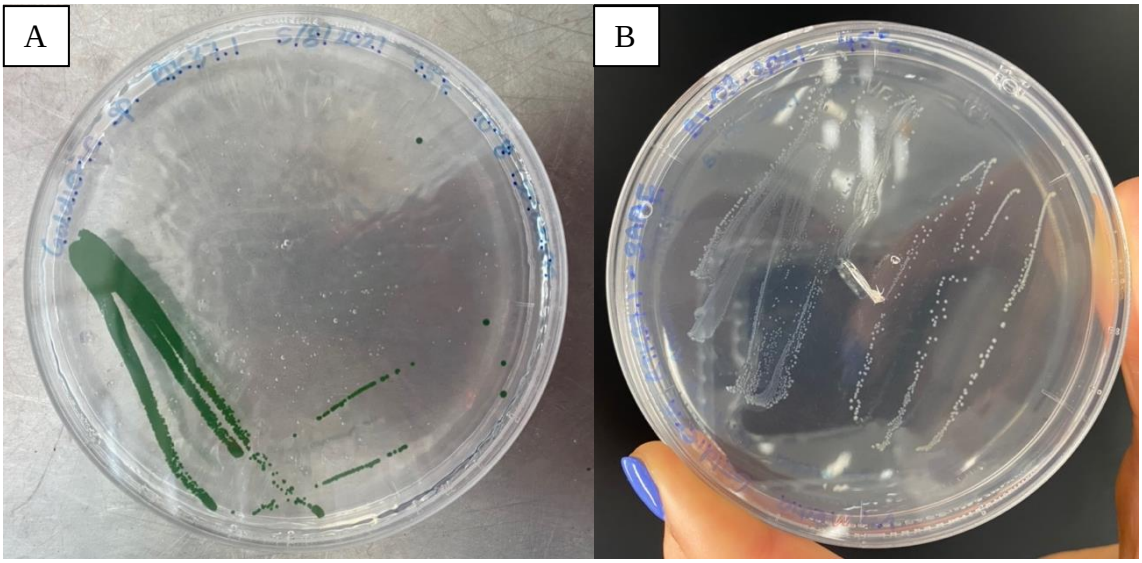

Figure 11: *Galdieria* sp. RTK37.1 colony growth on Phytagel V4 medium plates, grown at 45˚C, pH 2.5 under 400 µmol m^{-2} s^{-1}.

Figure 11. A shows an axenic culture of *Galdieria* sp. RTK 37.1.

Figure 11. B shows bacterial contamination, with no observed *Galdieria* sp. RTK37.1 growth.

3.5 Molecular Characterisation and Taxonomic Classification

Once an axenic culture of *Galdieria* sp. RTK37.1 was generated, genomic DNA was extracted to confirm the identity. For DNA extractions, 1 mL samples of *Galdieria* sp. RTK37.1 were microcentrifuged at 12,000 rpm for 10 minutes at 4°C (GYROZEN 1730R, Germany). DNA extraction was then completed using the NucleoSpin® Microbial DNA kit (Macherey - Nagel, Germany) following the manufacturer's recommended protocol. Mechanical lysis was achieved with a bead mill at 5 m s^{-1} for 10 minutes. DNA elution protocol was done using 25 µL of elution buffer (Tris-HCI). The purity recovered was assessed using Nanodrop UV Spectrophotometry (Thermo Fisher Scientific, USA) at an absorbance ratio of 260/230 nm and 260/280 nm. DNA extraction was also undertaken on the unknown bacterial isolate using the same method used for *Galdieria* sp. RTK37.1.

To taxonomically place the isolated *Galdieria* sp. RTK37.1 and bacterial contaminate, PCR was performed on the targeted housekeeping genes as summarised in Table 3. These target genes and primers used were based on research conducted by Colsell (2020)[104].

Table 3: Specific primers and target genes used during PCR. The genes targeted in *Galdieria* sp. RTK37.1 were the *18s rRNA*, *rbcL*, and *psaA*. The gene targeted for *Alicyclobacillus* sp. EB1 was *16s rRNA*.

Target Gene	Forward Primer	Reverse Primer
18s rRNA[105]	**CdmF** GTCAGAGGTGAAATTCTTGGATTTA	**CdmR** AAGGGCAGGGACGTAATCAACG
rbcL[106]	**RbcL1F** AACCTTTCATGCGTTGGAGAGA	**RbcL1R** CCTGCATGAATACCACCAGAAGC
psaA[107]	**psaA130F** AACWACWACTTGGATTTGGAA	**psaA130R** CCTCTWCCWGGWCCATCRCAWGG
16s rRNA[107]	**9F** AGAGTTGATCMTGGCTCAG	**1492R** GGHTACCTTGTTACGACTT

PCR amplification reaction mixtures contained 12 µL MyFi Mix (Bioline, USA), 4 µL forward primer (10 µM), 4 µL reverse primer (10 µM), 20 µL of PCR grade water and 10 µL of template DNA (40 ng μL^{-1}). Cycling conditions for the PCR reaction were specified by the MyFi Mix kit (Bioline, USA). The cycling conditions are outlined in Table 4.

Table 4: PCR cycling conditions for the specific primers used during this research to target genes within *Galdieria* sp. RTK37.1 and the bacterial contaminate.

Genes	Initial Denaturation	Denaturation	Annealing	Extension	Final Extension	Denaturation, Annealing & Extension Cycles
18s rRNA[105]	95°C 3 min	95°C 15 sec	55°C 15 sec	72°C 25 sec	72°C 2 min	30
rbcL[106]	95°C 3 min	95°C 15 sec	55°C 15 sec	72°C 25 sec	72°C 2 min	30
psaA[107]	95°C 3 min	95°C 15 sec	50°C 15 sec	72°C 25 sec	72°C 2 min	35
16s rRNA[107]	95°C 3 min	95°C 15 sec	50°C 15 sec	72°C 25 sec	72°C 2 min	35

Amplification of a PCR product was confirmed by gel electrophoresis using 1% (w/w) agarose gel. The PCR products were then cleaned using a DNA Clean and Concentrator kit (Zymo Research, USA) following the manufacturer's recommended protocol. Cleaned PCR products were sequenced via the Sanger Reaction Method for both the forward and reverse primers at Macrogen Ez-Seq (Seoul, South Korea).

For each primer-paired reaction, a consensus sequence was generated from raw sequence data on Geneious Prime (version 2022.0.1, Biomatters LTD, NZ) and poor-quality base cells were removed.

3.6 Optical Density Measurements

Cell growth was measured by a UV- visible spectrophotometer (Ultrospec 2100 pro, Amersham Biosciences, UK). The radiation absorbed by the biomass was directly related to the concentration of the biomass in the solution, providing a quantitative measurement[108]. A wavelength of 600 nm was used to ensure that the absorbance from cell pigmentation was decreased[67]. If required, the samples were diluted in sterile deionised water to values below 1.0 absorbance ($AU_{600\ nm}$)[67].

The specific growth rate, μ, was determined using Equation 3.

$$\mu = \frac{\ln(C_1) - \ln(C_i)}{t_1 - t_i} \tag{3}$$

Equation 3: The specific growth rate of a culture at a given time, where C_i is the initial concentration of the cells, C_1 is the concentration of the cells at t_1, t_i is the initial time and t_1 is the end time for the measurement.

3.7 Biomass Yield

Dry cell biomass weights were determined by collecting known volumes of effluent culture and centrifuging (Centrifuge 5810 C, Eppendorf, Germany) at 10,000 RPM for 5 minutes at 4°C in a pre-dried and weighed 50 mL Eppendorf tube. The supernatant was decanted and the cell pellet was washed three times with deionised water to remove remaining salts within the pellet. The cell pellet was frozen at -18°C for a minimum of 12 hours before the sample was dried in a vacuum oven (ATP Line, Binder, Germany) for 3 days, at 75°C and a vacuum pressure of 0.385 psi. Samples were confirmed dry when the weight did not change over the course of three days.

The dry cell weight (DCW) was calculated using Equation 4.

$$DCW = \frac{w_2 - w_1}{V} \tag{4}$$

Equation 4: Dry cell weight equation, where w_2 is the mass after the sample has been dried (g), w_1 is the mass of the empty Eppendorf tube (g) and V is the volume of the initial sample (L)

3.8 Cell Counting

Cell counts were done using the haemocytometer counting method as described by LeGresley *et al.*[109]. The haemocytometer used was an Improved Neubauer (0.1 mm deep) haemocytometer (Bright Line, Hausser Scientific, USA). Initially, the haemocytometer and glass slide was washed with 70% (v/v) ethanol and dried using lint-free tissue paper. The glass slide was then placed on top of the haemocytometer. Samples were initially diluted (10 x dilution) with deionised water in an Eppendorf tube, then 20 µL was pipetted under the glass slide onto the haemocytometer. The cells were counted using an optical Olympus BX60 microscope (Olympus, Japan) at 400 x magnification paired Amscope Digital Camera using the Amscope Software (Version 64.0, United Scope, USA). The cells were counted in the large four squares (Figure 12) representing a volume of 1 x 10^{-4} mL. The total cells in each square were counted and then an average of the four squares was reported.

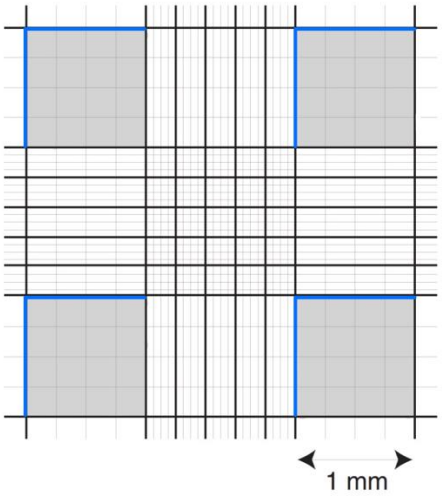

Figure 12: Haemocytometer counting diagram, where the grey squares represent the squares that were counted. The blue line outlines where, if cells were on these lines, they were ignored. Based on a diagram from LeGresley *et al.*[109].

Equation 5 was used to calculate the total number of cells:

$$C_{cell} = 1 \times 10^4 \, d_f n_{avg} \quad (5)$$

Equation 5: Total cell count equation, where C_{cell} is the total number of cells per volume, d_f is the dilution factor used and n_{avg} is the average number of cells counted in the large squares.

3.9 HPLC Substrate Concentration

The concentration of organic carbon substrates (i.e. glucose, succinate, galactose, sorbitol and acetate) was measured using High-Performance Chromatographic analysis. During heterotrophic and mixotrophic experiments (those which contained an organic carbon substrate), 1 mL samples were taken daily and micro-centrifuged at 12,000 rpm for 10 minutes at 4°C (GYROZEN 1730R, Korea). The supernatant was filtered through a 0.2 µm syringe filter (0.22 µm Nylon Membrane Filters, BIOFIL) and transferred into a 0.2 mL septum capped glass vial. The filtered supernatant was then analysed using high-performance liquid chromatography (HPLC) (UltiMate 3000 UPHLC, Thermo Fisher Scientific, USA) combined with a refractive index and UV-visible spectrophotometer set at a wavelength of 210 nm. The column used was an Aminex HPX-87H column 300 x 7.8 mm (BIORAD, USA). The mobile phase used was 5 mM H_2SO_4 with a set flow rate of 0.5 mL min^{-1}. The column temperature and pressure were set to 50°C and 1000 psi respectively. Results were analysed using Chromeleon software (version 7.3, ThermoFisher Scientific, USA).

Calibration curves for determining substrate concentration were generated using serial dilution stocks of known concentrations, as attached in Appendix E.

3.10 Ammonia Analysis Method

The dissolved ammonium concentration was measured to determine when *Galdieria sp.* RTK37.1 was limited in ammonia. Samples (10 mL) were centrifuged (Eppendorf Centrifuge 5810 C, Eppendorf, Germany) at 10,000 RPM for 5 minutes at 4°C to avoid the presence of cells interfering with measurements. The supernatant was then decanted and placed on a magnetic stirrer (500 RPM). The potential difference was determined by an Ammonia Electrode (ThermoFisher Scientific, USA) after 10 M of sodium chloride was added to the sample. Medium pH was measured using a Eutech pH Probe (Thermo Fisher Scientific, USA) after the measurement to confirm that the solution was above a pH 13, following the manufacturer's recommended protocol.

The ammonium concentration was then determined using a calibration curve. Calibration standards were generated through a serial dilution of V4 medium containing 0.4 g L^{-1} of ammonia chloride with V4 medium containing no ammonia chloride. Calibration curves are attached in Appendix F.

3.11 Oxygen Evolution Rate Measurement

The oxygen evolution rate was measured as a function of the light intensity, allowing insight into the ability for *Galdieria* sp. RTK37.1 to adapt to changes in trophic conditions and light intensity. The rate of oxygen evolution quantifies the concentration of dissolved oxygen generated by a population through photosynthesis.

The apparatus and method for this experiment were based on that reported and designed by Smith (2020)[110]. The apparatus set up consisted of a culture vessel, surrounded by a 10 mm thick water jacket, which was connected to a circuiting water bath through silica tubing. The temperature of the sample was maintained at a constant temperature of 45°C by a water bath controlled within $\pm$ 0.1°C. The culture vessel was placed on a magnetic stirrer, set at 800 RPM. A lighting array, consisting of warm white LED strips, surrounded the culture vessel and were connected to a dimmer control allowing the light intensity to be varied from 46 – 642 µmol m^{-2} s^{-1}. The oxygen evolution apparatus set up is shown below in Figure 13.

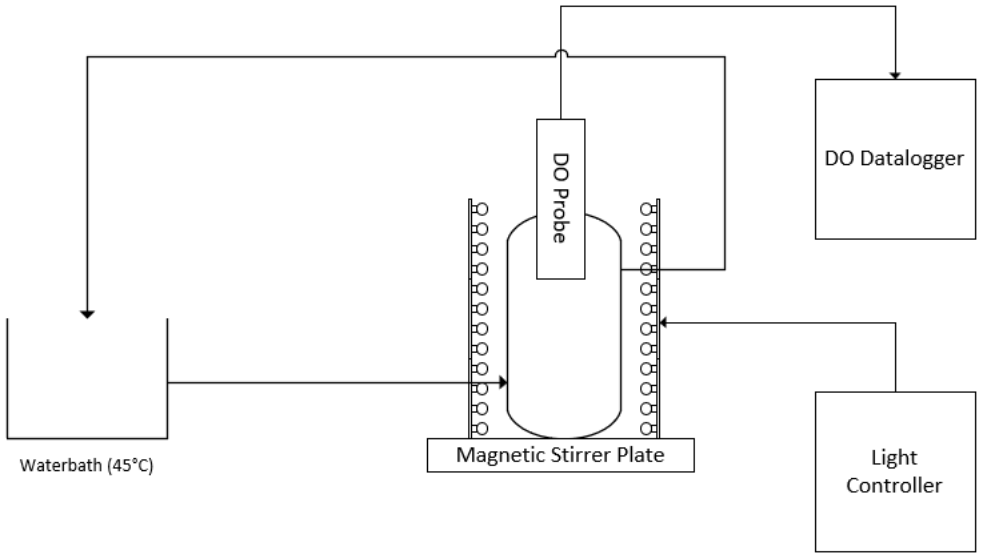

Figure 13: Experimental setup for Oxygen Evolution measurements, designed by Smith[110].

Dissolved oxygen concentration was measured using a polarographic style probe (Orion 083005MD, Thermo Fisher Scientific, USA) paired with a dissolved oxygen datalogger (Orion Star A223, Thermo Fisher Scientific, USA). Dissolved oxygen data was logged on a computer, through the StarCom software (version 1.0, Thermo Fisher Scientific, USA), allowing continuous timed measurements to be taken. The oxygen evolution rate was

determined by taking the linear regression of observed oxygen concentration with respect to time over 100 seconds.

Prior to any measurement being taken, the dissolved oxygen probe was calibrated using the water-saturated air method, as described in the user manual (Thermo Fisher, Scientific, USA). The electrolyte solution in the probe was changed before each measurement, and then the probe was polarized for 1 hour prior to ensure readings were consistent.

Fresh V4 medium was saturated with pure CO_2 for 1 hour by sparging before measurements. This ensured that the dissolved oxygen was set at 100% air saturation and the medium was only saturated with dissolved CO_2. This ensured that carbon limitation was avoided during the experiment. After saturation, 100 mL of medium was transferred into the culture vessel, and mixed (800 RPM) until the temperature and dissolved oxygen level were stabilised. Once equilibrium was achieved, 10 mL of fresh inoculum (*Galdieria* sp. RTK37.1, OD 3-6.5) was added to the culture vessel. Inoculum for the oxygen evolution rate experiment was grown in continuous chemostats until steady state conditions were achieved.

The temperature and dissolved oxygen concentration were measured every 3 seconds for 30 minutes. The experiment was repeated using fresh inoculum each time.

3.12 Light Intensity Measurement

Light intensities were measured using an MQ-610 extended range photon flux density meter (Apogee, USA). Measurements were taken in a dark room to avoid external light interfering with the results. The light intensities measured were recorded in µmol m^{-2} s^{-1} and were correlated to calibrated measurements taken using a spherical quantum sensor (Li-COR Spherical LI-193, USA) which was connected to a light sensor data logger. All light intensities mentioned in this research have been correlated to the spherical quantum sensor, as attached in Appendix G.

3.13 Relative Pigment Measurement

The relative pigment emitted by the cells was estimated using Cytations Imaging Reader (Biotek, USA), through Gen5 Software (version 1.02, Biotek, USA).

Samples were diluted in deionised water to an OD_{600nm} 0.6 and then 200 µL was pipetted into a Co-Star 96 welled plate. The linear shake duration was set at 10 s, the gain was

set at 80 and the total number of flashes was set to 3. The plate reader measured the absorbance at 600nm and completed a wavelength spectra scan from 300 nm – 800 nm in increments of 10 nm[111]. Fluorescence emitted by phycocyanin and chlorophyll-α were estimated by exciting the sample and measuring the emissions. To measure the relative amount of phycocyanin, samples were excited at 590 nm and the emissions measured at 670 nm[111]. For chlorophyll- α, the sample was excited at 485 nm and the emissions measured at 670 nm[111].

There was a discrepancy between the OD_{600nm} measurement between the UV spectrophotometer and the imaging reader, therefore a discrepancy curve was generated (Appendix H). All optical density measurements reported in this report are based on measurements provided by the UV- visible spectrophotometer (Ultrospec 2100 pro, Amersham Biosciences, UK). All measurements taken using the Cytations Imaging Reader (Biotek, USA) were adjusted using the discrepancy curve attached in Appendix H.

3.14 Nutritional Analysis

Effluent biomass was collected during steady state chemostat operation and centrifuged (Centrifuge 5810 C, Eppendorf, Germany) at 10,000 RPM for 5 minutes at 4°C in a pre-dried and weighed 50 mL Eppendorf tube. The supernatant was decanted and the cell pellet was washed three times with deionised water to remove remaining salts within the pellet. The cell pellet was frozen at -18°C for a minimum of 12 hours before the sample was dried in a vacuum oven (ATP Line, Binder, Germany) for 3 days, at 75°C and a vacuum pressure of 0.385 psi. Nutritional characterisation of *Galdieria* sp. RTK37.1 biomass was performed at the College of Sciences, Massey University (accredited to ISO 17025; New Zealand) following official methods of analysis of the Association of Official Analytical Communities (AOAC, 2005) international. Total crude protein and ash (w/w %) were determined via the Dumas method (AOAC method 986.06)[112] and furnace method (AOAC method 942.05)[113] respectively. Moisture and fat content was determined (w/w %) via the Air Oven method (AOAC 925.10, 930.15)[114] and the Mojonnier method (AOAC 922.06)[115] respectively. Carbohydrate (w/w %) was calculated by difference.

3.15 Data Analysis

Statistical analysis for the results was completed in GraphPad Prism (version 9.3.1) using data analysis functions. Results were considered to be statistically significant at 95% confidence levels using two-tailed unpaired t-tests and ANOVA, $p \leq 0.05$. Uncertainty was measured by standard deviation, by completing each measurement as either biologically or technical triplicates, as stated.

3.16 Batch Cultivation of *Galdieria* sp. RTK37.1

3.16.1 Incubator Set up

Batch experiments were completed in a modified MaxQ 600 incubator (Thermo Fisher Scientific, USA). LED lighting strips and a gas flow supply manifold had been added to the incubator to accommodate photoautotrophic and mixotrophic growth conditions. Mass flow controllers (MCS series, Alicat Scientific, USA) controlled the flow rate for compressed air and CO_2. Gas flowrates were maintained at 600 SCCM and 20 SCCM respectively, to maintain ~ a 3% (v/v) CO_2 concentration when gas sparging was required. Gas was humified through deionised water and filtered (0.2 μm PTFE filter) before entering the reactor.

The incubator was maintained at 45°C and 150 RPM throughout all batch experiments. LED lighting supplied the system with warm white light which was maintained at 170 µmol m^{-2} s^{-1} for photoautotrophic and mixotrophic growth experiments.

All cell manipulation and inoculation for batch experiments were completed in a laminar flow biohood to avoid contamination. All batch cultures were inoculated to AU_{600nm} of 0.1 and completed in triplicates. Negative controls were applied for each experiment.

3.16.2 Photoautotrophic Cultivation Experiments

During the photoautotrophic batch experiment, 100 mL serum bottles with septum caps were used. The serum bottles contained 50 mL of V4 medium. Filtered (0.2 µm PTFE syringe filter) compressed air and 3% (v/v) CO_2 was supplied through sterile needles (21 G, 120 mm) at 600 SCCM and 20 SCCM respectively (divided between triplicates). Ventilation of the system was provided by an additional needle covered in aluminium foil (23 G, 32 mm). LED warm white lighting surrounding the incubator was maintained at 170 µmol m^{-2} s^{-1}.

3.16.3 Mixotrophic Cultivation Experiments

During mixotrophic batch experiments, *Galdieria* sp. RTK 37.1 cells were grown in 100 mL serum bottles with a septum capped. The serum bottles contained 50 mL of V4 medium with the addition of 10 mM of an organic carbon source. Filtered (0.2 µm PTFE syringe filter) compressed air and 3% (v/v) CO_2 was supplied through sterile needles (21 G, 120 mm) at 600 SCCM and 20 SCCM respectively (divided between triplicates). Ventilation of the system was provided by an additional needle covered in aluminium foil (23 G, 32 mm). As with photoautotrophic samples, LED warm white lighting surrounding the incubator was maintained at 170 µmol m^{-2} s^{-1}.

3.16.4 Heterotrophic Cultivation Experiments

During heterotrophic batch experiments, *Galdieria* sp. RTK 37.1 cells were grown as described in mixotrophic batch experiments, with the exception that serum bottles were covered with aluminium foil to prevent exposure to light and no CO_2 or compressed air was sparged into the samples.

3.17 Continuous Cultivation of *Galdieria* sp. RTK37.1

After the completion of batch experiments, continuous cultivation of *Galdieria* sp. RTK37.1 was performed to investigate several light (in)dependant growth factors surrounding *Galdieria* sp. RTK37.1. This was completed to provide an understanding of the effect light has on the physiology of *Galdieria* sp. RTK37.1 and provide additional insight into the optimal growth conditions aiding in achieving large scale production of *Galdieria* sp. RTK37.1.

3.17.1 Airlift Photobioreactor Apparatus

The airlift photobioreactor used during this research was designed and constructed by Smith (2020)[110], based on designs by Mazumda (2015)[116] and Gopalakrishnan (2018)[110,116,117].

The airlift photobioreactor consisted of a 1500 mL concentric glass tube surrounded by a water jacket. The temperature inside the reactor was maintained through water circulation, which was controlled by a refrigerating water bath and submersion pump. A butyl rubber stopper was placed on the top of the reactor, containing stainless steel tubing for gas sparging, sampling and ventilation. LED lighting strips placed around a plastic circular tube was placed on the outside of the reactor.

The temperature inside the reactor was maintained at 45°C for all experiments. The LED lighting was on warm white light at an intensity of 94.6 μmol m^{-2} s^{-1}, unless stated otherwise. Gas sparging into the reactor was controlled by mass flow controllers (MCS series, Alicat Scientific, USA). A total gas flow rate (compressed air and CO_2) of approximately 2000 ml min^{-1} was used, maintaining a concentration of 3% (v/v) CO_2. The gas was split between two rotameters to ensure a constant gas flow rate of 1000 mL min^{-1} was maintained. Gas was humified through deionised water and filtered (0.2 μm PTFE filter) before entering the reactor.

3.17.2 Chemostat Design for Continuous Cultivation Experiments

For continuous cultivation experiments, two additional stainless steel tubes were added to the butyl rubber stoppers to allow for an inlet feed and outlet effluent ports. The outlet effluent tube height in the reactor was chosen to set the desired volume of culture, which was 1400 mL.

Fresh V4 medium was supplied into the reactor by a peristaltic pump (Huiyu Fluid, Beijing, China; Appendix I), which set the desired dilution rate (D = 0.12 d^{-1}) for the chemostat (Inlet flow rate 250 mL d^{-1}, outlet flow rate 500 mL d^{-1}). All media transferred was via sterilised silicon tubing (#14).

Sterilisation of the Chemostat Reactors

The chemostat reactors were initially rinsed with 4 wt% sodium hypochlorite to dislodge biofilm from the sides of the reactor, then rinsed with deionised water to remove the biomass and other contaminates. The inlet and outlet tubing of the reactor were then covered in aluminium foiling, ensuring the rubber bund was not placed on the reactor tightly to avoid pressure build-up within the system. The reactor was then autoclaved (dry sterilisation) at 134°C, 15 psi for 30 minutes. After sterilisation was complete the butyl rubber stopper was not removed from the reactor until all experiments were completed to avoid contamination.

Fresh V4 medium was sterilised by autoclaving at 121°C, 15 psi for 30 minutes. The butyl rubber stoppers remained on the bottles during sterilisation with the silicon tubing connected. After sterilisation, the inlet feed and outlet effluent tubing were attached to the reactor after being further sterilised with 70% (v/v) ethanol to limit airborne contamination. Sterile V4 medium was then pumped into the reactor until the desired volume was achieved.

3.17.3 Chemostat Reactor Experimental Method

The V4 medium was heated inside the reactor to 45°C. The total gas flow rate was set at approximately 2000 mL min^{-1} (1000 mL min^{-1} into each chemostat reactor), using 1900 mL min^{-1} compressed air and 60 mL min^{-1} CO_2 to maintain a 3% (v/v) CO_2 concentration. Once the reactors were at the desired conditions, axenic *Galdieria* sp. RTK 37.1 cells were inoculated into the reactors to achieved a desired OD_{600nm} of 0.1. The reactors were maintained in batch operation until an OD_{600nm} of ~ 3 was achieved, then the reactors were changed into continuous operation. A dilution rate of 0.12 d^{-1} (250 mL d^{-1}) was used during this research, which was based on the exponential growth rate measured during photoautotrophic batch growth experiments. Triplicate samples were collected from both reactors daily to measure the cell growth using UV- visible spectrophotometer (Ultrospec 2100 pro, Amersham Biosciences, UK). The temperature, ammonia concentration and pH were also measured throughout chemostat operation.

Photoautotrophic Cultivation Experiments

During photoautotrophic growth conditions of the chemostat reactors, warm white LED lighting was maintained at an intensity of 94.6 μmol m^{-2} s^{-1}. The reactors contained different initial inlet ammonia concentrations (Reactor 1 contained 0.2 g L^{-1} ammonia chloride (NH_4Cl) and Reactor 2 contained 0.4 g L^{-1} NH_4Cl) to investigate the effect ammonia limitation would have on the photoautotrophic steady state of *Galdieria* sp. RTK 37.1. During steady state conditions, pigment production analysis and cell counts were completed. Biomass was collected over 5 days to obtain dry biomass weights.

During light intensity and wavelength experiments (Chapter 6), reactor 1 was cultivated under warm white LED light at an intensity of 94.6 μmol m^{-2} s^{-1}. The light intensity was increased to 191.4 μmol m^{-2} s^{-1} then decreased to 8.1 μmol m^{-2} s^{-1}. Galdieria sp. RTK37.1 was then cultivated under red light (629 nm, 33.8 μmol m^{-2} s^{-1}) and then blue light (464 nm, 86.5 μmol m^{-2} s^{-1}). During steady state conditions, pigment production analysis and optical density were measured.

Mixotrophic Cultivation Experiments

To transfer to mixotrophic growth, 10 mM of glucose was added to the inlet V4 medium and this was pumped into the reactor. Warm white LED lighting was maintained at an intensity of 94.6 μmol m^{-2} s^{-1}. The reactor contained an inlet ammonia concentration of 0.4 g L^{-1} NH_4Cl. During steady state conditions, HPLC samples, pigment production analysis and cell counts were completed. Biomass was collected over 5 days to obtain dry biomass weights.

Heterotrophic Cultivation Experiments

Following mixotrophic growth experiments, the reactor was transferred to heterotrophic growth conditions by covering the reactor in aluminium foil to prevent exposure to light. CO_2 was still sparged into the reactor but would not impact the growth of *Galdieria* sp. RTK 37.1 due to light limitation. The reactor contained an inlet ammonia concentration of 0.4 g L^{-1} NH_4Cl and 10 mM of glucose. During steady state conditions, HPLC samples, pigment production analysis and cell counts were completed. Biomass was collected over 5 days to obtain dry biomass weights.

4 Chapter 4: Classification and Batch Characterisation of *Galdieria* sp. RTK37.1

4.1 Introduction and Aim

Batch cultivation involves a closed system where all required growth and maintenance nutrients are provided at the beginning of cultivation and no additional nutrients are added throughout[94], discussed in Section 2.6.1. During microalgae growth within a closed system, growth is exponential until the exhaustion of a limiting factor, typically a nutrient. After nutrient exhaustion, growth is no longer exponential as the system enters the stationary phase, where the rate of cell growth equals the rate of cell death[94]. Over time nutrients continue to decrease and cells expel toxins, which ultimately results in cell death[94].

During the exponential phase, growth is typically constant, largely depending on the species and cultivation parameters such as light intensity, temperature and nutrient availability[94]. Although maximum biomass and product production is achieved during exponential growth, this is not maintainable as cells will enter the stationary phase of growth[94]. This is a major consequence of batch cultivation[94]. To maintain cells in the exponential growth phase, cells must be supplied with fresh medium through subculturing[94]. This decreases cell density resulting in inconsistent biomass and product outputs[94]. Additionally, the requirement to subculture increases the likelihood of contamination and requires large amounts of labour due to continuous inoculation and harvesting[94]. Within batch systems cell properties such as size, internal composition and metabolic functions are dependent on the time of harvest, making metabolic studies difficult and often not an accurate estimate of what occurs intracellularly[94]. As a result, batch cultivation of algae is not favoured for large scale production in biotechnology applications[94].

Batch cultivation does have advantages, particularly surrounding the simplicity and low-cost associated with the system. Batch systems are often low volume and are therefore easier to manage and identify any remedy defects in the cultivation method. By completing batch cultivation of a species, optimal growth conditions can be identified and characterised which can then be transferred to larger scale continuous cultivation. During this research, *Galdieria* sp. RTK37.1 was grown in batch conditions to characterise growth during photoautotrophic, mixotrophic and heterotrophic conditions. This allowed viable organic

carbon substrates, light intensities and pH conditions to be identified and transferred for large scale cultivation undertaken in the forthcoming research Chapters 5 & 6.

The strain *Galdieria* sp. RTK37.1 used in this research was previously isolated from soils in Rotokawa geothermal fields (Taupō, New Zealand) in 2016 and had not previously been placed taxonomically. Additionally, due to continuous subculturing occurring over several years, an unknown bacterial contaminate was present as a coculture alongside *Galdieria* sp. RTK37.1. As a result, the strain of *Galdieria* sp. RTK37.1 was isolated, characterised and classified. Isolating the strain ensured that any bacterial contamination within culture samples did not interfere with the overall growth performance of *Galdieria* sp. RTK37.1. This is particularly important during mixotrophic and heterotrophic growth, as bacterial carbohydrate uptake rates, particularly glucose specific uptake, is higher than microalgae[118].

4.2 Experimental Methods and Materials

Cultures were grown according to Section 3.16. All cultures were grown in V4 medium, as described in Appendix C. During these experiments, *Galdieria* sp. RTK37.1 was cultivation in both solid (petri dishes) and liquid medium (laboratory flasks and airlift bioreactors). Isolation of *Galdieria* sp. RTK37.1 was done through dilution to extinction experiments, with the successful generation of an axenic culture confirmed by the absence of bacterial colonies on Phytagel solid medium plates (Appendix D) and observation under a microscope (Primostar star, Zeiss, Germany) at 1000x magnification. Batch experiments in photoautotrophic, mixotrophic and heterotrophic growth conditions were completed using 160 mL serum bottles, containing 50 mL of V4 mineral medium salts. Organic carbon substrates such as glucose, galactose, sorbitol, succinate and acetate, were investigated, at a concentration of 10 mM. Growth pH optimisation experiments were completed in 250 mL shake flasks, containing 100 mL of V4 medium. All experiments were performed as biological triplicates unless stated otherwise. All statistical analysis (two-tailed unpaired t-test) was completed in GraphPad Prism (version 9.3.1).

4.3 Results and Discussion

4.3.1 Isolation, Characterisation and Classification of *Galdieria* sp. RTK37.1

Taxonomic characterisation had not been completed on *Galdieria* sp. RTK37.1 and therefore was undertaken to confirm closely related species within the order Cyandiales. Characterisation was completed through genomic sequencing using primers outlined in Section 3.5. The primers used were Cdm (F & R), rbcL (1F & 1R) and psaA (130 F & 130 R) resulting in sequence data for target gene *18s rRNA*, *rbcL* and *psaA*. The retrieved *Galdieria* sp. RTK37.1 sequence was compared with other published sequences via GenBank BLAST (NCBI, USA) to determine the most closely related species or strains. Details outlining the species, strain, pair identity and accession numbers are provided in Appendix L. Gene sequences are provided in Appendix J (*Galdieria* sp. RTK37.1) and Appendix K (Bacterial contaminate).

The target gene *rbcL* of *Galdieria* sp. RTK37.1 most closely relates to the New Zealand Type IV *Galdieria sp.* strains isolated and characterised by Toplin *et al*[119]. Specifically, strains isolated from the Taupō and Waiotopu regions of New Zealand (#EF675175, 100% sequence identity)[119]. Figure 14 outlines the characterisation placement of *Galdieria* sp. RTK37.1 among other closely related *Galdieria sp.* and Cyandiales species. *Rhodella violacea* was used as the outgroup.

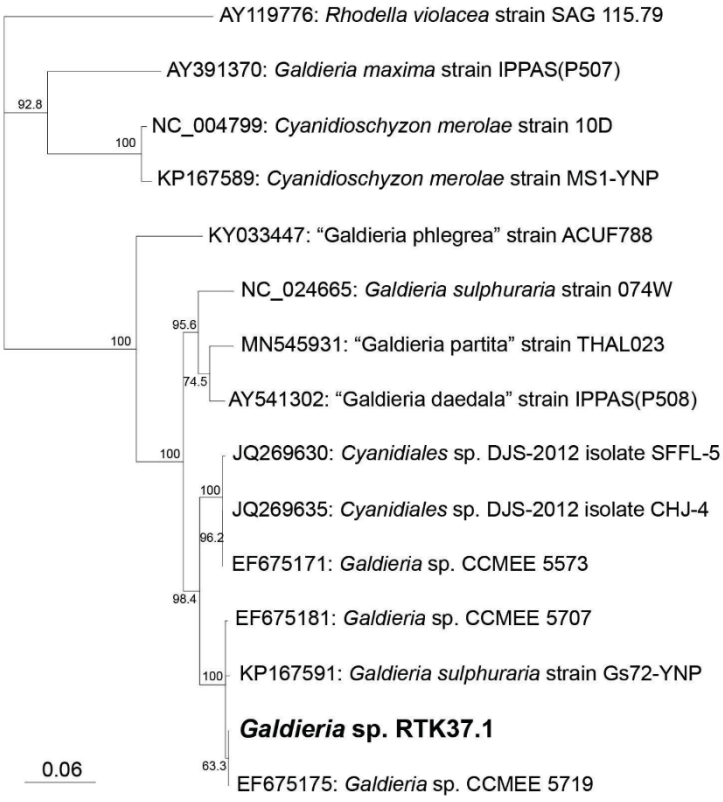

Figure 14: Neighbour-joining phylogram based on the *rbcL* gene sequence of *Galdieria* sp. RTK37.1 and representatives of order Cyandiales. The tree was nonstructured via a Jukes-Cantor Model. Bootstrap values for nodes calculated via 1,000 resampling; where no bootstrap value is provided values < 0.5. Scale bar represents 0.06 substitutions per nucleotide position. *Rhodella violacea* AY119776 was used as the Outgroup.

The *18s rRNA* gene sequence of *Galdieria* sp. RTK37.1 closely relates to other *G. sulphuraria*, specifically strains from Yellow Stone National Park, USA, as shown in Figure 15 (#KP167587, 97.47% sequence identity). *Rhodella violacea* was used as the outgroup.

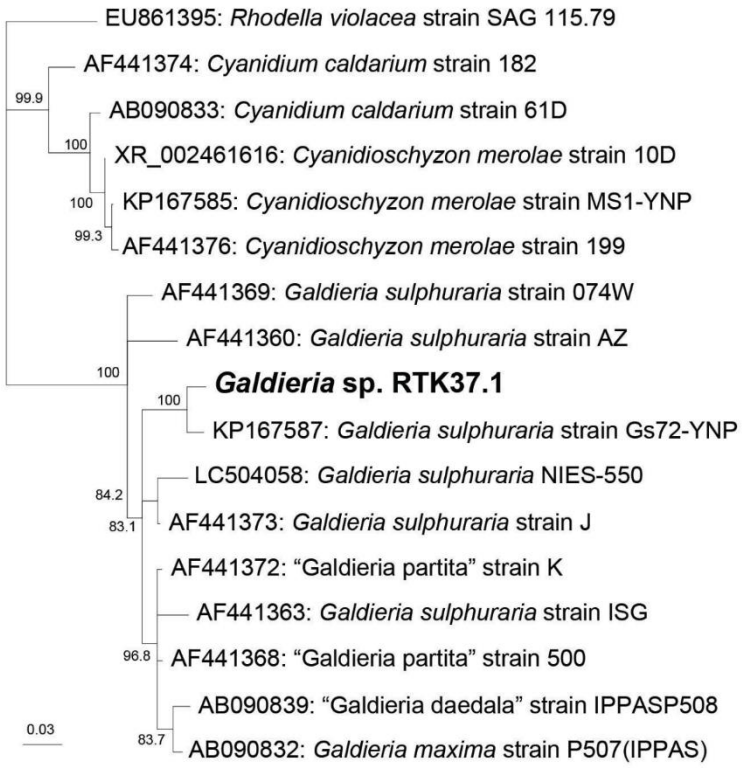

Figure 15: Neighbour-joining phylogram based on the *18s rRNA* gene sequence of *Galdieria* sp. RTK37.1 and representatives of order Cyandiales. The tree was nonstructured via a Jukes-Cantor Model. Bootstrap values for nodes calculated via 1,000 resampling; where no bootstrap value is provided values < 0.5. Scale bar represents 0.03 substitutions per nucleotide position. *Rhodella violacea* EU861395 was used as the Outgroup.

The *psaA* gene sequence of *Galdieria* sp. RTK37.1 closely relates to other *G. sulphuraria* strains, specifically from Sonoma County, California, USA, as shown in Figure 16 (MN518834, 93.33% sequence identity). *Rhodella violacea* was used as the outgroup. It appears that *Galdieria* sp. RTK37.1 appears to be forming its own monophyletic grouping, likely representing a novel lineage.

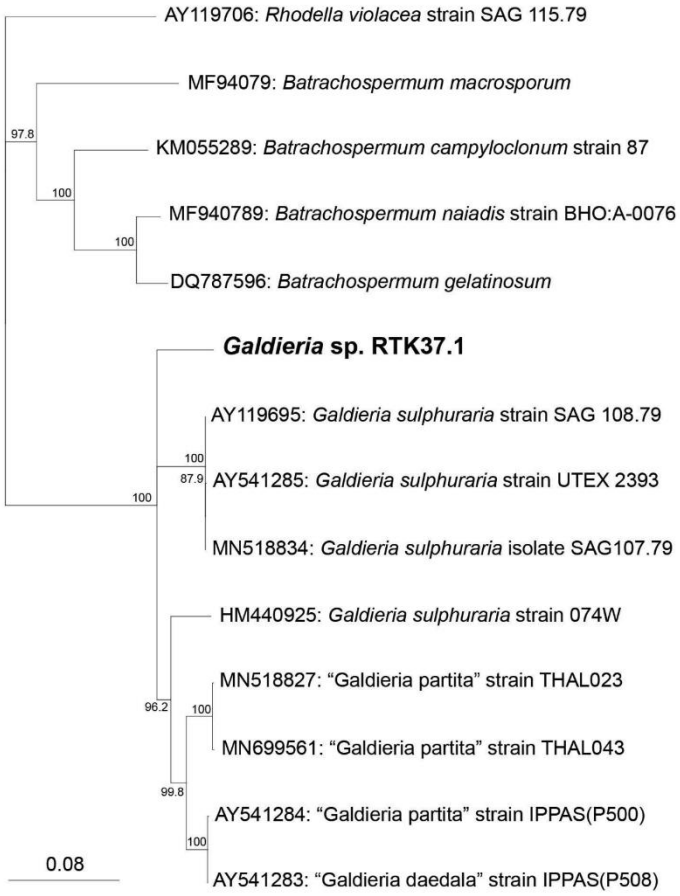

Figure 16: Neighbour-joining phylogram based on the *psaA* gene sequence of *Galdieria* sp. RTK37.1 and representatives of order Cyandiales. The tree was nonstructured via a Jukes-Cantor Model. Bootstrap values for nodes calculated via 1,000 resampling; where no bootstrap value is provided values < 0.5. Scale bar represents 0.08 substitutions per nucleotide position. *Rhodella violacea* AY119706 was used as the Outgroup.

Molecular characterisation and taxonomic classification confirm that *Galdieria* sp. RTK37.1 is most closely related to *Galdieria sulphuraria*, within the genus *Galdieria*.

Identification of the Bacterial Contaminate

As a bacterial contamination was persistent in cultures of *Galdieria* sp. RTK37.1, genomic extractions of the bacterial contaminate were completed to identify the species of bacteria successfully growing in co-culture with *Galdieria* sp. RTK37.1. Through comparative analysis of the *16s rRNA* gene sequence, the bacterial contaminate was determined most likely to be within the *Alicyclobacillus* genus, most closely related to *Alicyclobacillus tengchongensis* (99.50% sequence identity) as outlined in Figure 17. The microscope image of an axenic culture of *Alicyclobacillus* sp. EB1 isolated from cultures of *Galdieria* sp. RTK37.1 is shown in Figure 18.

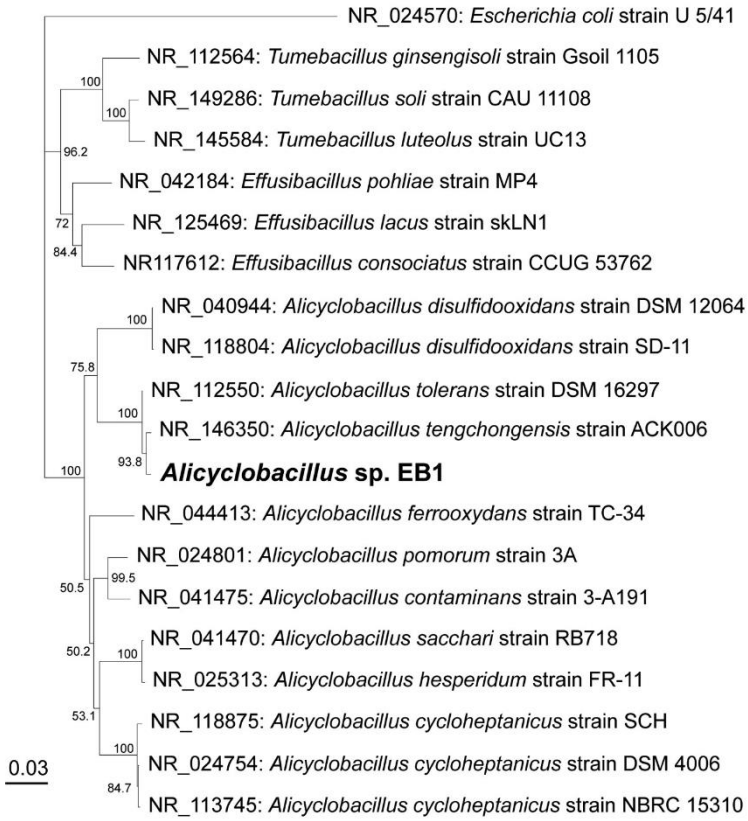

Figure 17: Neighbour-joining phylogram based on the *16s rRNA* gene sequence of *Alicyclobacillus* sp. EB1 and representatives of genus *Alicyclobacillus*, *Tumebacillus* and *Effusibacillus*. The tree was nonstructured via a Jukes-Cantor Model. Bootstrap values for nodes calculated via 1,000 resampling; where no bootstrap value is provided values < 0.5. Scale bar represents 0.03 substitutions per nucleotide position. *E.coli* NR024570 was used as the Outgroup.

Alicyclobacillus tengchongensis is a Gram-positive, aerobic, acidophilic, endospore-forming thermotolerant rod-shaped bacterial species[120]. *Alicyclobacillus tengchongensis* has very similar optimal growth conditions to *Galdieria* sp. RTK37.1, highlighting the ability of the bacterial species to thrive when grown in the same conditions as *Galdieria* sp. RTK37.1[120,121]. The growth temperature range for *Alicyclobacillus tengchongensis* is 30-50°C, with the optimal temperature for growth at 45°C[120,121]. *Alicyclobacillus tengchongensis* can grow in pH conditions ranging from 2 - 6, with the optimal pH for growth at pH 3.2[120,121]. *Alicyclobacillus tengchongensis* is a heterotroph, commonly cultivated on glucose[120]. As the V4 liquid medium does not contain substrates that support heterotrophic growth of non-phototrophic microorganisms, it is likely that *Alicylcobacillus* sp. EB1 grow via the use of metabolic byproducts excreted or released from *Galdieria* sp. RTK37.1[120].

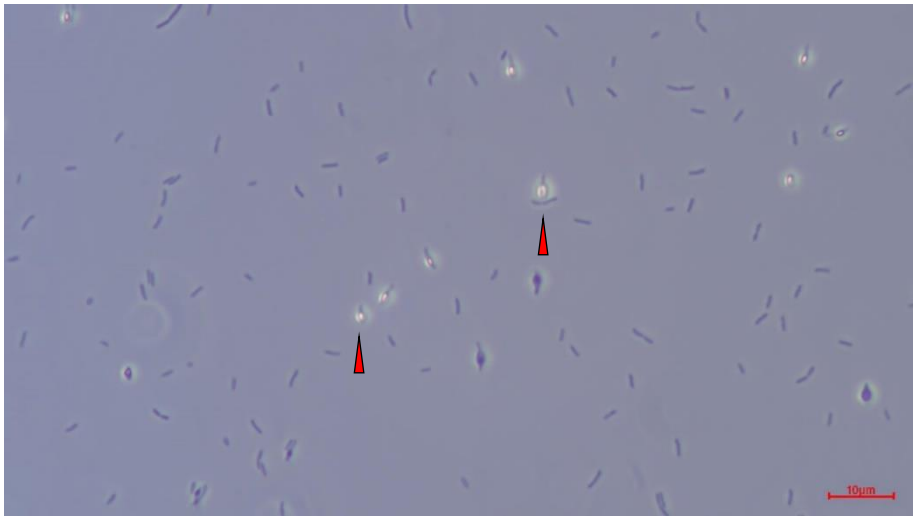

Figure 18: Microscope image of axenic cultures of *Alicyclobacillus* sp. EB1, isolated from cultures of *Galdieria* sp. RTK37.1 at 1000x objective. *Alicyclobacillus* sp. EB1was grown on 15 g/L phytagel plates, at pH 2.5, 45°C. Red triangles indicate vegetative *Alicyclobacillus* sp. EB1 cells with endospores. Scale bar is 10 µm.

4.3.2 *Galdieria* sp. RTK37.1 growth rate and biomass yield differ in different trophic growth conditions

Galdieria sp. RTK37.1 was grown photoautotrophically, mixotrophically and heterotrophically to investigate the maximum growth rate and biomass yields achieved during batch growth. The growth curve for *Galdieria* sp. RTK37.1 grown in these various trophic conditions is shown in Figure 19. Biomass yields and maximum growth rates (μ_{max}) during the different trophic growth conditions are summarised in Table 5.

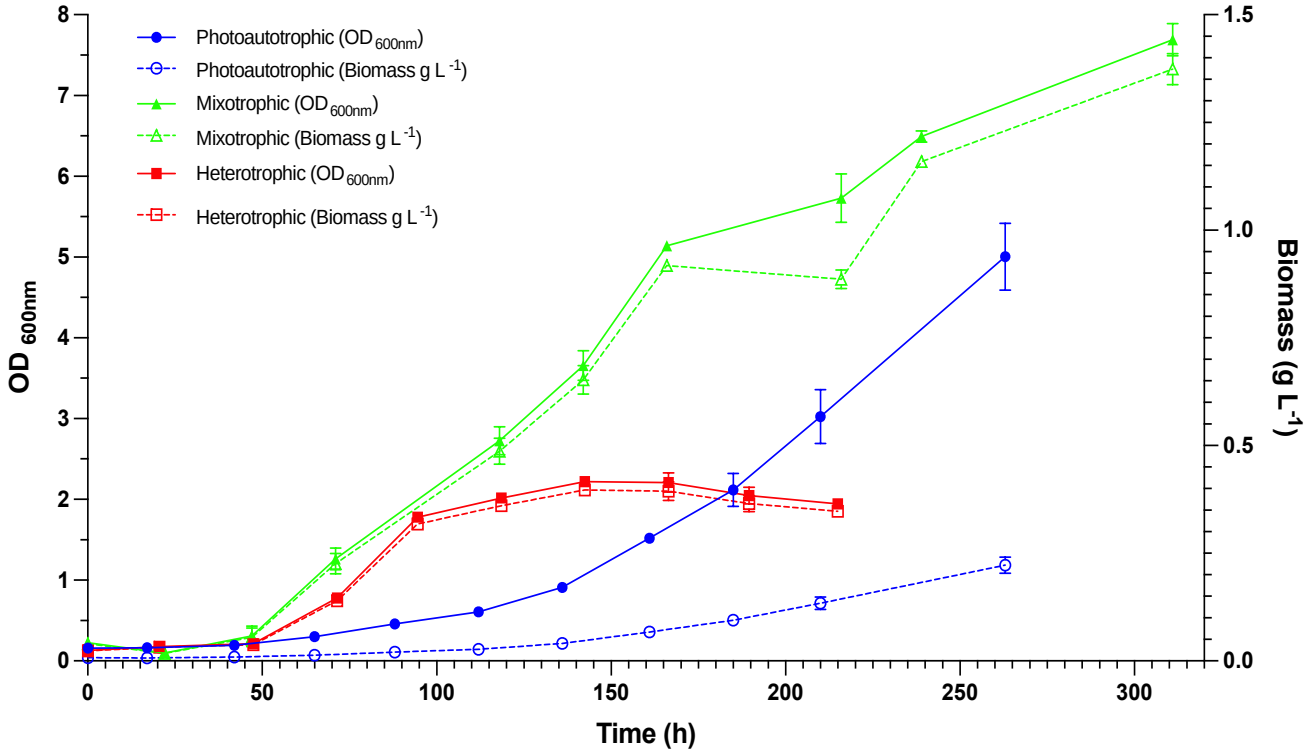

Figure 19: Growth curve outlining the optical density and biomass concentration of *Galdieria* sp. RTK37.1 grown in photoautotrophic, mixotrophic and heterotrophic growth conditions. *Galdieria* sp. RTK37.1 cells were grown at a pH 2.5, 45°C in 160 mL serum bottle supplied with 50 mL of V4 media. During photoautotrophic and mixotrophic growth conditions, cells were provided with 3% (v/v) CO_2, under 170 µmol m^{-2} s^{-1} warm white LED lighting. During heterotrophic and mixotrophic, 10 mM glucose was used as organic carbon substrates. Error bars denote standard deviation.

After 216 hours of growth, mixotrophic *Galdieria* sp. RTK37.1 had the greatest biomass concentration (as determined by dry cell weights, DCW) at 0.9 (± 0.02) g L^{-1}compared with heterotrophic and photoautotrophic grown cells which had biomass concentration of 0.4 (± 0.007) g L^{-1} and 0.2 (± 0.01) g L^{-1} respectively (*t-test: p-value: < 0.0025*). This is a significant 75% increase in biomass concentration during mixotrophic conditions compared with heterotrophic cells (*t-test: p-value < 0.04*) and a 130% increase from photoautotrophic grown cells (*t-test: p-value: < 0.0025*). These results align with results from previously known literature, which stated that after 216 hours, mixotrophic grown *G. sulphuraria* cells obtained biomass yields 42% greater than heterotrophically grown cells, and 100% greater than photoautotrophic grown cells. However during this study, 25 mM glucose was used as the carbon substrate, and cells were under 30 µmol m^{-2} s^{-1} illumination where required[54].

During mixotrophic and heterotrophic growth, the optical density of the cell culture followed the same graphical pattern as the biomass yields obtained. This was not observed during photoautotrophic growth conditions, as the biomass yields do not increase at the same rate as the optical density measurement observed during mixotrophic and heterotrophic growth (Figure 19). This is likely due to the high presence of pigmentation associated with photoautotrophic growth in photosynthetic organisms[82]. During photoautotrophic growth, cells require specific pigments to absorb the light energy required for photosynthesis[82]. These pigments are required in lesser concentrations during mixotrophic and heterotrophic growth conditions therefore it is likely the cells downregulate them, although as seen in Figure 20 pigmentation is still visible suggesting that pigments are constitutively expressed[82]. The occurrence of variable pigmentation can result in spectrophotometric inaccuracies when determining optical density.

The cell pigmentation of *Galdieria* sp. RTK37.1 grown photoautotrophically, mixotrophically and heterotrophically is shown in Figure 20. Photoautotrophic *Galdieria* sp. RTK37.1 exhibits a darker green pigmentation than mixotrophic and heterotrophic *Galdieria* sp. RTK37.1, suggesting that during photoautotrophy the cell has an increased concentration of pigments. The presence of these pigments likely impacts spectrophotometric measurements, corresponding to a higher optical density during photoautotrophy.

A

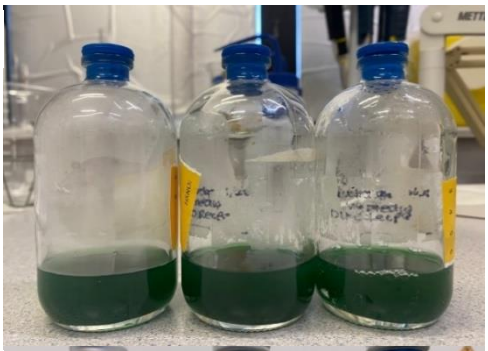

B

C

Figure 20: Cell pigmentation of *Galdieria* sp. RTK37.1 grown photoautotrophically (A), mixotrophically (B) and heterotrophically (C). *Galdieria* sp. RTK37.1 cells were grown at a pH 2.5, 45°C in 160 mL serum bottle supplied with 50 mL of V4 medium. During photoautotrophic and mixotrophic growth conditions, cells were provided with 3% (v/v) CO_2, under 170 µmol m^{-2} s^{-1} warm white LED lighting. During heterotrophic and mixotrophic, 10 mM glucose was used as organic carbon substrates.

Figure 20. A is cell pigmentation for photoautotrophically grown *Galdieria* sp. RTK37.1.

Figure 20. B is cell pigmentation for mixotrophically grown *Galdieria* sp. RTK37.1.

Figure 20. C is cell pigmentation for heterotrophically grown *Galdieria* sp. RTK37.1.

Table 5: Tabulated data of maximum growth rate, biomass production, consumption rates and biomass yields for *Galdieria* sp. RTK37.1 grown photoautotrophically, mixotrophically and heterotrophically. *Galdieria* sp. RTK37.1 cells were grown at a pH 2.5, 45°C in 160 mL serum bottle supplied with 50 mL of V4 medium. During photoautotrophic and mixotrophic growth conditions, cells were provided with 3% (v/v) CO_2, under 170 µmol m^{-2} s^{-1} warm white LED lighting. During heterotrophic and mixotrophic growth, galactose and glucose were used as organic carbon substrates (10mM). Uncertainty error denotes standard deviation.

Growth Condition	Substrate	Maximum Growth Rate	Rate of Biomass Production	Rate of Carbohydrate Consumption	Rate of Carbohydrate Consumption per Biomass Weight	Biomass Yield per mole of Carbohydrate
		μ_{max}	r_b	r_s	r_s	$Y_{b/s}$
		(h^{-1})	($mg_{biomass}$ L^{-1} h^{-1})	($mol_{carbohydrate}$ L^{-1} h^{-1})	($mmol_{carbohydrate}$ $mg_{biomass}^{-1}h^{-1}$)	($mg_{biomass}$ $mol_{carbohydrate}^{-1}$)
Photoautotrophic	3% w/w CO_2	0.011 ± 0.004	2.45 ± 2	ND	ND	ND
Mixotrophic	10 mM glucose 3% w/w CO_2	0.030 ± 0.001	64.1 ± 4	131 ± 36	33.9 ± 5	0.265 ± 0.04
	10 mM galactose 3% w/w CO_2	0.031 ± 0.002	74.6 ± 6	139 ± 65	31.6 ± 4	0.254 ± 0.03
Heterotrophic	10 mM glucose	0.045 ± 0.002	12.7 ± 4	86.7 ± 20	21.5 ± 8	0.105 ± 0.07
	10 mM galactose	0.044 ± 0.002	15.3 ± 5	75.5 ± 19	15.7 ± 6	0.122 ± 0.08

ND: Substrate consumption and biomass yields per substrate were not able to be determined for photoautotrophic growth conditions due to the limitation in measuring CO_2 consumption and light capture of the cells.

The fastest exponential growth rate was achieved by heterotrophic *Galdieria* sp. RTK37.1, growing at rates 4 times faster than photoautotrophic and 1.5 times faster than mixotrophic grown cells (Table 5). These observed maximum growth rates concurred with previous reported heterotrophic growth rates of *G. sulphuraria*, which stated that during heterotrophic growth *G. sulphuraria* growth rates were 85% faster than photoautotrophic cells[55,67]. Heterotrophically grown cells appeared to reach the stationary phase of growth after 100 hours (further discussed in Section 4.3.3), due to the complete consumption of glucose (Lower detection limit, LDL < 0.75 mM). However, during mixotrophy *Galdieria* sp. RTK37.1 did not reach the stationary phase after 100 hours but continued to grow at rates and biomass

yields greater than those observed during photoautotrophy. Additionally, there was a 2.5 times increase in biomass yield per mole of glucose compared with heterotrophically grown *Galdieria* sp. RTK37.1 (*t-test: p-value: < 0.0015*). This is evidence in the ability for *Galdieria* sp. RTK37.1 to combine the mechanisms of photoautotrophy and heterotrophy to achieve faster growth rates and greater biomass yields during mixotrophic growth conditions.

Although this data outlines some important conclusions surrounding the biomass yields during different trophic conditions, it is important to consider that heterotrophic cells were likely limited during batch growth (i.e. as was not continuously supplied glucose). Whereas, photoautotrophic and mixotrophic cells were continuously sparged with CO_2 and under constant LED illumination. As a result, heterotrophic grown *Galdieria* sp. RTK37.1 were cultivated in a batch system while photoautotrophic and mixotrophic grown *Galdieria* sp. RTK37.1 was cultivated in a static liquid continuous gas system. As CO_2 was continuously supplied into the closed system there would have been a discrepancy between the amount of growth substrates available in each trophic condition. This is made clear in the results as heterotrophically grown *Galdieria* sp. RTK37.1 reached a stationary phase after 100 hours, while photoautotrophic cells continued to grow linearly. Due to this, is it not justifiable to make conclusions based on the final biomass concentrations between the trophic conditions tested, unless the substrates were provided in equal molarity (i.e. CO_2 should have been provided as headspace gas instead of continuously sparged). This would have resulted in equivalence between the trophic conditions, allowing for a more conclusive comparison.

4.3.3 The metabolism rate of carbon substrates depends on the trophic conditions.

Prior research has reported that *Galdieria* spp. are capable of heterotrophic growth on glucose, galactose, sorbitol and succinate[39,54], although in this experiment it was confirmed that *Galdieria* sp. RTK37.1 could only grow on glucose and galactose. Growth curves for batch cultivated *Galdieria* sp. RTK37.1 grown mixotrophically and heterotrophically is shown in Figure 21, in comparison to the carbohydrate consumption rate profiles for each specific substrate. Glucose and galactose were both used to determine whether there was a significant difference between the growth rates and final biomass yields of the cells grown in the presence of these different substrates. It was concluded that the effect glucose and galactose had on the growth rate and biomass yields of the cells were not significantly different (*t-test: p-value > 0.5*). Consequently, either substrate would be suitable for continuous cultivation during these growth conditions. Optical density measurements and substrate consumption curves for the additional carbon substrates investigated (sorbitol, succinate and acetate), in which there was no observed growth of *Galdieria* sp. RTK37.1 are provided in Appendix I.

During heterotrophic growth of *Galdieria* sp. RTK37.1, glucose and galactose were exhausted after 100 hours of growth (LDL < 0.75 mM). However, in mixotrophic growth conditions, glucose and galactose were exhausted after only 70 hours of growth, as were below the detectable limit. As summarised in Table 5, the biomass normalised rate of carbohydrate consumption in mixotrophic growth was 36% faster for glucose and 50% faster for galactose compared with heterotrophically grown cells. This is interesting as it has previously been suggested that during mixotrophic growth conditions, algal cells such as *Chlorella zofingiensis*, downregulate the activity of the TCA cycle compared with heterotrophic cells[70,122]. These results suggest that due to the increased carbohydrate consumption rate observed during mixotrophic conditions, *Galdieria* sp. RTK37.1 may not downregulate the activity of the TCA cycle. Although further investigation into the mixotrophic regulation of *Galdieria* sp. RTK37.1 through transcriptome analysis would be required to confirm this.

The onset of stationary phase growth coincided with the exhaustion of glucose and galactose during heterotrophic growth. Whereas, during mixotrophic growth when the presence of glucose or galactose was undetectable, the biomass concentration continued to increase at a linear rate. Continued growth is assumed to be due to the continuous supply of CO_2 and light, indicating the cells' ability to utilise aerobic respiration and photosynthesis to obtain maximum biomass yields.

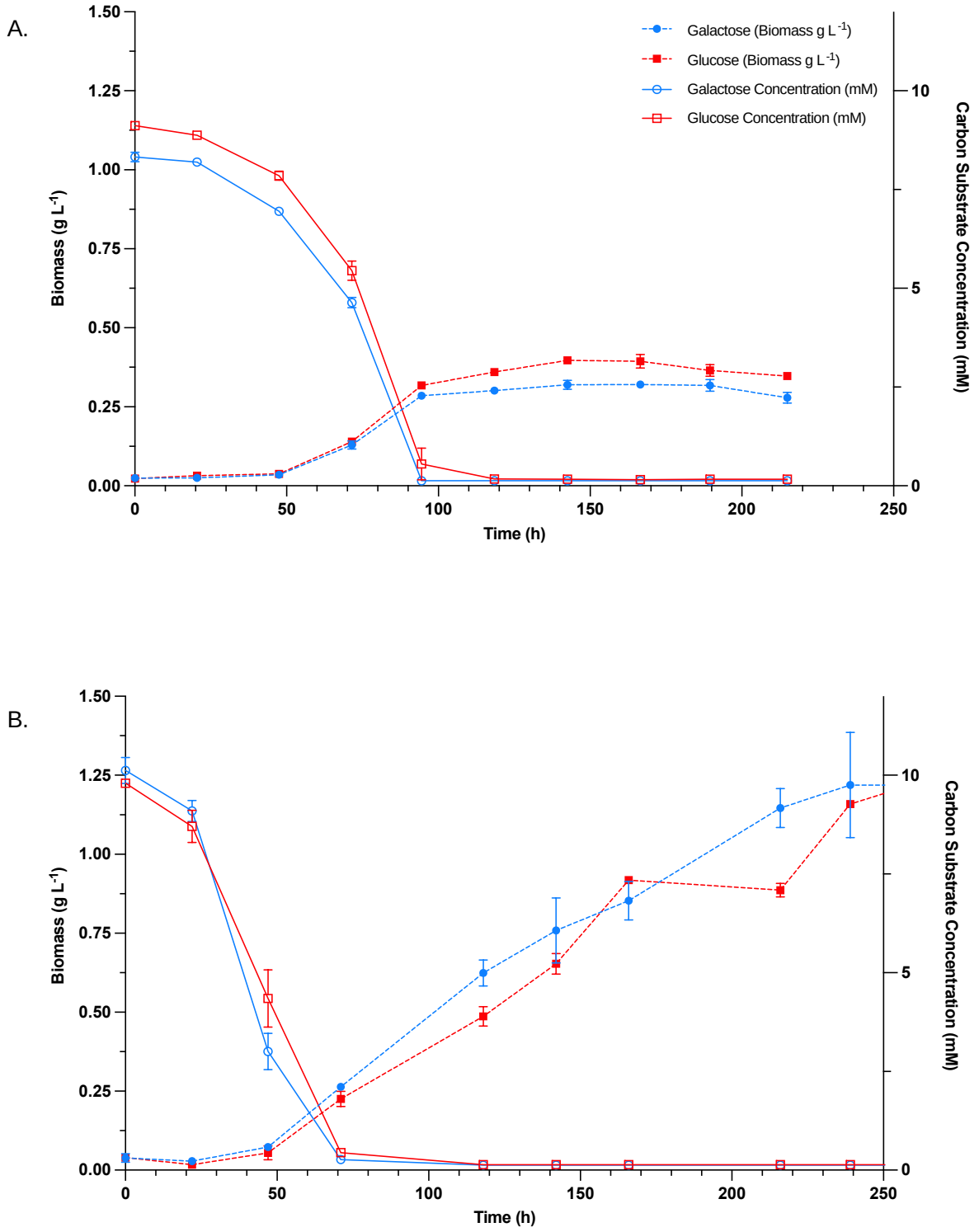

Figure 21: Growth curve outlining the biomass yield of *Galdieria* sp. RTK37.1 and substrate concentration in heterotrophic (A) and mixotrophic (B) growth condition. *Galdieria* sp. RTK37.1 cells were grown at a pH 2.5, 45°C in 160 mL serum bottle supplied with 50 mL of V4 medium. 10mM of either glucose and galactose were provided as the organic carbon substrates. During mixotrophic growth conditions, cells were provided with 3% (v/v) CO_2, under 170 µmol m^{-2} s^{-1} warm white LED lighting. Error bars denote standard deviation.

Figure 21. A is the growth curve for heterotrophic growth conditions of *Galdieria* sp. RTK37.1.

Figure 21. B is the growth curve for mixotrophic growth conditions of *Galdieria* sp. RTK37.1.

4.3.4 pH conditions impact the growth rate of *Galdieria* sp. RTK37.1

Galdieria sp. RTK37.1 was grown in different pH conditions to conclude the optimal pH for the maximum growth rate of *Galdieria* sp. RTK37.1, as shown in Figure 22. *Galdieria* sp. RTK37.1 grow successfully in all pH conditions tested (pH 0.5 – 5). These results agree with previous research which reported that *Galdieria* spp. can grow photoautotrophically in pH conditions ranging from 0.5 – 7[4].

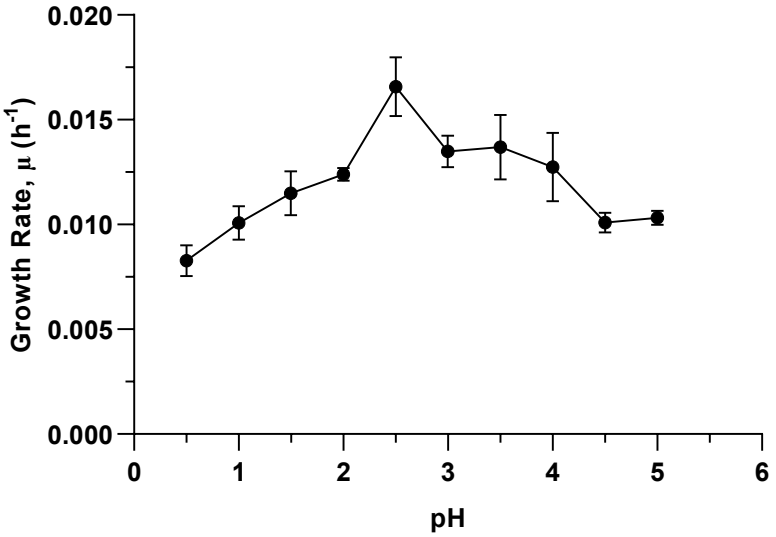

Figure 22: Exponential growth rates of *Galdieria* sp. RTK37.1 grown photoautotrophically in various pH conditions. *Galdieria* sp. RTK37.1 cells were grown at 45°C in 250 mL shake flasks supplied with 100 mL of V4 media. Cells were provided with 3% (v/v) CO_2, under 170 µmol m^{-2} s^{-1} warm white LED lighting. Error uncertainties denote standard deviation.

In literature, the optimal pH conditions for *Galdieria* spp. is defined between a pH 0.5 - 3[1,4]. The growth rate and therefore doubling rate remain relatively constant between these varying pH conditions[1,4]. This data, however, suggests a clear optimal pH condition which results in the highest observed growth rate for *Galdieria* sp. RTK37.1 at pH 2.5. As shown in Figure 22 above, as the pH increases the growth rate increases until pH 2.5, where the fastest growth rate was observed corresponding to a doubling time of 40 hours. As the pH continues to increase following pH 2.5, the growth rate slows down again. It is worth noting that it is possible that the highest growth rate of *Galdieria* sp. RTK37.1 was observed at pH 2.5 due to the cell adapting over several years of cultivation at this specific pH.

4.4 Conclusions

To determine and identify the taxonomic position of *Galdieria* sp. RTK37.1, sequencing of the *rbcL*, *psaA* and *18s rRNA* gene were performed. Genomic sequencing confirmed that *Galdieria* sp. RTK37.1 closely relates to other strains of *G. sulphuraria*, within the genus *Galdieria.* Genomic sequencing of the *16s rRNA* gene confirmed that the bacterial contaminate, *Alicyclobacillus* sp. EB1, belongs to the genus *Alicyclobacillus*, most closely relating to *Alicyclobacillus tengchongenesis* (99.50% sequence identity).

From batch experiments, it was concluded that *Galdieria* sp. RTK37.1 can utilise glucose and galactose during heterotrophic and mixotrophic growth, but could not utilise succinate, sorbitol and acetate as mentioned in previous literature[39,54]. This is likely due to *Galdieria* sp. RTK37.1 adapting to different conditions results in the cell losing the ability to metabolise these substrates. Mixotrophic *Galdieria* sp. RTK37.1 displayed the greatest biomass yield, while heterotrophic *Galdieria* sp. RTK37.1 had the fastest growth rate. The ability for *Galdieria* sp. RTK37.1 to grow mixotrophically was implied by the continued linear growth after no carbon substrate (glucose or galactose) was detected within the system. Whereas, in heterotrophic growth, when the available carbon substrate was exhausted this resulted in the onset of stationary growth. During the various photoautotrophic pH experiments, it was observed that *Galdieria* sp. RTK37.1 grown at a pH of 2.5 achieved the fastest growth rate.

This investigation into the batch growth performance has characterised the growth of *Galdieria* sp. RTK37.1 photoautotrophically, mixotrophically and heterotrophically. Viable carbon substrate and optimal pH conditions for this strain were identified and were utilised to successfully grow *Galdieria* sp. RTK37.1 in a continuous cultivation system in the forthcoming research Chapters 5 & 6. Additionally, growth rate data provided an estimate for dilution rates to achieve desired steady states and avoid 'wash out' during continuous cultivation. It is concluded that glucose was to be used during mixotrophic and heterotrophic cultivation of *Galdieria* sp. RTK37.1. Although galactose and glucose had a similar effect on the growth and biomass production of the cell, glucose is a more reasonable economic choice as is readily available in the industry and a cheaper substrate option[123]. All following *Galdieria* sp. RTK37.1 was cultivated at a pH 2.5.

5 Chapter 5: Continuous Cultivation of *Galdieria* sp. RTK37.1 in a Chemostat

5.1 Introduction and Aim

A chemostat (Figure 23) is a laboratory apparatus that allows continuous cultivation to be achieved in microalgae species[124]. The apparatus consists of a vessel enclosing liquid media to support the growth of the desired species under investigation, with a sterile liquid feed inlet (*F*) and an effluent outflow[124]. The volume, *V,* of medium remains constant throughout the operation allowing for steady state conditions to be achieved. Mixing of the system can be supplied by an impeller or gas sparging[124]. Continuous culture techniques allow submaximal growth rates to be achieved in microorganism cultivation under defined, nutrient-limited conditions[95]. This allows the culture conditions to remain virtually constant, achieving steady state[95].

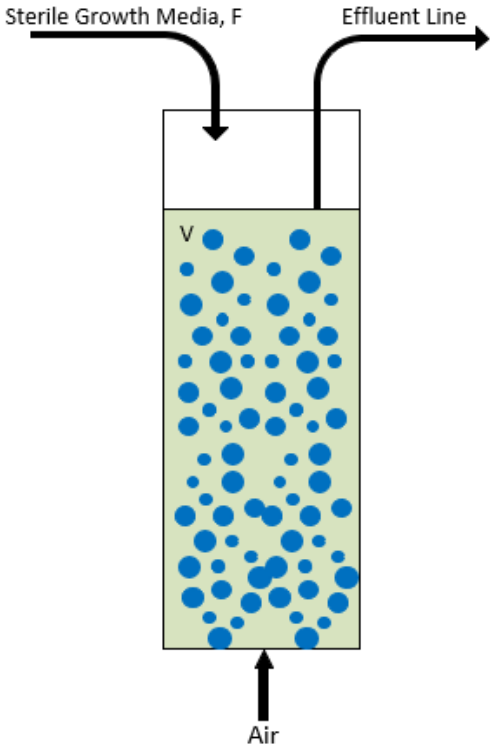

Figure 23: Basic chemostat configuration.

Previous research conducted by Graverholt and Eriksen (2007), concluded that *Galdieria* spp. are highly suited for high cell density cultivations but highlighted the lacking research surrounding achieving stable growth in continuous cultivation[90]. Following on from this, this research involved continuous cultivation of *Galdieria* sp. RTK37.1 to investigate growth in different trophic conditions, including photoautotrophy, mixotrophy and heterotrophy. Initially the suitability of *Galdieria* sp. RTK37.1 to achieve steady state during continuous cultivation was explored. The effect various trophic conditions and growth-limiting factors has on the microalgae species was investigated. This provided additional process information surrounding the optimal growth conditions for the successful cultivation of *Galdieria* sp. RTK37.1 to assist in large scale production.

The specific hypothesises investigated in this chapter were:

1. *Galdieria* sp. RTK37.1 is a true mixotroph.
2. Stable continuous cultivation of *Galdieria* sp. RTK37.1 is achievable during photoautotrophic, mixotrophic and heterotrophic growth conditions.

5.2 Chemostat Theory

For a chemostat to be considered ideal, homogenous mixing must be achieved by effective aeration or stirrers[124]. This allows the assumption that all contents within the reactor have uniform composition[124]. Therefore, there is no variability in biomass concentration within the reactor. Due to this assumption, the concentration of the effluent stream is equal to the concentration within the reactor vessel, defined as C[124]. Additionally, the concentration of dissolved oxygen and CO_2 is the same throughout the bulk liquid phase, which is critical for photoautotrophic and mixotrophic growth of algae species as inorganic carbon is a growth substrate[124].

During steady state conditions within a chemostat reactor, it is assumed that the rate of cell addition (through the feed stream) and the rate of cell production is equal to the rate of cell removal from the system[124]. For the chemostat specifically used during this research, the liquid feed was sterile of biomass, resulting in the viable cell concentration in the feed stream being zero, $C_O = 0$. Therefore, the rate of production, r_x, (Equation 6) is solely based on cell formation per unit time within the reactor, which is based on the number of viable cells and the specific growth rate at that unit time[124].

$$r_x = \mu C \tag{6}$$

Equation 6: Rate of productivity, where μ is defined as the specific growth rate, t is defined as time.

The specific growth rate is defined in Equation 7:

$$\mu = \frac{(\ln C - \ln C_0)}{t - t_0} \tag{7}$$

Equation 7: Specific growth rate, where C is defined as the biomass concentration, t is defined as time.

The dilution rate, *D*, is equal to the liquid vessel volumes (*V*) which will pass through the vessel per unit time (Equation 8)[124]. This is the reciprocal of the hydraulic retention time, which denotes the holding time of viable cells within the system[124].

$$D = \frac{F}{V} \tag{8}$$

Equation 8: Dilution rate, where *F* is defined as the flow rate, *V* is reactor volume**.**

For a chemostat system where the culture is in a state of exponential growth and the specific growth rate is independent of the cell concentration, *C*, and substrate concentration, *s*, the steady state growth can be defined by the material balance in Equation 9. In the case where the inlet feed is sterile, then the dilution rate is equal to the specific growth rate[124]. It is assumed that the rate of cell death is negligible compared to cell growth:

$$Materials\ in - Materials\ out + Generated - \ Consumed = Accumulation$$

Therefore, the steady state mass balance for biomass:

$$F(C_0 - C) + Vr_x = 0 \tag{9}$$

$$DC_0 = (D - \mu)C \tag{9}$$

Equation 9: Steady state mass balance

This model mentioned above does not describe what is observed during continuous cultivation when there is a growth-limiting substrate, typically a nutrient. The concentration of the growth-limiting substrate is related to the specific growth rate of the species using Monod's equation (Equation 10)[125].

$$\mu = \frac{\mu_{max} S}{s + K_S} \tag{10}$$

Equation 10: Monod's Equation[125]. μ_{max} is the maximum achievable growth rate observed when the concentration of the growth-limiting substrate is significantly larger than Monod coefficient[125], K_s.

K_s is the concentration of the growth-limiting nutrient where the specific growth rate is at half the maximum value, as defined below[125].

$$K_S \; is \; the \; saturation \; constant, [s] at \frac{1}{2}\mu_{max}$$

When considering Monod's equation, the steady state material balance for the system is then defined as (Equation 11):

$$\left(\frac{\mu_{max} S}{s + K_S} - D\right) C + DC_0 = 0 \tag{11}$$

Equation 11: Steady state material balance using Monod's Equation[125].

The yield factor can then be defined as (Equation 12):

$$Y = \frac{g_{biomass \; formed}}{g_{biomass \; consumed}} \tag{12}$$

Equation 12: Yield Factor.

$$D(C_0 - C) - \frac{\mu_{max} sC}{Y(s + K_s)} = 0$$

When the feed stream is sterile, the material balance can be simplified as described below (Equation 13):

$$C_{sterile \; feed} = Y\left(C_0 - \frac{DK_s}{\mu_{max} - D}\right) \tag{13}$$

$$s_{sterile \; feed} = \frac{DK_S}{\mu_{max} - D} \tag{13}$$

Equation 13: Steady state material balance when feed stream is sterile.

5.2.1 Light Limitation in Chemostats

During photoautotrophic and mixotrophic growth conditions light limitation is an important factor to consider. Light limitation differs from nutrient based limitations within a chemostat, as photons cannot be homogeneously mixed. In chemostats, light is often supplied externally, resulting in a photon flux that decays exponentially towards the centre of the reactor. This results in the theory of light-limited growth differing significantly from substrate limited growth. This concept is further discussed in Chapter 6.

5.2.2 Optimal Operation of Chemostats

Achieving steady state growth of a microalgae species in a chemostat depends on the dilution rate and therefore the flow rate, as stated by Equation 8.

When a system is operating with a very slow flow rate, the dilution rate exceeds zero resulting in the growth-limiting substrate tending to zero causing cell growth to be limited. The effluent cell concentration is then dependent on the inlet substrate concentration and the yield factor.

As the dilution rate increases in the system (i.e. with increasing flow rate) the cell concentration decreases linearly and then rapidly begins to diminish as the dilution rate tends towards the maximum growth rate of the cells[124]. At the point where the dilution rate equals the maximum growth rate, the cell concentration tends to zero[124,126]. This is due to the dilution rate surpassing the maximum growth of the cells, resulting in the only achievable steady state condition being when the cell concentration equals zero[124,126]. This is called wash out[124,126]. When a system is operated near wash it, it is very sensitive to changes in the dilution rate[124,126]. The critical dilution rate, where the steady state biomass concentration becomes zero due to wash out, can be estimated by Equation 14 below:

$$D_{crit} = \frac{\mu_{max} s_0}{K_S + s_0} \tag{14}$$

Equation 14: Critical Dilution Rate. Where μ_{max} is the maximum achievable growth rate observed when the concentration of the growth-limiting substrate is significantly larger than Monod's coefficient[125], K_s. K_s is Monod's coefficient, at [s] at ½ μ_{max}, s is defined as the growth-limiting substrate.

For most cell cultures $K_s << s_0$ therefore $D_{crit} \approx \mu_{max}$. Therefore, to avoid wash out the operating dilution rate must always be less than the critical dilution rate (and therefore the maximum growth rate)[124,126]. To optimise a chemostat reactor the system needs to be operated

in conditions where the initial concentration of the growth limiting substrate are significantly greater than the saturation constant[124,126]. This will result in the dilution rate being close to the maximum growth rate, but slow enough to ensure that wash out will not occur[124,126]. This will result in the greatest achievable biomass production while maintaining steady state conditions[124,126]. The optimal dilution rate of a chemostat, which results in the highest biomass production, is defined in Equation 15. Although, operating the chemostat at the optimal dilution rate is often not practical due to the optimal dilution rate being near the critical dilution rate which results in small variations of the reactor causing large fluctuations in cell concentration[126].

$$D_{opt} = \mu_{max}\left(1 - \sqrt{\frac{K_s}{K_s + s_i}}\right) \tag{15}$$

Equation 15: Optimal Dilution Rate. Where μ_{max} is the maximum achievable growth rate observed when the concentration of the growth limiting substrate is significantly larger than Monod's coefficient[125], K_s. K_s is Monod's coefficient, at [s] at ½ μ_{max}, s is defined as the growth limiting substrate.

5.2.3 Issues in Chemostats

The most common issues during chemostat operation are caused by slow circulating regions resulting in highly dense regions of biomass. This invalidates the assumption of perfect mixing[124,126]. The presence of high density regions within the reactor leads to cell interchange between the bulk liquid volume and unmixed regions[124,126]. This acts as an unsterile feed stream into the reactor[124,126]. This additional feed stream results in a faster obtainable dilution rate, as these high density regions will take longer to dilute out of the reactor[124,126]. This allows wash out to be is avoided, but results in an oscillating effect observed in cell growth[124,126]. A similar effect is observed when cell cultures adhere to the reactor wall as a biofilm, resulting in the cells diluting from the system at a slower rate[124,126]. Biomass adhering to the reactor wall can be defined as a chemostat with immobilised cells[124,126]. The concentration of suspended cells (C_s) and immobilised cells (C_{im}) must be considered in the model discussed in Section 2[124,126].

The effect flocculation has on chemostats is an important aspect to consider during operation, particularly if a bacterial contaminate is present within cell cultures[124,127,128]. Research has shown that bacterial contamination increases the formation of flocs in algae species and increases cell wall adhersion[127,128]. One study found that the flocculation activity of *Chlorella vulgaris* increased by 98% compared to axenic cultures[128]. As a result of bacterial

contamination, unsteady growth within chemostats can cause oscillating growth patterns and higher wash out rates[124,127,128].

5.3 Experimental Methods and Materials

Cultures were grown according to Section 3.17. All cultures were grown in V4 medium, as described in Appendix C. During this research chapter, *Galdieria* sp. RTK37.1 was cultivated in batch airlift reactors until a desired optical density has been achieved (OD_{600nm} ~3), and then the reactors will be switched to chemostat operation (D = 0.12 d^{-1}). During mixotrophic and heterotrophic growth conditions, 10 mM glucose was used as the carbon substrate. This was concluded to be the best substrate option from research conducted in Chapter 4. Unless stated otherwise, all experiments were completed as technical replicates. All statistical analysis (two-tailed unpaired t-test) was completed in GraphPad Prism (version 9.3.1).

5.4 Results and Discussion

5.4.1 *Galdieria sp. RTK37.1* achieved different steady states during different trophic growth conditions.

Stable growth of *Galdieria* sp. RTK37.1 in photoautotrophic, mixotrophic and heterotrophic growth conditions was possible during continuous cultivation. The growth curve for continuously cultivated *Galdieria* sp. RTK37.1 during these trophic conditions is shown in Figure 24. Growth was monitored using biomass concentration, optical density and cell count measurements due to the variability in pigment production, glycogen storage and cell size observed during growth in the different trophic conditions.

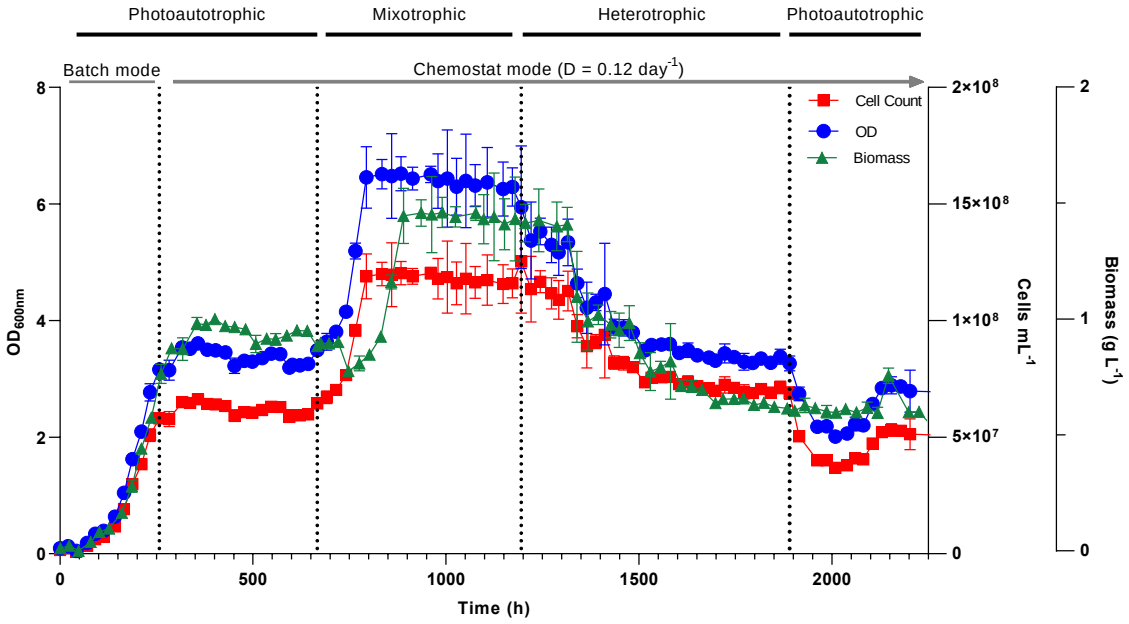

Figure 24: Growth curve outlining the optical density, cell count and biomass concentration for *Galdieria* sp. RTK37.1 grown in photoautotrophic, mixotrophic and heterotrophic growth conditions in continuous cultivation. *Galdieria* sp. RTK37.1 cells were grown at pH 2.5, 45°C in a 1.5 L chemostat reactor, at a dilution rate of 0.12 d^{-1}. During photoautotrophic and mixotrophic growth conditions, cells were provided with 3% (v/v) CO_2 under 94.6 µmol m^{-2} s^{-1} warm white LED lighting. During heterotrophic and mixotrophic growth conditions, 10 mM glucose was used as the organic carbon substrate. Error bars denote standard deviation.

Although, the steady state optical density for photoautotrophic and heterotrophic grown *Galdieria* sp. RTK37.1 are equal, this was not deemed an accurate measurement for cell growth. As discussed previously (Section 4.3.2), the occurrence of variable pigmentation can result in spectrophotometric inaccuracies when determining optical density[82]. Relative pigment production is dependent on the trophic condition *Galdieria* sp. RTK37.1 is grown in, as observed in Figure 25. During photoautotrophy (A: Reactor 1), *Galdieria* sp. RTK37.1 emitted a greater relative fluorescence amount of pigments, resulting in a darker green culture. While, during heterotrophy, the pigment fluorescence emitted was decreased and cultures were a lighter shade of green (B: Reactor 2). Pigment production is further discussed in Section 5.4.3.

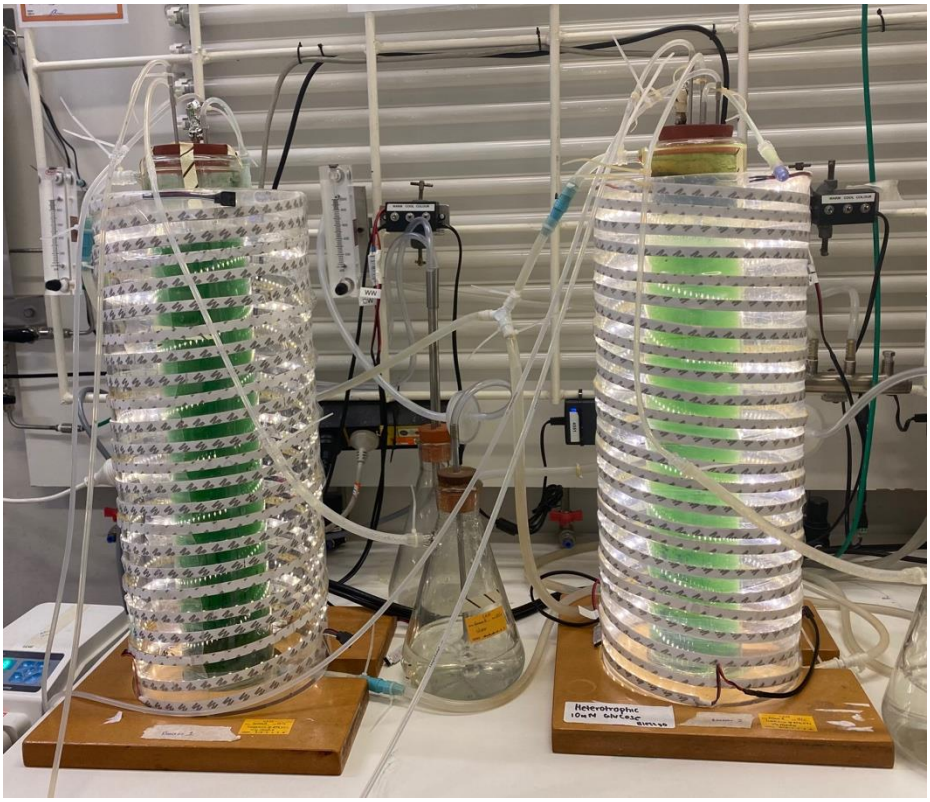

Figure 25: Cell pigmentation of *Galdieria* sp. RTK37.1 grown in photoautotrophic (A: Reactor 1) and heterotrophic (B: Reactor 2) growth conditions in continuous cultivation. *Galdieria* sp. RTK37.1 cells were grown at pH 2.5, 45°C in a 1.5 L chemostat reactor, at a dilution rate of 0.12 d^{-1}. During photoautotrophic growth conditions, cells were provided with 3% (v/v) CO_2 under 94.6 µmol m^{-2} s^{-1} warm white LED lighting. During heterotrophic growth conditions, 10 mM glucose was used as the organic carbon substrate and the reactor was covered in aluminium foil to exclude light.

Figure 25. A cell pigmentation for photoautotrophically grown *Galdieria* sp. RTK37.1.

Figure 25. B cell pigmentation for heterotrophically grown *Galdieria* sp. RTK37.1.

ND: These images were taken after the completion of heterotrophic growth conditions; all aluminium foil had been removed.

Biomass concentrations (as determined by DCW) for photoautotrophic *Galdieria* sp. RTK37.1 were 0.93 (± 0.01) g L^{-1}, this concentration significantly increased by 34% to 1.43 (± 0.02) g L^{-1} when cells were grown in mixotrophic conditions (t-*test: p-value < 0.0001*), and then decreased by 56% to 0.63 (± 0.02) g L^{-1} in heterotrophic growth conditions (*t-test: p-value < 0.0001*), as summarised in Table 6. Obtaining greater biomass concentrations during photoautotrophy compared with heterotrophy was not observed during batch experiments and has not been reported in previous known literature. This inconsistency between biomass concentrations is likely due to the differing growth limiting factors during continuous and batch cultivation. As discussed in Chapter 4, heterotrophically grown *Galdieria* sp. RTK37.1 was cultivated as a batch system while photoautotrophic and mixotrophic grown *Galdieria* sp. RTK37.1 were cultivated as static liquid continuous systems, continuously sparged CO_2 and under constant LED illumination. In continuous cultivation, there is a constant inflow of growth substrates and removal of effluent. As a result of this, it is not valid to compare batch cultivated biomass concentrations with continuously cultivated biomass concentrations.

As this research represents the first chemostat cultivation of any *Galdieria* spp. during different trophic conditions, it is unclear whether obtaining greater biomass concentrations in photoautotrophy compared with heterotrophy is typical during continuous cultivation. In heterotrophic growth, glucose was continuously supplied into the reactor at a set concentration of 10 mM. During cultivation, no glucose was detected in the reactor (LDL < 0.75 mM), therefore it was assumed that glucose had been fully metabolized and was limited, resulting in steady state growth. In contrast, during photoautotrophic growth, the cells were continuously sparged with CO_2 and under constant LED illumination. It was assumed that CO_2 was provided in excess, and that light was the limiting nutrient (provided light at 96.4 μmol m^{-2} s^{-1}). Light is a difficult substrate to quantify due to the presence of the photon flux and mutual shading, therefore the discrepancy between the amount of growth substrate provided during each trophic condition is unclear. As heterotrophic growth resulted in a lower biomass concentration, the ratio between glucose and light likely differed, and light was most likely provided in a greater relative amount during photoautotrophy than the equivalent amount of energy available per unit concentration of glucose was during heterotrophy.

Table 6: Tabulated data of steady state cell counts, rate of biomass production and biomass yield for *Galdieria* sp. RTK37.1 growth in photoautotrophic, mixotrophic and heterotrophic growth conditions during continuous cultivation. *Galdieria* sp. RTK37.1 cells were grown at pH 2.5, 45°C in a 1.5 L chemostat reactor. During photoautotrophic and mixotrophic growth conditions, cells were provided with 3% (v/v) CO_2 under 94.6 µmol m^{-2} s^{-1} warm white LED lighting. During heterotrophic and mixotrophic growth conditions, 10 mM glucose was used as the organic carbon substrate. Uncertainty errors denote standard deviation.

Growth Condition	**Carbon Substrate**	**Dilution Rate**	**Cell Count**	**Biomass Dry Cell Weight**	**Rate of Biomass Production**	**Biomass Yield per Ammonia concentration**	**Crude Protein Yield per Ammonia concentration**	**Biomass Yield per gram of Glucose**
		D		**C_b**	**r_b**	**$Y_{b/a}$**	**$Y_{p/a}$**	**$Y_{b/g}$**
		(d^{-1})	(Cells mL^{-1})	(g L^{-1})	(mg L^{-1} h^{-1})	($g_{biomass}$ $g_{ammonia}^{-1}$)	($\%_{protein}$ $g_{ammonia}$)	($g_{biomass}$ $g_{glucose}^{-1}$)
Photoautotrophic	3% w/w CO_2	0.12	6.08E+07	0.93 ± 0.01	46.5 ± 12	2.58 ± 0.4	1.55	ND
Mixotrophic	10 mM Glucose 3% w/w CO_2	0.12	1.17E+08	1.43 ± 0.12	79.9 ± 11	3.71 ± 0.7	1.77	7.94 ± 0.7
Heterotrophic	10 mM Glucose	0.12	6.98E+07	0.63 ± 0.02	36.3 ± 8	11.8 ± 2	6.61	3.5 ± 0.1

ND: Substrate consumption and biomass yields per substrate were not determined for photoautotrophic growth conditions due to the limitation in measuring CO_2 consumption and light capture of the cells.

Although heterotrophic *Galdieria* sp. RTK37.1 cells had lesser biomass concentration (as determined by CDW), it achieved the highest yield per mass of ammonia. During heterotrophic growth, 87% of the initial ammonia remained (Figure 26), a significantly higher concentration compared with photoautotrophic grown *Galdieria* sp. RTK37.1 cells, where only 7% of the initial ammonia remained (*t-test: p-value* < $2E^{-9}$). In contrast, mixotrophic *Galdieria* sp. RTK37.1 cells fully exhaust all ammonia (LDL < 0.01 g L^{-1}). Ammonia was likely a growth limiting factor during mixotrophic growth. The consumption of ammonia is discussed in more detail in Section 5.4.2.

The increased biomass yields and cell count during mixotrophic growth highlights the ability for *Galdieria* sp. RTK37.1 to adjust and regulate intracellular components to metabolism the addition of glucose for additional cell growth. This outlines the growth versatility of *Galdieria* sp. RTK37.1 and its ability to successfully grow in natural

environments when access to light and dissolved CO_2 is often limited[54]. These results indicate that mixotrophic growth is favoured to obtain high concentrations of biomass production, a potential benefit for biotechnological applications requiring high density cultures.

Following steady state heterotrophic growth, the reactor was switched back to photoautotrophic growth to determine if the same initial photoautotrophic steady state could be achieved. After removing glucose from the inlet feed bottles, and exposing the cells to warm white LED lighting (94.6 μmol m^{-2} s^{-1}) there was an immediate decrease in cell growth. This is likely due to the cells having to upregulate photosynthetic pigments and intracellular pathways to perform photosynthesis again. After ~ 230 hours of photoautotrophic conditions, *Galdieria* sp. RTK37.1 reached a similar steady state to that observed previously.

The dilution rate (0.12 d^{-1}) was chosen based on the maximum growth rate observed during the initial batch operation. To ensure 'wash out' did not occur, the dilution rate chosen was approximately half the maximum growth rate (50% μ_{max}). Using a slower (than optimal) dilution rate, and axenic culture of *Galdieria* sp. RTK37.1 was due to the consequence of a previous chemostat experiment (Appendix P). During this initial trial experiment, which used *Galdieria* sp. RTK37.1 contaminated with *Alicyclobacillus* sp. EB1, significant floc formations on the side of the reactor were observed (image not presented). This was likely a result of bacterial contamination increasing the flocculation activity of the algae cells[124,127,128]. Another likely reason for the increased flocculation activity was due to the dilution rate (0.3 d^{-1}) operating near the maximum growth rate of *Galdieria* sp. RTK37.1 ($\mu_{max,batch}$ ~ 0.3 d^{-1}). As the system was operating near 'wash out', this likely increased the flocculation activity to ensure cells remained within the reactor. The presence of immobilised cells on the side of the reactor would have acted as non-sterile feed, limiting the cells from washing out of the reactor. This explains why wash out was not observed, but an oscillating effect as the cells were slowly diluted out while the reactor was refed from the floc formations on the reactor wall.

5.4.2 *Galdieria* sp. RTK37.1 consume different amounts of ammonium depending on the growth condition

To investigate growth-limiting factors during continuous cultivation of *Galdieria* sp. RTK37.1, the inlet and effluent reactor concentrations of ammonium were monitored during steady state photoautotrophic, mixotrophic and heterotrophic conditions, as shown in Figure 26.

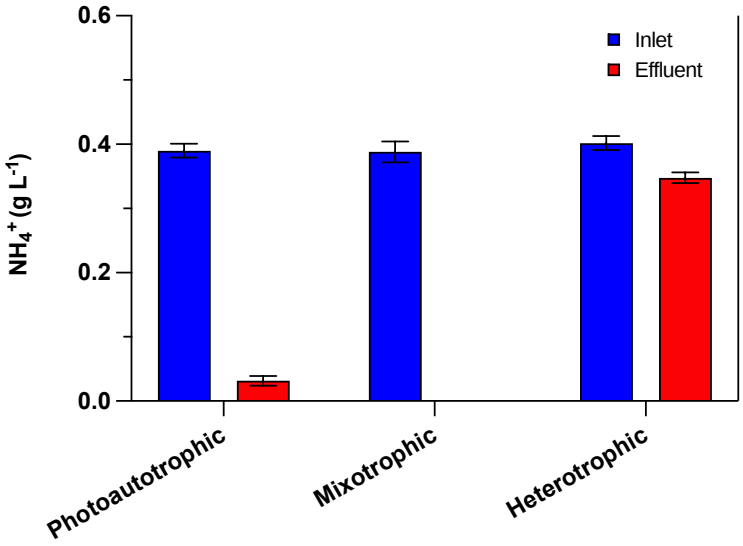

Figure 26: Inlet and effluent ammonium concentration measured during steady state growth of *Galdieria* sp. RTK37.1 grown in photoautotrophic, mixotrophic and heterotrophic growth conditions during continuous cultivation. *Galdieria* sp. RTK37.1 cells were grown at pH 2.5, 45°C in a 1.5 L chemostat reactor, at a dilution rate of 0.12 d^{-1}. During photoautotrophic and mixotrophic growth conditions, cells were provided with 3% (v/v) CO_2 under 94.6 µmol m^{-2} s^{-1} warm white LED lighting. During heterotrophic and mixotrophic growth conditions, 10 mM glucose was used as the organic carbon substrate. Error bars denote standard deviation.

During mixotrophic growth, *Galdieria* sp. RTK37.1 was assumed to be limited in ammonia, as no ammonium was detected in the bulk liquid of the reactor (LDL < 0.01 g L^{-1}). Interestingly, during steady state heterotrophic growth, *Galdieria* sp. RTK37.1 only consumed 12.5% of ammonium from the medium (*t-test: p-value* < $2E^{-9}$) and therefore ammonia was not a growth-limiting substrate, resulting in a higher biomass yield per mass of ammonia. It appears that during heterotrophic growth conditions, *Galdieria* sp. RTK37.1 required significantly less ammonia for cell growth which has not been discussed in previous known literature. It is unclear why *Galdieria* sp. RTK37.1 consumed significantly less ammonia when grown heterotrophically. One hypothesis explaining this phenomenon is that as internal concentrations of ammonia rise it can become toxic to the photosynthetic reactions within the

chloroplast[129]. Therefore, it is required that ammonia assimilation occurs rapidly within the cell, a process carried out by the enzyme glutamine synthetase through the GS-GOGOAT (glutamine synthase and glutamine oxoglutarate aminotransferase) pathway[129]. This leads to ammonia assimilation being reported as a photosynthetic process[129]. As photosynthetic reactions are not required during heterotrophic growth there is a lesser requirement for ammonia to be assimilated other than for cell growth. Although ultimately this is only a hypothesis.

Yields calculations adjusted to crude protein percentage per ammonia consumption (Table 6) suggest that heterotrophic *Galdieria* sp. RTK37.1 are more efficiently able to assimilate ammonia into protein. Referring back to the maximum growth rates of *Galdieria* sp. RTK37.1 in batch cultivation (Table 5), the fastest growth rate observed was during heterotrophy. This suggests an ideal ratio between carbon and ammonia, allowing the cell to prioritise cell replication over energy storage. While, during light utilising growth (photoautotrophy and mixotrophy), additional energy requirements for photosynthesis and carbon fixation compared with aerobic respiration promotes the production and storage of glycogen and other carbohydrates. This results in slower growth rates (Table 5), and less crude protein yield per percentage of ammonia consumed (Table 6).

Questions remain unanswered surrounding ammonia metabolism and therefore further experiments would need to be completed to fully understand why significantly less ammonia is metabolised by heterotrophically grown *Galdieria* sp. RTK37.1 (*t-test: p-value* $< 2E^{-9}$). This experiment should be repeated to ensure reproducibility of this result along with batch experiments to identify whether these results are continuous cultivation specific. Additionally, transcriptome analysis should be completed to identify metabolic differences during each trophic condition.

As ammonia was either fully exhausted or remained in very low concentrations during light utilising growth (mixotrophic and photoautotrophic), it suggests *Galdieria* sp. RTK37.1 as a feasible option in ammonium removal for biotechnological applications[130]. Particularly in landfill leachate, where ammonium is a more challenging contaminant to remove due to its excessive concentration and high biotoxicity[130].

5.4.3 Relative pigment production is dependent on the trophic condition of *Galdieria* sp. RTK37.1

In order to understand the pigment production of *Galdieria* sp. RTK37.1 during different growth conditions, the fluorescence emissions of *Galdieria* sp. RTK37.1 primary absorbing pigments, chlorophyll- α (absorption peaks at 450nm and 680 nm)[5,82] and phycocyanin (absorption peak at 618 nm)[5,82], were measured. These pigments allow the cell to absorb light energy and utilise it during photosynthesis[5,82]. The absorption spectra in Figure 27 concurs with previously reported absorption spectrums for *G. sulphuraria*[5,82], outlining the increased height in absorption peaks for pigments produced during mixotrophic growth and photoautotrophic growth conditions compared with the flatter heterotrophic absorption spectra.

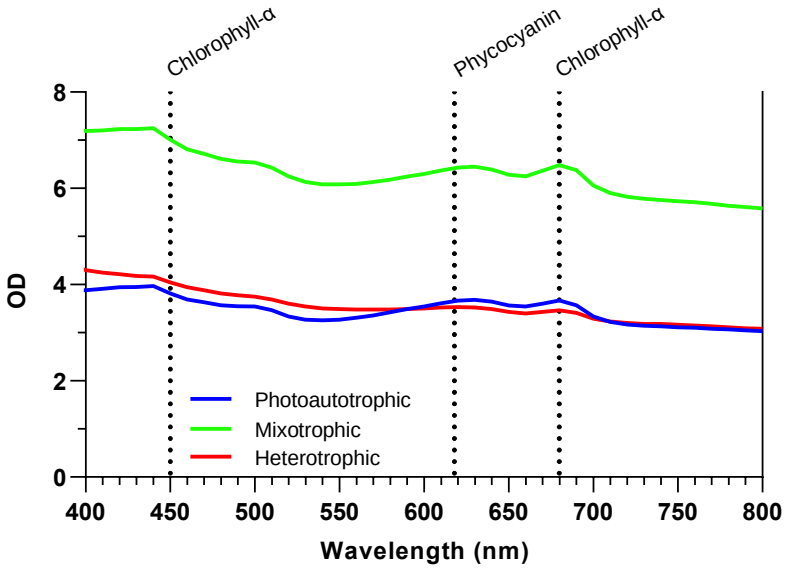

Figure 27: Absorbance spectra of steady state *Galdieria* sp. RTK37.1 grown in photoautotrophic, mixotrophic and heterotrophic growth conditions during continuous cultivation. *Galdieria* sp. RTK37.1 cells were grown at pH 2.5, 45°C in a 1.5 L chemostat reactor, at a dilution rate of 0.12 d^{-1}. During photoautotrophic and mixotrophic growth conditions, cells were provided with 3% (v/v) CO_2 under 94.6 µmol m^{-2} s^{-1} warm white LED lighting. During heterotrophic and mixotrophic growth conditions, 10 mM glucose was used as the organic carbon substrate. Absorption peaks at 450 nm and 680 nm corresponds to the chlorophyll- α pigment, while the absorption peak at 618 nm corresponds to the phycocyanin pigment[5,82].

The relative fluorescence intensity of pigments, phycocyanin and chlorophyll-α, produced by *Galdieria* sp. RTK37.1 is shown in Figure 28. Phycocyanin and chlorophyll-α produced during mixotrophic growth was 35% (*t-test: p-value* < *0.01*) and 26% (*t-test: p-value* < *0.007*) greater respectively than pigments produced during photoautotrophic conditions. While during heterotrophy, the fluorescence intensity of phycocyanin and

chlorophyll-α produced was significantly less. During mixotrophy, phycocyanin and chlorophyll-α were 72% (*t-test: p-value < 0.0002*) and 73% (*t-test: p-value* < $6E^{-5}$) greater respectively. The decrease in pigment expression during heterotrophic growth suggest that the cells downregulate light absorbing pigments as photosynthesis is not performed by the cells.

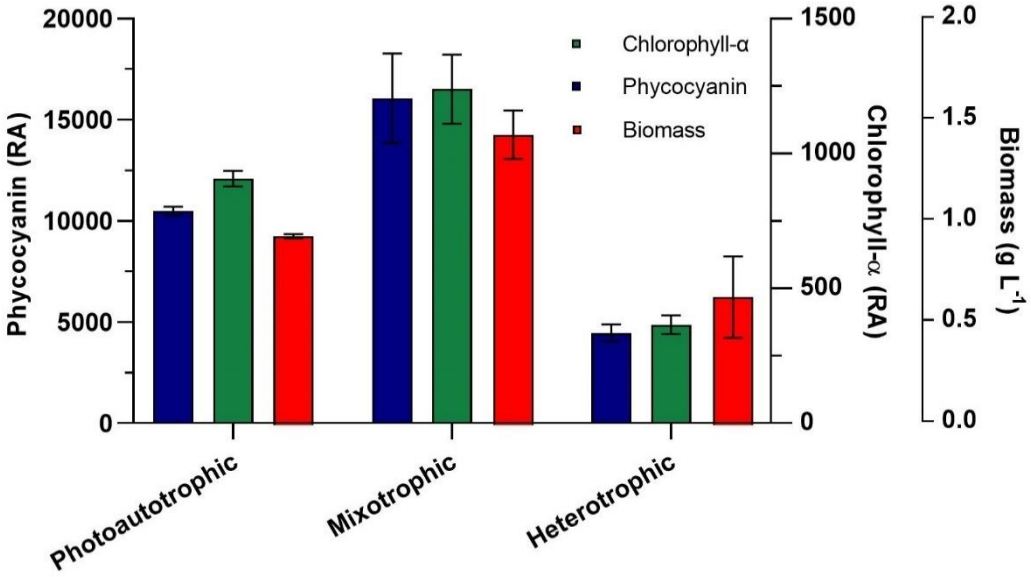

Figure 28: The relative fluorescence intensity of pigments phycocyanin and chlorophyll-α produced by *Galdieria* sp. RTK37.1 during photoautotrophic, mixotrophic and heterotrophic growth, against biomass concentration. *Galdieria* sp. RTK37.1 cells were grown at pH 2.5, 45°C in a 1.5 L chemostat reactor, at a dilution rate of 0.12 d^{-1}. During photoautotrophic and mixotrophic growth conditions, cells were provided with 3% (v/v) CO_2 under 94.6 µmol m^{-2} s^{-1} warm white LED lighting. During heterotrophic and mixotrophic growth conditions, 10 mM glucose was used as the organic carbon substrate. Error bars denote standard deviation.

Despite the reduction in pigment fluorescence during heterotrophic growth, the ability for *Galdieria* sp. RTK37.1 to produce pigments, particularly phycocyanin, without light is a major industrial advantage. As mentioned previously (Section 2.5.1), phycocyanin is typically produced under photoautotrophic conditions which have expensive lighting requirements. Lighting is a major limitation for industrial phycocyanin production[90,42,91,92], and therefore the ability for *Galdieria* sp. RTK37.1 to produce this pigment without light is a concept that is becoming heavily investigated[40,42]. These results justify using heterotrophic *Galdieria* sp. RTK37.1 for large scale production of phycocyanin, as through continuous cultivation high density cultures can be maintained while continuous extracting biomass for phycocyanin or chlorophyll- α purification.

It has been reported that during ammonia starvation, cells will selectively degrade phycobiliproteins decreasing pigment production[89]. Although, in mixotrophically grown *Galdieria* sp. RTK37.1, which cells were assumed to be limited in ammonia, pigments were still produced. The fluorescence intensities during mixotrophic growth were greater than the photoautotrophic pigments, likely as a result of the increased biomass concentration from the addition of glucose. There is the possibility, that decreasing the light intensity during mixotrophic growth while maintaining the addition of an organic carbon, would result in similar pigment production to photoautotrophic growth. This would decrease lighting costs while maintaining the production output of pigments. Although, this concept would need to be validated through further experiments.

5.4.4 The nutritional composition of *Galdieria* sp. RTK37.1 differs in different trophic conditions

To understand the effect trophic condition and limiting substrates has on the nutritional composition of *Galdieria* sp. RTK37.1, nutritional analyse of *Galdieria* sp. RTK37.1 grown photoautotrophically, mixotrophically and heterotrophically was obtained (Table 7). *Galdieria* sp. RTK37.1 was grown in ammonia-limited photoautotrophic conditions to investigate the effect limiting ammonia had on the nutritional composition. Ammonia-limited photoautotrophic *Galdieria* sp. RTK37.1 achieved the same overall biomass yield as photoautotrophic cells which were not ammonia-limited, as seen in the growth curve in Appendix Q.

Table 7: Nutritional composition of *Galdieria* sp. RTK37.1 grown in photoautotrophic, mixotrophic and heterotrophic growth conditions. *Galdieria* sp. RTK37.1 was grown at pH 2.5, 45°C in a 1.5 L chemostat reactor, at a dilution rate of 0.12 d^{-1}. During photoautotrophic and mixotrophic growth conditions, cells were provided with 3% (v/v) CO_2 under 94.6 µmol m^{-2} s^{-1} warm white LED lighting. During heterotrophic and mixotrophic growth conditions, 10 mM glucose was used as the organic carbon substrate.

Sample	Moisture %	Ash %	Crude Protein %	Fat %	Carbohydrate %
Photoautotrophic (Ammonia-limited)	8.2	1.8	49	11.3	29.8
Photoautotrophic	7.1	1.5	60.4	11.3	19.5
Mixotrophic	5.1	1.7	47.8	10.3	35.1
Heterotrophic	5.1	2.2	56.2	10.6	25.8

The nutritional composition of ammonia-limited photoautotrophic *Galdieria* sp. RTK37.1 had a greater percentage of carbohydrates, and a lesser percentage of crude proteins compared to non-ammonia limited photoautotrophic cells. This is likely due to the cell repressing growth as a result of limiting conditions, leading to a reduction in crude proteins. Following this, *Galdieria spp.* have been reported to accumulate glycogen under macronutrient limiting conditions[76,131], which is likely the reason ammonia-limited photoautotrophic cells have a greater composition of carbohydrate. This explains the increased percentage of carbohydrates in mixotrophic cells, as cells were not only ammonia-limited but also assumed

to be limited in light and glucose (LDL < 0.75 mM). The percentage of carbohydrates in heterotrophic *Galdieria* sp. RTK37.1 differed from previously reported carbohydrate content which states that carbohydrate content typically does not change between photoautotrophic and heterotrophic *G.sulphuraria* cells[132]. Although, in *Galdieria maxima*, the metabolism of glucose during heterotrophy results in a 4-factor increase in carbohydrate content as a result of synthesising a storage polysaccharide which is accumulated in the cytoplasm[132,133]. There is the potential that *Galdieria* sp. RTK37.1 metabolises glucose and stores a similar polysaccharide resulting in the increased carbohydrate content, but further investigation into the carbohydrates stored by *Galdieria* sp. RTK37.1 would be required to confirm this.

Mixotrophic cells displayed the lowest percentage of crude proteins, which may indicate the cells' ability to undertake true mixotrophic growth, utilising both respiration and photosynthesis simultaneously. The decrease in crude proteins may be due to a reduction in photosynthetic protein abundance, which has been reported to occur in *Galdieria* spp. when grown mixotrophically[54], particular the protein RuBisCO activase. This may indicate that mixotrophic *Galdieria* sp. RTK37.1 are less capable of carbon fixation during mixotrophy compared with photoautotrophic *Galdieria* sp. RTK37.1. This shows that the cell is no longer exclusively utilising photosynthesis, but coordinating energy and carbon metabolism methods between photosynthesis and aerobic respiration which attributes to the higher biomass yield obtained during mixotrophy (Figure 24).

Unfortunately, although triplicates samples were collected for analysis, biomass requirements necessitated the pooling of replicates. Hence, statistical analysis was not performed to determine if the difference observed were significant. Future investigations into the nutritional compositions of *Galdieria* sp. RTK37.1 is recommended to improve the certainty of these results.

5.4.5 Net specific oxygen evolution rate is dependent on the growth condition of *Galdieria* sp. RTK37.1

To further investigate the photosynthetic potential of *Galdieria* sp. RTK37.1 grown in different trophic conditions, the net specific oxygen evolution rate was measured (Table 8). *Galdieria* sp. RTK37.1 grown in photoautotrophic growth conditions had the highest rate of photosynthesis, 66% faster than mixotrophically grown cells (*t-test: p-value < 0.0006*). Due to the low oxygen evolution rate of *Galdieria* sp. RTK37.1 cells grown heterotrophically, it was assumed no oxygen was produced, and therefore the cells did not undertake photosynthesis.

Table 8: The net specific rate of oxygen produced by *Galdieria* sp. RTK37.1 grown in photoautotrophic, mixotrophic and heterotrophic growth conditions during continuous cultivation. The net specific oxygen evolution rate for each growth condition is the rate of oxygen measured for that specific steady state minus the rate of oxygen produced by *Galdieria* sp. RTK37.1 under no illumination. *Galdieria* sp. RTK37.1 was grown at pH 2.5, 45°C in a 1.5 L chemostat reactor, at a dilution rate of 0.12 d^{-1}. During photoautotrophic and mixotrophic growth conditions, cells were provided with 3% (v/v) CO_2 under 94.6 µmol m^{-2} s^{-1} warm white LED lighting. During heterotrophic and mixotrophic growth conditions, 10 mM glucose was used as the organic carbon substrate. Uncertainty errors denote standard deviation.

Growth Condition	Substrate	Net Specific Oxygen Evolution Rate ($nmol\ O_2\ mg_{biomass}^{-1}\ h^{-1}$)
Photoautotrophic	3% w/w CO2	125 ± 20
Mixotrophic	10 mM Glucose 3% w/w CO2	42 ± 1
Heterotrophic	10 mM Glucose	< 0.01

Cells grown under heterotrophic growth conditions had very low rates of oxygen evolution, indicating that photosynthesis is repressed during heterotrophic growth. Due to the addition of glucose and the cells being in light exclusion, it is likely that heterotrophic *Galdieria* sp. RTK37.1 were respiring by consuming oxygen, instead of undergoing photosynthesis. As observed in Figure 24, the cells require ~230 hours to regulate and produce the required photosynthetic proteins to absorb and utilise light energy. During this experiment, heterotrophic *Galdieria* sp. RTK37.1 were not able to adjust to the rapid change in growth condition and therefore were not able to upregulate intracellular processes to perform photosynthesis. When comparing this result to the pigment fluorescence intensities during heterotrophic growth (Figure 28), phycocyanin (*t-test: p-value* < $2E^{-6}$) and chlorophyll-α (*t-test: p-value* < $4E^{-6}$) were significantly decreased compared with phycocyanin and chlorophyll-α emitted during photoautotrophy. This further justifies decreased net specific oxygen evolution rate during heterotrophy, as the cells lacked photosynthetic proteins required

to enable photosynthesis[40,42]. Additionally, aerobic respiration requires the consumption of oxygen, which would have contributed to the decreased oxygen concentration during heterotrophy.

Mixotrophic *Galdieria* sp. RTK37.1 have a decreased net specific oxygen evolution rate compared with photoautotrophic cells. This suggests that during mixotrophic growth photosynthesis is downregulated by the addition of glucose, a result observed in previous research[4], but photosynthesis is not fully repressed like that observed during heterotrophy. This is further evidence towards the coordination of photoautotrophic and heterotrophic metabolism during mixotrophic growth, outlining the net specific oxygen evolution rate of mixotrophic *Galdieria* sp. RTK37.1 combines the oxygen produced by photosynthesis and the oxygen consumed through aerobic respiration.

Comparing the oxygen evolution rates and the pigment fluorescence intensities expressed during mixotrophic growth (Figure 28), there is a discrepancy in the results. The highest fluorescence intensity was expressed by mixotrophically grown *Galdieria* sp. RTK37.1, although the oxygen evolution rate of these cells was less than photoautotrophically grown cells. This elevated pigment expression from mixotrophic cells is likely due to the increased biomass and does not accurately highlight an increased pigment production rate per biomass concentration.

5.5 *Galdieria* sp. RTK37.1 is a true Mixotroph

As discussed, mixotrophic growth was initially considered a combination of photoautotrophic and heterotrophic metabolism until it was determined that for cells to be considered true mixotrophs, they had to display synergistic effects between photosynthesis and respiration[6]. This often results in the maximum biomass yield exceeding the combined photoautotrophic and heterotrophic biomass yields[70,71]. Although some *Galdieria* spp. have been shown to be true mixotrophs[54], the results of this research show that the combined maximum biomass concentrations achieved during heterotrophic and photoautotrophic growth did not exceed those obtained during mixotrophic growth. But this observation alone is not enough to conclude that this strain of *Galdieria* sp. RTK37.1 is not capable of true mixotrophic growth. During photoautotrophic growth, it is likely that the only growth limiting substrate was the accessibility to light. Shading from biomass on the outer layer of the reactor would have limited the light penetration into the centre of the reactor. During heterotrophic growth, it was assumed that all glucose was exhausted as it was not detected in samples collected during steady state growth (LDL < 0.75 mM). During mixotrophic, light availability and glucose are both factors required for growth and therefore were both assumed to be limited. Additionally, ammonia was not detected in mixotrophic effluent samples while was detected during photoautotrophic and heterotrophic steady state effluent. Operating a chemostat with three growth-limiting substrates generates a complex system. It is likely that due to the number of growth-limiting factors, the overall obtainable biomass concentration was limited during mixotrophic growth compared with photoautotrophic and heterotrophic conditions which were likely only limited in one substrate.

As biomass concentrations obtained during mixotrophic growth were significantly greater than photoautotrophic (*t-test: p-value < 0.0001*) and heterotrophic biomass yields (*t-test: p-value < 0.0001*), it justifies that *Galdieria* sp. RTK37.1 is utilising both metabolism methods. Although these results alone do not prove that photosynthetic and respiratory processes are occurring simultaneously within the cell, they outline mixotrophic conditions as a good strategy to increase biomass productivity in *Galdieria* sp. RTK37.1 There is the argument that cells could be alternating between photoautotrophic and heterotrophic metabolism methods[4]. But, due to this research being performed in a chemostat it was assumed that the content within the reactor was homogenous[124]. Therefore, it is valid to assume that all cells in the reactor were undertaking the same metabolic mechanisms. If immobilised cells were present on the reactor wall, it would be justifiable to conclude that those cells were

undertaking photoautotrophic metabolism due to their close proximity to the light source. While cells located near the centre of the reactor may be undertaking heterotrophic metabolism due to light limitation from mutual shading. As immobilised cells were not present during these experiments it is justifiable to conclude that all *Galdieria* sp. RTK37.1 were undertaking the same metabolic mechanism.

The decreased net specific oxygen evolution rate measured during mixotrophy indicates a decrease in photosynthesis oxygen production and suggests oxygen consumption due to aerobic respiration (Table 8). This decreased rate is likely due to reduced photosynthetic proteins, which is justified by the decrease in mixotrophy crude proteins percentage compared with photoautotrophy (Table 7). This reduction in photosynthesis proteins abundance has been reported in mixotrophically grown *G. sulphuraria* through metabolic and proteomic studies[54], particular the protein RuBisCO activase. RuCisCO activase is an enzyme that converts RuBisCO ((ribulose bisphosphate carboxylase/oxygenase) from an inactive state to an active state[54]. During photoautotrophic growth, RuBisCO is required during carbon fixation to catalyse the carboxylation of RuBP (ribulose-1, 5-bisphosphate). The activation of RuBisCO requires ATP, which is obtained from light dependant reactions (Section 2.3.1). Although, net specific oxygen evolution rates and nutritional analysis both indicate a decrease in photosynthesis occurring within mixotrophic *Galdieria* sp. RTK37.1, the cell is still able to achieve greater biomass productivity than heterotrophic and photoautotrophic *Galdieria* sp. RTK37.1. This demonstrates the synergistic effect between photosynthesis and aerobic respiration during mixotrophy, highlighting that *Galdieria* sp. RTK37.1 is a true mixotrophic.

The intracellular mechanisms of a cell undertaking true mixotrophy, simultaneously utilising photoautotrophy and heterotrophy has not been fully clarified[70]. As a result, various researchers have proposed mixotrophic metabolism networks. Some researchers have speculated that CO_2 generated from aerobic respiration is reutilised by photosynthesis during mixotrophy, thus resulting in higher specific growth rates compared to the combination of photoautotrophic and heterotrophic growth rates[69,134,135]. Zhang *et al*. (2017) proposed another coordination between photosynthesis and aerobic respiration metabolism networks[70], which results show a clear reduction in photosynthetic reactions, concurring with observations made throughout this research. Zhang *et al*. (2017) observed downregulation of citrate synthesis during mixotrophic cultivation of *Chlorella zofingiensis* compared with heterotrophy, indicating that less organic carbon is catabolised by the TCA cycle to produce ATP in

mixotrophic conditions[70]. Although, interestingly this result was not observed during metabolic and proteomic studies undertaken by Curien *et al.* (2021), who observed a constant abundance of respiratory proteins in mixotrophic and heterotrophic *G. sulphuraria* cultures[54]. Zhang *et al*. (2017) and Curien *et al*. (2021) both reported that RuBisCO abundance was decreased during mixotrophy compared with photoautotrophy demonstrating a decrease in photosynthesis[54,70], similarly observed during mixotrophic growth of *Galdieria* sp. RTK37.1. Although evidence shows downregulation of both photosynthesis (compare with photoautotrophic cells) and the TCA cycle (compared with heterotrophic cells), mixotrophic biomass yields were greater than the sum of yields obtained during photoautotrophic and heterotrophic conditions[70]. It was then proposed that only part of the ATP and NADPH produced through photosynthesis is directed to carbon reactions, and the remaining is used for cell metabolism[70]. Glucose consumed from the culture medium is likely used for energy storage, which results in the increased biomass concentration observed during mixotrophic growth[70]. Although this is only a proposed mechanism, it provides a basis for results obtained during this research[70].

Completing transcriptome analysis would further justify *Galdieria* sp. RTK37.1 as a true mixotrophic, as would highlight the regulation of intracellular components throughout the different trophic conditions. Transcriptome analysis on different trophic growth conditions for *Galdieria* spp. has not been investigated and would provide a clearer understanding of the different metabolism methods. Additionally, investigating the citrate synthase activity of *Galdieria* sp. RTK37.1 during different trophic conditions by chemical assay kits would further justify whether the TCA cycle is downregulated during mixotrophic growth. This would allow for further justification around the metabolic networks of mixotrophic *Galdieria* sp. RTK37.1.

5.6 Conclusion

Investigations into the suitability *Galdieria* sp. RTK37.1 for continuous cultivation during different trophic growth conditions has revealed that stable growth is achievable during photoautotrophic, mixotrophic and heterotrophic growth conditions. These results highlight that *Galdieria* sp. RTK37.1 is suitable for continuous cultivation and has the potential to be upscaled for larger biotechnology applications.

Mixotrophic growth conditions resulted in the greatest biomass production, making it an ideal condition for achieving high biomass yields. Net specific oxygen evolution rates and nutritional analysis both suggested a decrease in photosynthesis occurring within mixotrophic *Galdieria* sp. RTK37.1, although the cell was still able to achieve greater biomass productivity than heterotrophic and photoautotrophic *Galdieria* sp. RTK37.1. This suggests a synergistic effect between photosynthesis and aerobic respiration during mixotrophy, highlighting that *Galdieria* sp. RTK37.1 is a true mixotroph.

6 Chapter 6: The Effect Light has on the Growth, Oxygen Evolution rate and Pigment Yield of *Galdieria* sp. RTK37.1

6.1 Introduction

Light intensity and wavelength condition are some of the most important cultivation parameters during photoautotrophic growth. Light affects both the production and composition of biomass due to the impact it has on photosynthesis[68,82].

There has been a wide range of research into the effect light has on the growth and pigment production of *Galdieria* spp., although the majority of this research was conducted during batch growth[4,5,71]. This has resulted in limited understanding surrounding the effect light intensity and spectral composition has on the growth and biomass yield of *Galdieria* spp. grown in continuous cultivation[71]. Additionally, published data outlines that the spectral composition of light for algae species is not necessarily transferable between specific strains[71]. Therefore, this research chapter aims to investigate the effect of light intensity and spectral composition has on the growth, oxygen evolution rate and pigment yields of continuously cultivated *Galdieria* sp. RTK37.1.

6.1.1 Light Intensity

Light intensity is of primary importance during photoautotrophic microalgae cultivation, as it is directly proportional to the rate of photosynthesis and biomass production[68]. As discussed in Section 2.4.4, cell concentration will increase exponentially until all photons impinging onto the surface of the culture is absorbed[136] or the saturation point is exceeded[68,82]. Operating at light intensities beyond the saturation point results in photoinhibition, where overexposure to light causes radiation damage to components within the photosynthetic apparatus resulting in decreased rates of photosynthesis and cell growth[4]. Operating at low light intensities limits cell growth and results in lower biomass yields[136].

6.1.2 Wavelength Conditions

Photosynthetically active radiation is light at wavelengths between 400 – 700 nm[137]. This is the portion of the light spectrum that is used during photosynthesis[137]. The ability for microalgae species to utilise light energy within this photosynthetically active radiation spectrum depends on the specific pigment composition of the cell[82]. This allows the cell to absorb light energy, exciting the pigments to a higher energy state resulting in a net ATP production[82]. The distinct photosystem of *G. sulphuraria* contains light harvesting pigments chlorophyll-α and phycocyanin[5]. Due to the presence of these pigments, *G. sulphuraria* can absorb light within the spectrum region at 450 nm and 680 nm, and 618 nm respectively. The spectra of LED lighting used for continuous cultivation of *Galdieria* sp. RTK37.1 is shown in Figure 29[110].

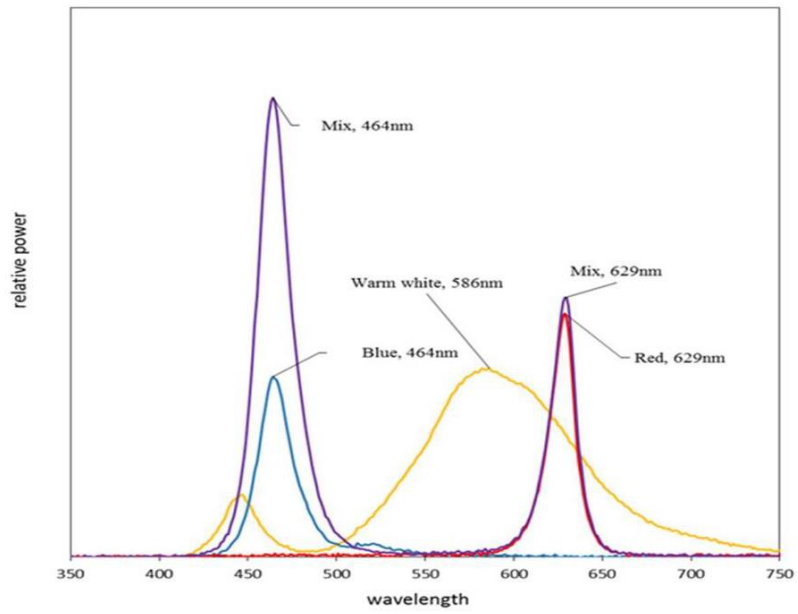

Figure 29: Spectra of LED lighting used during continuous cultivation of *Galdieria* sp. RTK37.1. As reported by Smith (2020). Reprinted with permission[110].

Blue and red light have absorption peaks at 464 nm and 629 nm respectively. The absorption peak for warm white light (586 nm), the light condition used in the majority of this research, has a comparatively wide absorption peak compared with the other coloured LEDs. Due to this wide absorption peak, both chlorophyll-α and phycocyanin pigments in *Galdieria* sp. RTK37.1 can absorb this light energy and utilise it during photoautotrophic growth. This is seen in the absorbance spectra in Figure 27, where absorption peaks for chlorophyll- α and

phycocyanin are expressed during the continuous cultivation of *Galdieria* sp. RTK37.1 in photoautotrophic and mixotrophic conditions.

Previous investigations into the influence different light spectra have on continuously cultivated *G. sulphuraria* ($D = 0.29\ d^{-1}$) by Baer *et al*. highlighted that light composition has a strong effect on biomass and pigment productivity[71]. It was determined that the highest biomass production of *G. sulphuraria* was under red light illumination (625 nm), while green (525 nm) and blue light (490 nm) resulted in reduced biomass production[71]. Aside from this research, the majority of research into the lighting requirements for *Galdieria* spp. has been performed in batch[4,5,71] and therefore further investigation into the effect light has on nutrient-limited *Galdieria* sp. RTK37.1 was undertaken.

6.1.3 Light Limitation in Chemostats

During microalgae continuous cultivation, nutrient limitation can be eliminated by ensuring the growth media contains sufficient amounts of each essential nutrient[136]. Inorganic carbon (CO_2) supply is often sufficient through constant sparging and can be monitored through total inorganic carbon measurements[136]. Nutrient limitations within continuous culture systems are normally distributed homogenously and can be modelled using Monod's equation (Equation 10). This is not the case for light limitation, which during photoautotrophic growth conditions light is often the only limiting factor on cell growth[136]. Light limitation is a significant challenge due to light attenuation, and as photons cannot be homogenously mixed a photon flux is formed within reactors[138]. This results in an exponential decay of light availability with increasing distance from the illumination source[138]. Mutual shading from highly concentrated cells at the surface, known as the photic zone, can lead to regions with low light energy where cell growth is limited[136]. The principles of light limitation in chemostats differ greatly from usual chemostats which are limited in a nutrient provided through the media[138]. Chemostats, which can be modelled using Monod's equation (Equation 10), is based on the nutrient supply rate becoming directly correlated to the dilution rate. Light-limited chemostats supply light independently of the dilution rate. As a result, steady state conditions are achieved due to mutual shading from highly concentrated cells at the surface[138].

6.1.4 Research Aim

Although the theory and technique behind light-limited chemostats is something that requires further investigation, this research focuses on providing an understanding of how light intensity and spectra composition impacts growth and biomass yields of *Galdieria* sp. RTK37.1 during continuous cultivation. Following on from the research completed by Baer *et al.* (*'Optimization of spectral light quality for growth and product formation in different microalgae using a continuous photobioreactor'*)[71], *Galdieria* sp. RTK37.1 will be grown photoautotrophically in continuous cultivation, operating at a lower dilution rate (D = 0.12 d^{-1}) to achieve stable growth[71]. This provides an understanding of how light affects the overall biomass production, oxygen evolution rate and pigment (phycocyanin and chlorophyll-α) fluorescence intensity of *Galdieria* sp. RTK37.1.

The specific hypothesis investigated in this chapter was:

3. The growth and pigment production of *Galdieria* sp. RTK37.1 depends on the light intensity and wavelength condition during continuous cultivation

6.2 Experimental Methods and Materials

Cultures were grown according to Section 3.17. All cultures were grown in V4 medium, as described in Appendix C. During these experiments, *Galdieria* sp. RTK37.1 was cultivated in a 1.5 L chemostat photobioreactor (D = 0.12 d^{-1}), under various warm white light intensities and different wavelength conditions. Initially, *Galdieria* sp. RTK37.1 was cultivated photoautotrophically under warm light LED at an intensity of 94.6 μmol m^{-2} s^{-1}. During steady state growth, pigment emissions and optical density measurements were recorded. Following this, the light intensity was increased to 191.3 μmol m^{-2} s^{-1}, then decreased to 8.1 μmol m^{-2} s^{-1} until steady state growth was achieved under each light intensity. *Galdieria* sp. RTK37.1 was then cultivated in red light (629 nm, 33.8 μmol m^{-2} s^{-1}) and blue light (464 nm, 86.5 μmol m^{-2} s^{-1}) to investigate the effect different wavelength conditions had on biomass and pigment productivity. Light intensities during the red and blue light were variable due to the incapability to alter the intensity. The light intensity dependence of *Galdieria* sp. RTK37.1 photosynthesis rate was also investigated, as described in Section 3.11. All experiments were completed as technical replicates unless stated otherwise. All statistical analysis (two-tailed unpaired t-test) was completed in GraphPad Prism (version 9.3.1).

6.3 Results and Discussion

6.3.1 *Galdieria* sp. RTK37.1 achieved different steady states during various light intensity and wavelength conditions.

Stable growth of *Galdieria* sp. RTK37.1 under various light intensity and wavelength conditions was achieved during continuous cultivation. The growth curve for continuously cultivated photoautotrophic *Galdieria* sp. RTK37.1 during these light conditions is shown in Figure 30. Growth was monitored using optical density and correlated to biomass concentrations obtained during initial photoautotrophic *Galdieria* sp. RTK37.1 cultivated in warm white LED lighting (94.6 µmol m^{-2} s^{-1}).

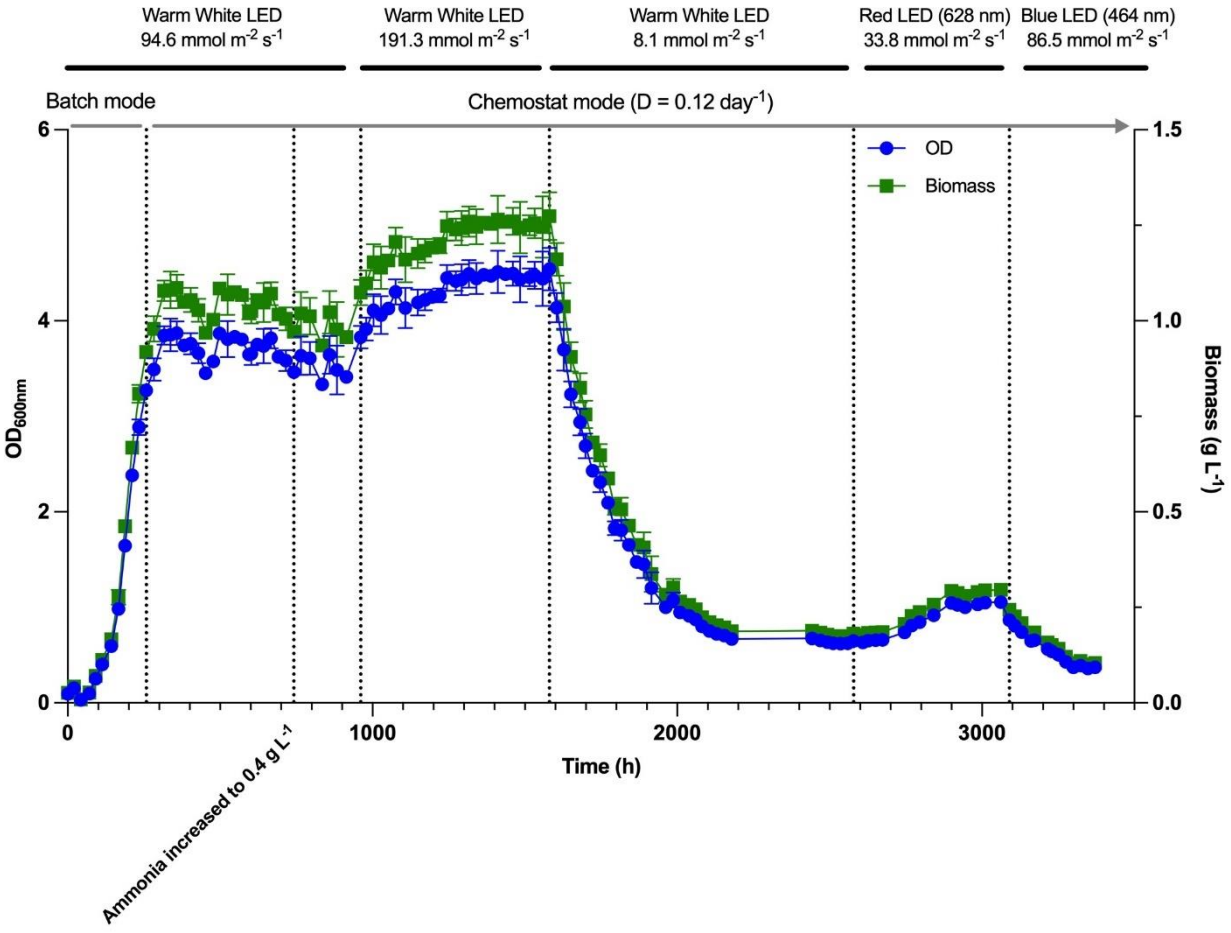

Figure 30: Growth curve outlining the optical density and biomass concentration for photoautotrophic *Galdieria* sp. RTK37.1 grown in various light intensity and wavelength conditions. *Galdieria* sp. RTK37.1 cells were grown at pH 2.5, 45°C in a 1.5 L chemostat reactor, at a dilution rate of 0.12 d^{-1}. Cells were provided with 3% (v/v) CO_2 initially under 94.6 µmol m^{-2} s^{-1} warm white LED lighting. The light intensity was increased to 191.3 µmol m^{-2} s^{-1}, then reduced to 8.1 µmol m^{-2} s^{-1} as illustrated. Following cultivated in warm white LED, *Galdieria* sp. RTK37.1 cells were cultivated in red light (629 nm, 33.8 µmol m^{-2} s^{-1}) and blue light (464 nm, 86.5 µmol m^{-2} s^{-1}). Error bars denote standard deviation.

Table 9: Biomass concentrations for *Galdieria* sp. RTK37.1 grown under various light intensity and wavelength conditions. *Galdieria* sp. RTK37.1 were grown at pH 2.5, 45°C in a 1.5 L chemostat reactor, at a dilution rate of 0.12 d^{-1}. Cells were provided with 3% (v/v) CO_2 initially under 94.6 μmol m^{-2} s^{-1} warm white LED lighting. The light intensity was increased to 191.3 μmol m^{-2} s^{-1}, then reduced to 8.1 μmol m^{-2} s^{-1} as illustrated. Following cultivated in warm white LED, *Galdieria* sp. RTK37.1 was cultivated in red light (629 nm, 33.8 μmol m^{-2} s^{-1}) and blue light (464 nm, 86.5 μmol m^{-2} s^{-1}). Uncertainty errors denote standard deviation

	Warm White Light	**Warm White Light**	**Warm White Light**	**Red Light**	**Blue Light**
Wavelength	586 nm	586 nm	586 nm	629 nm	464 nm
Light Intensity	94.6 μmol m^{-2} s^{-1}	191.3 μmol m^{-2} s^{-1}	8.1 μmol m^{-2} s^{-1}	33.8 μmol m^{-2} s^{-1}	86.5 μmol m^{-2} s^{-1}
Biomass Dry Cell Weight C_b (g L^{-1})	0.93 ± 0.01	1.23 ± 0.03	0.17 ± 0.001	0.29 ± 0.002	0.10 ± 0.004

As the light intensity increased from 94.6 μmol m^{-2} s^{-1} to 191.3 μmol m^{-2} s^{-1}, steady state biomass concentration only increased by 24%, while in contrast the biomass concentrations of *Galdieria* sp. RTK37.1 grown under an intensity of 94.6 μmol m^{-2} s^{-1} was 82% greater than biomass concentrations during the lower light intensity, 8.1 μmol m^{-2} s^{-1} (Table 9). It is likely that biomass concentration during continuous cultivation of *Galdieria* sp. RTK37.1 linearly increases with light intensity to the point where light then becomes limited. This limitation is a consequence of mutual shading caused by high density cultures located in closer proximity to the light. As biomass concentration increases, light is less able to penetrate resulting in greater exponential photon flux. Therefore, it is likely that as the light intensity increases beyond 94.6 μmol m^{-2} s^{-1} biomass concentration begins to limit light availability for photosynthesis. This observation was further validated by the appearance of immobilised cells during cultivation under warm white LED at 191.3 μmol m^{-2} s^{-1}. As the light intensity was increased, the flocculation activity of the cells appeared to increase resulting in the presence of immobilised cells on the reactor wall. *Galdieria* sp. RTK37.1 likely increases flocculation activity to increase their proximity to the light source and overcome light limitations within the reactor. This phenomenon of light dependant adhesion to reactors walls is common in photoautotrophic microalgae (i.e. *Chlamydomonas reinhardtii)* to optimise photosynthetic efficiency[139]. Interestingly, no immobilised cells were observed during mixotrophic cultivation (Chapter 5) of *Galdieria* sp. RTK37.1 (1.43 (± 0.02) g L^{-1}) which obtain greater biomass concentrations than *Galdieria* sp. RTK37.1 (1.23 (± 0.03) g L^{-1})

cultivated under 191.3 μmol m^{-2} s^{-1} warm white LED. This further validates *Galdieria* sp. RTK37.1 as a true mixotroph as the cell utilised glucose during mixotrophic cultivation and therefore were not required to adhere to the reactor wall to fulfil photosynthetic requirements. Although cultivating *Galdieria* sp. RTK37.1 under a higher light intensity resulted in increased biomass concentrations (Table 9) and pigment production (Figure 31) the presence of immobilised cells during continuous cultivation is not desired. As discussed in Section 5.2.3, high density regions within a chemostat often result in non-optimal operation as the immobilised cells act as non-sterile fed streams. Ultimately, it is deemed more beneficial to operate at lower light intensities, sacrificing greater biomass production rates to allow for the control and optimal operation during continuous cultivation of *Galdieria* sp. RTK37.1.

Biomass concentrations of *Galdieria* sp. RTK37.1 was decreased when cultivated in blue and red light, highlighting that these wavelengths are less optimal than warm light LED at higher intensities (94.6 μmol m^{-2} $s^{-}1$, 191.3 μmol m^{-2} s^{-1}) for the photosynthetic growth of *Galdieria* sp. RTK37.1. Warm white LED light has a wider adsorption peak (Figure 29), resulting in both chlorophyll-α and phycocyanin pigments of *Galdieria* sp. RTK37.1 having the ability to absorb light energy and utilise it during photoautotrophic growth. Alternately, during *Galdieria* sp. RTK37.1 cultivation under red light, it is likely that only phycocyanin pigments were able to utilise the light due to the absorption peak (629 nm) corresponding absorption spectra of phycocyanin (618 nm). Furthermore, under blue light, it is likely that only the chlorophyll-α pigments in *Galdieria* sp. RTK37.1 were able to utilise the light as the absorption peak of red light (464 nm) corresponds to the absorption spectra of chlorophyll-α (450 nm). This result is further validated by pigment emissions shown in Figure 31.

6.3.2 Relative pigment production of *Galdieria* sp. RTK37.1 is dependent on light

As completed in Section 5.4.3, the relative pigment production of *Galdieria* sp. RTK37.1 during various light conditions was investigated to determine the effect light intensity and wavelength condition has on pigment production. The fluorescence of *Galdieria* sp. RTK37.1 primary absorbing pigments, chlorophyll-α (absorption peaks at 450 nm and 680 nm)[5,82] and phycocyanin (absorption peak at 618 nm)[5,82], were measured, as shown in Figure 31.

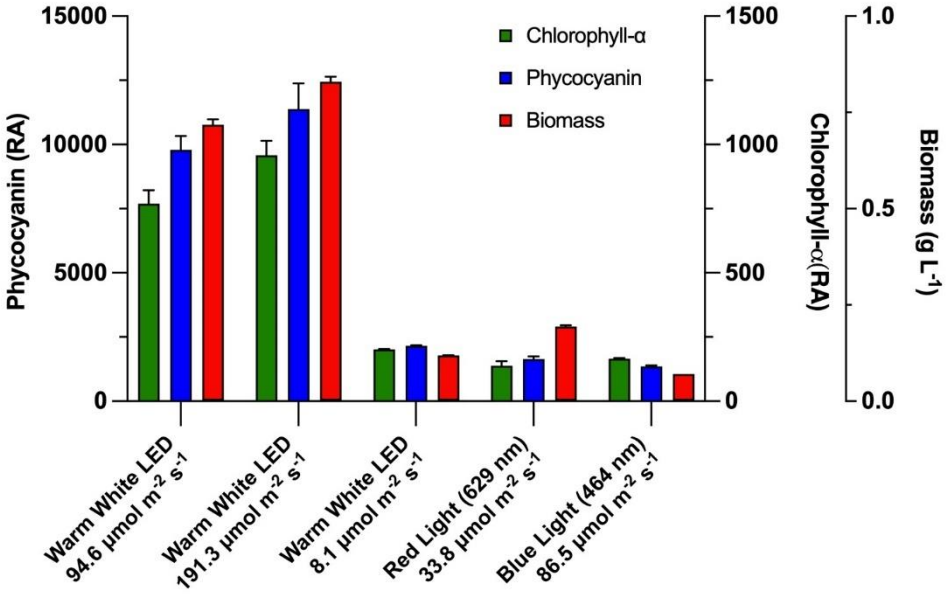

Figure 31: The relative fluorescence intensity of pigments Phycocyanin and Chlorophyll- α produced by photoautotrophic *Galdieria* sp. RTK37.1 during continuous cultivation, against biomass concentration. *Galdieria* sp. RTK37.1 was grown at pH 2.5, 45°C in a 1.5 L chemostat reactor, at a dilution rate of 0.12 d^{-1}. Cells were provided with 3% (v/v) CO_2 and grown under warm white LED light at intensities ranging from 8.1 µmol m^{-2} s^{-1}, 94.6 µmol m^{-2} $s^{-1}$and 191.3 µmol m^{-2} s^{-1}. Following cultivated in warm white LED light, *Galdieria* sp. RTK37.1 was cultivated in red light (629 nm, 33.8 µmol m^{-2} s^{-1}) and blue light (464 nm, 86.5 µmol m^{-2} s^{-1}). Error bars denote standard deviation.

During red light, *Galdieria* sp. RTK37.1 produced a greater relative amount of phycocyanin compared with *Galdieria* sp. RTK37.1 cultivated in blue light concurring with previously reported literature for *G. sulphuraria* grown in continuous cultivation[71]. Although the relative amount of phycocyanin emitted was greatly decreased compared with phycocyanin emitted when *Galdieria* sp. RTK37.1 was cultivated under warm white LED light (94.6 µmol m^{-2} s-1, 191.3 µmol m^{-2} s^{-1}). Under blue light, *Galdieria* sp. RTK37.1 emitted an increased amount of chlorophyll-α compared with cultures cultivated in red light[71]. This is

likely a result of blue light wavelength (464 nm) corresponding to the chlorophyll-α pigment absorption spectrum (480 nm)[71].

The absorption spectrum in Figure 32 outlines the increased height of absorption peaks during cultivation under the higher warm white light intensities (94.6 μmol m^{-2} s^{-1}, 191.3 μmol m^{-2} s^{-1}). The absorption peaks for pigments emitted during cultivation of *Galdieria* sp. RTK37.1 under low intensity warm white, red and blue light is not visible in the absorption spectrum. This justifies that these lighting conditions are not viable for photoautotrophic growth of *Galdieria* sp. RTK37.1 when pigment and greater overall biomass production is essential.

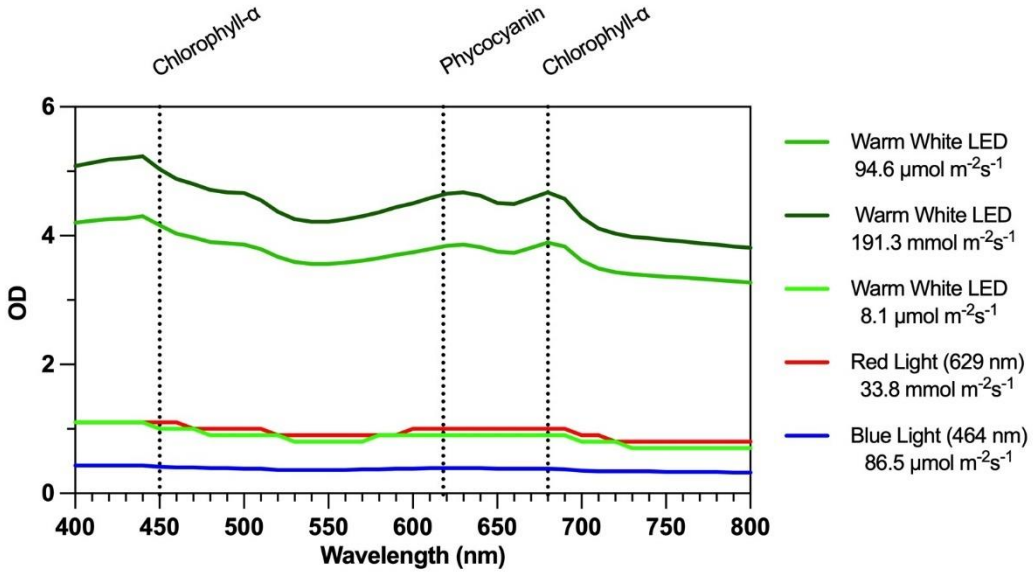

Figure 32: Absorbance spectra of steady state *Galdieria* sp. RTK37.1 grown in various light intensities and wavelength conditions. *Galdieria* sp. RTK37.1 was grown at pH 2.5, 45°C in a 1.5 L chemostat reactor, at a dilution rate of 0.12 d^{-1}. Cells were provided with 3% (v/v) CO_2 and grown under warm white LED light at intensities ranging from 8.1 μmol m^{-2} s^{-1}, 94.6 μmol m^{-2} $s^{-1}$and 191.3 μmol m^{-2} s^{-1}. Following cultivated in warm white LED light, *Galdieria* sp. RTK37.1 was cultivated in red light (629 nm, 33.8 μmol m^{-2} s^{-1}) and blue light (464 nm, 86.5 μmol m^{-2} s^{-1}). Error bars denote standard deviation.

6.3.3 *Galdieria* sp. RTK37.1 photosynthesis rates are dependent on light intensity

To determine the light dependency on photosynthesis rates during photoautotrophic growth of *Galdieria* sp. RTK37.1 (OD_{600nm} ~ 3.5), cells were illuminated under warm white LED lighting ranging from 47 to 642 µmol m^{-2} s^{-1} and the net specific oxygen evolution rate (Figure 33) was measured according to Section 3.11. The maximum net specific oxygen evolution rate was 133 (± 9) nmol O_2 $mg_{biomass}^{-1}$ h^{-1} at a light intensity of 101 µmol m^{-2} s^{-1}.

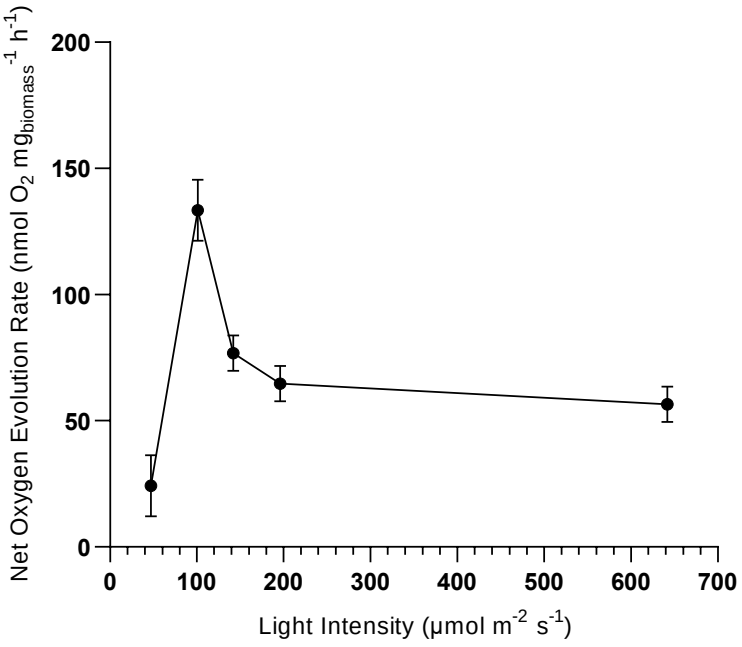

Figure 33: The light intensity dependence of photosynthesis in *Galdieria* sp. RTK37.1 under various warm white LED light intensities. Cells used during these experiments was taken from steady state continuously cultivated photoautotrophic *Galdieria* sp. RTK37.1. Cells were maintained at pH 2.5, 45°C in a 1.5 L chemostat reactor, at a dilution rate of 0.12 d^{-1}, provided with 3% (v/v) CO_2 under 94.6 µmol m^{-2} s^{-1} warm white LED lighting. Error bars denote standard deviation.

Oesterhelt *et al.* (2007) conducted a similar experiment, investigating the light intensity dependence of photosynthesis rates in *G. sulphuraria* under light intensities ranging from 0 – 250 µE m^{-2} s^{-1} (µE m^{-2} s^{-1} is equivalent to µmol m^{-2} s^{-1})[4]. During this experiment, an abrupt decrease in the oxygen evolution rate was observed at a light intensity of 225 µmol m^{-2} s^{-1}, which suggested photoinhibition[4,68]. It was concluded that *G. sulphuraria* does not require high light intensities due to its occurrence within endolithic ecosystems[4]. Interestingly, the net specific oxygen evolution rates of *Galdieria* sp. RTK37.1 decreased at light intensities higher than ~ 101 µmol m^{-2} s^{-1}, lower than that observed by Oesterhelt *et al.* (2007). Additionally, the

net oxygen evolution rate of *Galdieria* sp. RTK37.1 appeared to stabilise as the light intensity increased, not decreased abruptly like observed by Oesterhelt *et al*. (2007). This suggests that photoinhibition was not occurring during this experiment[68], but indicates that *Galdieria* sp. RTK37.1 has an optimal light intensity at ~ 101 μmol m^{-2} s^{-1}. This optimal light intensity is further justified by the biomass concentration (Table 9) observed during continuous cultivation of photoautotrophic *Galdieria* sp. RTK37.1. Increasing the light intensity from 8.1 μmol m^{-2} s^{-1} to 94.6 μmol m^{-2} s^{-1}, increased biomass production by 82% while increasing the light intensity to 191.3 μmol m^{-2} s^{-1} only resulted in a 24% increase in biomass concentration justifying that the increase in light intensity did not provide a significant effect into biomass productivity and was likely decreasing overall photosynthetic rates.

6.4 Conclusion

It was concluded that the cultivation of *Galdieria* sp. RTK37.1 under high intensity warm white LED light decreased rates of photosynthesis and increased adhesion on the reactor wall. Operating chemostats with high density regions often results in oscillating growth behaviours, making it difficult to obtain stable growth[124,126]. Cultivation of *Galdieria* sp. RTK37.1 under blue and red light decreased biomass concentrations and pigment production, leading to the conclusion that warm white LED lighting at ~ 101 μmol m^{-2} s^{-1} was optimal.

Overall, this research chapter has highlighted light intensity and wavelength conditions as major considerations for the successful growth of *Galdieria* sp. RTK37.1 in large scale cultivation systems. Operating chemostats under non-optimal light intensities and wavelength conditions not only affect microalgae growth but also the ability to control and achieved desired stable growth due to increased reactor wall adhesion.

7 Chapter 7: General Discussion and Conclusions

This thesis aimed to investigate light (in)dependant growth of *Galdieria* sp. RTK37.1 in a continuous bioreactor to further understand the physiology for large scale cultivation for biotechnology application of the species.

The main hypothesises of this research were:

1. *Galdieria* sp. RTK37.1 is a true mixotroph.
2. Stable continuous cultivation of *Galdieria* sp. RTK37.1 is achievable during photoautotrophic, mixotrophic and heterotrophic growth conditions
3. The growth and pigment production of *Galdieria* sp. RTK37.1 depends on the light intensity and wavelength condition during continuous cultivation

7.1 Summary of Key Results

The following section details key results obtained throughout this research. The strain *Galdieria* sp. RTK37.1 was identified, through isolation and characterisation, to be most closely related to other strains of *G. sulphuraria*, within the genus *Galdieria*. Specifically strains of *G. sulphuraria* isolated from the Taupō and Waiotopu regions of New Zealand (*rbcL* gene)[119]. The initial bacterial contaminate, *Alicyclobacillus* sp. EB1, was determined to be closely related to *Alicyclobacillus tengchongensis*, a Gram-positive, aerobic, acidophilic thermotolerant bacterial species. The presence of *Alicyclobacillus* sp. EB1 suggests heterotrophic metabolism as the bacterial cells were capable of growing on excreted metabolites from *Galdieria* sp. RTK37.1. Co-culture between *Galdieria* spp. and *Alicyclobacillus* spp. has not been reported in previous known literature and therefore investigation is required to understand the metabolic relationship between these two species. Initial batch experiments determined that *Galdieria* sp. RTK37.1 can grow in photoautotrophic, mixotrophic and heterotrophic growth conditions. Carbon substrates, glucose and galactose, were able to support heterotrophic growth. Mixotrophically grown cells obtained the greatest biomass yield, with linear growth continuing after the complete exhaustion (LDL < 0.75 mM) of the organic carbon source. Additionally, there was a clear optimal pH condition for *Galdieria* sp. RTK37.1, at a pH 2.5.

After successful batch cultivation (50 mL) of *Galdieria* sp. RTK37.1, continuous cultivation in a 1.5 L bioreactor was pursued. All experimental results obtained during this

stage of the research were a major step towards successfully upscaling *Galdieria* spp. for use in biotechnical applications, as achieving stable growth under various continuous trophic conditions has not previously been published in the literature. As observed in Figure 24, stable growth of *Galdieria* sp. RTK37.1 in photoautotrophic, mixotrophic and heterotrophic growth conditions is possible during continuous cultivation. This is a significant observation and shows clear evidence towards successfully upscaling this genus of algae for biotechnical purposes, such as phycocyanin production. Cultivation in a continuous chemostat ensures that the growth of *Galdieria* sp. RTK37.1 can be manipulated, allowing the consumption of ammonia, carbohydrate and other growth substrates to be controlled. Additionally, the output of products, including biomass concentration and pigment production, can be controlled through different trophic and light conditions.

Results indicated that mixotrophic growth is favoured to obtain high density biomass production and achieve high relative amounts of pigments phycocyanin and chlorophyll-α. There is evidence (Figure 28) that reducing the light intensity (a major limiting factor in industrial cultivation of photosynthetic microalgae species[90,42,91,92]) while maintaining the addition of an organic carbon, pigment production during mixotrophic growth would be similar to what was observed during photoautotrophic growth. This would reduce lighting costs while maintaining the production output of pigments making it more economic to utilise mixotrophic *Galdieria* spp. Although, this would need to be quantified through further light dependent mixotrophic experiments. Heterotrophic *Galdieria* sp. RTK37.1 biomass concentration (0.63 ± 0.02 g L^{-1}) were lower than photoautotrophic (0.93 ± 0.01 g L^{-1}) and mixotrophic (1.43 ± 0.12 g L^{-1}) biomass concentrations, but stable growth was obtainable while maintaining the production of pigments. This justifies the biotechnology viability of heterotrophic *Galdieria* sp. RTK37.1 in phycocyanin production. Additionally, this research outlines that light is not necessary to achieve high density axenic *Galdieria* sp. RTK37.1 biomass during continuous cultivation.

One of the most thought-provoking results obtained during this experiment was the significantly decreased ammonia consumption during the growth of heterotrophic *Galdieria* sp. RTK37.1 (*t-test: p-value* < $2E^{-9}$). Heterotrophically grown *Galdieria* sp. RTK37.1 only consumed 12.5% of the available ammonia, while photoautotrophically grown cells consumed 93% and mixotrophically grown cells consumed 100% (LDL < 0.01 g L^{-1} NH_4Cl). It appears that during continuous heterotrophic growth conditions, *Galdieria* sp. RTK37.1 required significantly (*t-test: p-value* < $2E^{-9}$) less ammonia

for cell growth, which has not been discussed in previous known literature. It is unclear why during heterotrophy significantly less ammonia is consumed but one hypothesis outlines that it may be due to a decreased requirement for ammonia assimilation[129]. As photosynthetic reactions are no longer required during heterotrophy, the need to assimilate toxic ammonia is decreased other than that required for cell growth[129]. Although ultimately this is only a hypothesis, further understanding of ammonia metabolism would need to be investigated to fully understand why this result was observed. Additionally, it is unclear whether this phenomenon is only observed during continuous cultivation or all heterotrophic growth of *Galdieria* sp. RTK37.1.

Leading on from this, ammonia was either fully exhausted or nearly completely consumed during light utilising growth (mixotrophic and photoautotrophic). This result suggests the usage of *Galdieria* sp. RTK37.1 as a feasible option for ammonia removal for biotechnological applications[130]. Particularly in landfill leachate, where ammonia is a more challenging contaminant to remove due to its excessive concentration and high biotoxicity[130].

Continuous cultivation of *Galdieria* sp. RTK37.1 under various light intensities and wavelength conditions provided a further understanding of light (in)dependant growth of the species. It was determined that light intensity and wavelength conditions are major considerations for the successful growth of *Galdieria* sp. RTl37.1 in large scale cultivation systems. Operating chemostats under non-optimal light intensities and wavelength conditions not only affected the growth of *Galdieria* sp. RTK37.1 but also the ability to control and achieved desired stable growth due to increased reactor wall adhesion. The cultivation of *Galdieria* sp. RTK37.1 under high warm white LED light intensities (191.3 μmol m^{-2} s^{-1}) increased adhesion to the reactor wall, likely due to light limitation in the reactor. Although cultivating *Galdieria* sp. RTK37.1 under a higher light intensity resulted in increased biomass concentrations (Table 9) and pigment production (Figure 31), the presence of immobilised cells during continuous cultivation is not desired as can result in non-optimal operation from immobilised cells acting as non-sterile fed streams. Therefore, it was concluded that it is more beneficial to operate at lower light intensities, sacrificing higher biomass production rates to allow for the control and optimal operation during continuous cultivation of *Galdieria* sp. RTK37.1. Additionally, the cultivation of *Galdieria* sp. RTK37.1 under blue and red light decreased biomass concentrations and pigment production, which lead to the

conclusion that warm white LED (586 nm) lighting at ~ 101 μmol m^{-2} s^{-1} was the most optimal light intensity and wavelength conditions for the growth of *Galdieria* sp. RTK37.1.

7.1.1 Addressing the Hypotheses

Galdieria sp. RTK37.1 is a Mixotroph

Mixotrophic growth is defined as the ability for a cell to combine the mechanisms of photoautotrophic and heterotrophic growth, utilising both inorganic carbons through photosynthesis and organic carbon through respiration simultaneously[6]. This research concluded that *Galdieria* sp. RTK37.1 is a true mixotroph. Biomass concentrations obtained during mixotrophic growth were significantly greater than concentrations for either photoautotrophy or heterotrophy (*t-test: p-value < 0.0001*), justifying that the cell is utilising both metabolism methods. Observed net specific oxygen evolution rates suggest that mixotrophic cells were undertaking photosynthesis, although at a decreased rate compared to photoautotrophic cells. Nutritional analysis of mixotrophic *Galdieria* sp. RTK37.1 outlined a decrease in crude protein percentage compared with heterotrophic and photoautotrophic cells, likely due to a decrease in photosynthesis proteins (particularly RuBisCO). Net specific oxygen evolution rates and nutritional analysis both indicate a decrease in photosynthesis occurring within mixotrophic *Galdieria* sp. RTK37.1, but as the cell is still able to achieve greater biomass productivity than heterotrophic and photoautotrophic *Galdieria* sp. RTK37.1 it demonstrates the synergistic effect between photosynthesis and aerobic respiration during mixotrophy.

Stable continuous cultivation of Galdieria sp. RTK37.1 is achievable during photoautotrophic, mixotrophic and heterotrophic growth conditions

Stable growth of *Galdieria* sp. RTK37.1 in photoautotrophic, mixotrophic and heterotrophic growth conditions is possible during continuous cultivation. The ability to grow *Galdieria* sp. RTK37.1 continuously, while achieving submaximal specific growth rates indicates that *Galdieria* sp. RTK37.1 can be grown in larger scale reactors (reactor volume in this research was 1.5 L). Stable growth proves that through defined nutrient or light limitations the growth of *Galdieria* sp. RTK37.1 can be controlled. This is a major industrial benefit as growth can be manipulated to obtain desired biomass and product yields. Continuous cultivation promotes the growth of *Galdieria* sp. RTK37.1 over a long duration while still allowing the biomass to be removed for the retrieval of products, such as phycocyanin.

The growth and pigment production of Galdieria sp. RTK37.1 depends on the light intensity and wavelength condition during continuous cultivation

Galdieria sp. RTK37.1 achieved different steady states during various light intensity and wavelength conditions, highlighting that light is a major consideration for the successful growth of *Galdieria* sp. RTK37.1 in large scale cultivation systems. This research highlighted that operating chemostats under non-optimal light intensities and wavelength conditions not only affects microalgae growth but also the ability to control and achieved desired steady states due to increased reactor wall adhesion.

7.2 Repeatability and Reliability of Results

Throughout cultivation of *Galdieria* sp. RTK37.1, the presence of *Alicyclobacillus* sp. EB1 or another contaminating bacterial species was monitored by continuously plating the sample on Phytagel plates (Appendix D) and observing it under a microscope. The cultures remained axenic until all trophic experiments were completed, which was deemed to be most important, as during stages of mixotrophic and heterotrophic growth bacterial carbohydrate uptake rates, particularly glucose specific uptake, is higher than microalgae[118]. It was confirmed that samples became contaminated with *Alicyclobacillus* sp. EB1 during light intensity and wavelength experiments (Chapter 6), but it was concluded that the presence of this culture would not impact the results as the bacterial species was a heterotroph, likely growing on products excreted during cell lysis.

A lack of previous literature investigating the growth of *Galdieria* spp. in continuous cultivation makes comparing these results to those published challenging (i.e. majority of research surrounding *Galdieria* spp. is in batch conditions). Ideally, the continuous cultivation experiments completed in this research should be repeated to ensure the reproducibility of the results. Specifically, ammonia concentration analysis should be repeated due to the unexpected low consumption of ammonia during heterotrophic growth, which is something not previously reported in the literature. Additionally, as the uncertainty around the nutritional composition of *Galdieria* sp. RTK37.1 grown in various trophic conditions was not determined due to lacking biomass provided for the analysis, it would be beneficial to repeat experiments and collect larger volumes of biomass for nutritional analysis. This would ensure that the results obtained were valid and not impacted by low volumes. All other results were taken as either biological or technique replicates (as specified) and therefore were assumed to be valid enough to make conclusions.

7.3 Overall Outcomes and Contributions from this Research

Prior to this work, continuous cultivation of *Galdieria* spp. was limited to only photoautotrophic conditions[71]. This research outlined that *Galdieria* sp. RTK37.1 can be grown in continuous cultivation under a range of light (in)dependent conditions. This demonstrates *Galdieria* sp. RTK37.1 as a promising strain for larger scale production, with evidence towards its ability to be used for phycocyanin production and as a feasible option in ammonia removal. The ability to control the growth of *Galdieria* sp. RTK37.1 allows product outputs to be manipulated through the supply of various light conditions and (in)organic carbon substrates. Additionally, this research outlines the ability for *Galdieria* sp. RTK37.1 to adapt to a wide range of conditions, achieving stable growth even under multiply limiting factors.

This research further validates the conclusions of Curien *et al.* (2021) that some *Galdieria* spp. are capable of true mixotrophy[54], a growth mechanism that has numerous industrial benefits. As it is believed that decreasing light availability in mixotrophic conditions will still maintain biomass and product yields similar to that observed in photoautotrophic *Galdieria* sp. RTK37.1, this will greatly impact the economics of cultivation, particular for phycocyanin production.

Overall, *Galdieria* spp. are extremely versatile. As research and scale up work continues, the species is likely to be of great benefit biotechnologically speaking. *Galdieria* spp. have the ability to decrease the impact of major issues, such as the greenhouse gas effect and livestock evolution (Chapter 1), and the potential to be utilised for other economic benefits such as phycocyanin production. This research provides the initial evidence towards large scale cultivation of *Galdieria* spp., justifying future work to take advantage of everything this extremophilic microalgae offers.

7.4 Future Work

In terms of continuing the investigation into the feasibility of light (in)dependent continuous cultivation of *Galdieria* sp. RTK37.1, it is suggested that this research be repeated in a larger reactor volume. This would further justify large scale cultivation of *Galdieria* sp. RTK37.1, and ensure reproducibility of the results in this research.

As steady state growth is achieved as a consequence of a growth limiting substrate, it would be beneficial to further investigate the effect multiply limiting factors has on the overall growth and biomass yield of *Galdieria* sp. RTK37.1. As detailed in this research, it was assumed that during mixotrophy, there were three limiting factors (ammonia, light and glucose). Operating the chemostat with three limiting factors would have generated a complex system. Therefore, further investigation into how each of these growth limiting factors, both individually and combined, impacted the overall growth of mixotrophic *Galdieria* sp. RTK37.1 is required. Furthermore, the theory and technique surrounding light-limited chemostats requires further investigation. This would provide a further understanding of how light availability is varied during photosynthetic growth to ensure that stable growth would be achievable in larger cultivation systems.

Transcriptome analysis should be completed for the biomass samples collected over steady state growth (in photoautotrophic, mixotrophic, and heterotrophic conditions), this would further justify *Galdieria* sp. RTK37.1 as a true mixotrophic. Transcriptome analysis would highlight the regulation of intracellular components throughout the different trophic conditions. Transcriptome analysis on the different trophic growth conditions for *Galdieria* spp. has not been investigated and would provide a clearer understanding of the different metabolism methods of the genus. Isotopic labelling of $^{13}CO_2$ (through isotope ratio mass spectrometry) would show CO_2 uptake during mixotrophy, concluding photosynthesis is occurring during mixotrophic growth of *Galdieria* sp. RTK37.1.

Additionally, further investigation into ammonia consumption under different trophic conditions is recommended to justify the results concluded in this research. The minimal ammonia consumption observed during heterotrophy has not previously been reported and could offer major knowledge surrounding the growth kinetics of *Galdieria* spp. during heterotrophic growth. To further justify the economic feasibility of cultivating *Galdieria* spp. for pigment production, the concentration and purity of pigments, phycocyanin and

chlorophyll-α, should be quantified. Extracting these pigments will highlight the purity obtainable, improving the economic potential of *Galdieria* spp. for phycocyanin production.

8 References

1 Reeb, V. & Bhattacharya, D. Red algae in the genomic age. *Cellular Origin, Life in Extreme Habitats and Astrobiology. Cellular Origin, Life in Extreme Habitats and Astrobiology. Springer, Dordrecht, Netherlands*, 409-426 (2010).

2 Chisti, Y. & Moo-Young, M. in *Encyclopedia of Physical Science and Technology (Third Edition)* (ed Robert A. Meyers) 247-271 (Academic Press, 2003).

3 Tuchman, N. C. in *Algal Ecology* (eds R. Jan Stevenson, Max L. Bothwell, & Rex L. Lowe) 299-319 (Academic Press, 1996).

4 Oesterhelt, C., Schmälzlin, E., Schmitt, J. M. & Lokstein, H. Regulation of photosynthesis in the unicellular acidophilic red alga Galdieria sulphuraria†. *The Plant Journal* 51, 500-511, doi:10.1111/j.1365-313X.2007.03159.x (2007).

5 Sarian, F. D., Rahman, D., Schepers, O. & van der Maarel, M. Effects of Oxygen Limitation on the Biosynthesis of Photo Pigments in the Red Microalgae Galdieria sulphuraria Strain 074G. *PloS one* 11, e0148358, doi:10.1371/journal.pone.0148358 (2016).

6 Venkata Subhash, G. *et al.* Carbon streaming in microalgae: extraction and analysis methods for high value compounds. *Bioresource Technology* 244, 1304-1316, doi:https://doi.org/10.1016/j.biortech.2017.07.024 (2017).

7 Lelieveld, J., Crutzen, P. J., and Dentener, F. J. Changing concentration, lifetime and climate forcing of atmospheric methane. *Tellus B Chem. Phys. Meteorol*, 128-150 (1998).

8 Ritchie, H. & Roser, M. *Carbon Dioxide and Greenhouse Gas Emissions*, <'https://ourworldindata.org/co2-and-other-greenhouse-gas-emissions'> (2020).

9 Government, A. *Greenhouse Effect*, <https://www.environment.gov.au/climate-change/climate-science-data/climate-science/greenhouse-effect> (2021).

10 IPCC. Climate Change 2007: Synthesis Report. *Contribution of Working Groups I, II and III to the Fourth Assessment Report of the Intergovernmental Panel on Climate Change* (2007).

11 Shaftel, H., Callery, S., Bailey, D. & Randel, J. *The Effects of Climate Change*, <https://climate.nasa.gov/effects/> (2021).

12 Jain, P. C. Greenhouse effect and climate change: scientific basis and overview. *Renewable Energy* 3, 403-420, doi:https://doi.org/10.1016/0960-1481(93)90108-S (1993).

13 Foley, J. *A Five Step Plan to Feed the World*, <https://www.nationalgeographic.com/foodfeatures/feeding-9-billion/> (2014).

14 Gilbert, R. *Protein Sources For The Animal Feed Industry*, <http://www.fao.org/3/y5019e/y5019e00.htm#Contents> (2004).

15 Roser, M., Ritchie, H. & Esteban, O.-O. *World Population Growth*, <https://ourworldindata.org/world-population-growth> (2013).

16 Seckbach, J. *Enigmatic Microorganisms and Life in Extreme Environments*. (Springer Netherlands, 1999).

17 Fukuda. Physiological studies on a thermophilic blue-green alga, Cyanidium Calderium. *Bot. Mag.* 71, 79-86 (1958).

18 Barsanti L, E. V., Frassanito A M, Passarelli V, Gualtieri P. Algal Toxins: Nature, Occurence, Effect and Detection. (2008).

19 Sahoo, D. & Seckbach, J. *The Algae World*. (Springer, 2015).

20 Fritsch, F. E. *Structure and Reproduction of the Algae*. (2021).

21 Seckbach, J. & Oren, A. in *Algae and Cyanobacteria in Extreme Environments* (ed Joseph Seckbach) 3-25 (Springer Netherlands, 2007).

22 Kristjánsson, J. K. & Hreggvidsson, G. O. Ecology and habitats of extremophiles. *World Journal of Microbiology and Biotechnology* 11, 17-25, doi:10.1007/BF00339134 (1995).

23 Lafraie, M. A. & Betz, A. Anaerobic fermentation in Cyanidium caldarium. *Planta* 163, 38-42, doi:10.1007/bf00395895 (1985).

24 Seckbach, J. *Evolutionary Pathways and Enigmatic Algae: Cyanidium caldarium (Rhodophyta) and Related Cells*. (Springer Netherlands, 1994).

25 Allen, M. B. Studies with cyanidium caldarium, an anomalously pigmented chlorophyte. *Archiv für Mikrobiologie* 32, 270-277, doi:10.1007/BF00409348 (1959).

26 Lewin, R. Cyanidium caldarium-a Cryptococcalean? *Phycol. News Bull.* 14, 6-7 (1961).

27 Kremer, B. P. (ed W. Schwemmler H.E.A Schenk) 963-970 (W. deGruyter and co, 1983).

28 Reeb, V. & Bhattacharya, D. 409-426 (2010).

29 Sheath, R. G. in *Freshwater Algae of North America* (eds John D. Wehr & Robert G. Sheath) 197-224 (Academic Press, 2003).

30 CINIGLIA, C., YOON, H. S., POLLIO, A., PINTO, G. & BHATTACHARYA, D. Hidden biodiversity of the extremophilic Cyanidiales red algae. *Molecular Ecology* 13, 1827-1838, doi:https://doi.org/10.1111/j.1365-294X.2004.02180.x (2004).

31 Merola, A. *et al.* Revision of Cyanidium caldarium. Three species of acidophilic algae. *Giornale botanico italiano* 115, 189-195, doi:10.1080/11263508109428026 (1981).

32 Pinto, G., Ciniglia, C., Cascone, C. & Pollio, A. in *Algae and Cyanobacteria in Extreme Environments* (ed Joseph Seckbach) 487-502 (Springer Netherlands, 2007).

33 Gross, W., Seipold, P. & Schnarrenberger, C. Characterization and purification of an aldose reductase from the acidophilic and thermophilic red alga Galdieria sulphuraria. *Plant physiology* 114, 231-236 (1997).

34 Sentsova, O. Y. in *Evolutionary Pathways and Enigmatic Algae: Cyanidium caldarium (Rhodophyta) and Related Cells* (ed Joseph Seckbach) 167-174 (Springer Netherlands, 1994).

35 Pinto, G. *et al.* Comparative approaches to the taxonomy of the genus Galdieria Merola (Cyanidiales, Rhodophyta). *Cryptogamie Algologie* 24, 13-32 (2003).

36 Cozzolino, S., Caputo, P., De Castro, O., Moretti, A. & Pinto, G. Molecular variation in Galdieria sulphuraria (Galdieri) Merola and its bearing on taxonomy. *Hydrobiologia* 433, 145-151, doi:10.1023/A:1004035224715 (2000).

37 Schönknecht, G. *et al.* Gene transfer from bacteria and archaea facilitated evolution of an extremophilic eukaryote. *Science* 339, 1207-1210 (2013).

38 Jain, K. *et al.* Extreme features of the Galdieria sulphuraria organellar genomes: a consequence of polyextremophily? *Genome Biol Evol* 7, 367-380, doi:10.1093/gbe/evu290 (2014).

39 Barbier, G. *et al.* Comparative genomics of two closely related unicellular thermo-acidophilic red algae, Galdieria sulphuraria and Cyanidioschyzon merolae, reveals the molecular basis of the metabolic flexibility of Galdieria sulphuraria and significant differences in carbohydrate metabolism of both algae. *Plant physiology* 137, 460-474 (2005).

40 Gross, W., Küver, J., Tischendorf, G., Bouchaala, N. & Büsch, W. Cryptoendolithic growth of the red alga Galdieria sulphuraria in volcanic areas. *European Journal of Phycology* 33, 25-31 (1998).

41 Gross, W. & Oesterhelt, C. Ecophysiological studies on the red alga Galdieria sulphuraria isolated from southwest Iceland. *Plant biology* 1, 694-700 (1999).

42 Maria Cizkova, M. V. a. V. Z. The Red Micoalga Galdieria as a Promising Organism for Applications in Biotechnology *Physiology to Applications* (2019).

43 Náhlík, V. *et al.* Growth under Different Trophic Regimes and Synchronization of the Red Microalga Galdieria sulphuraria. *Biomolecules* 11, 939 (2021).

44 Tanaka, A. & Makino, A. Photosynthetic research in plant science. *Plant Cell Physiol* 50, 681-683, doi:10.1093/pcp/pcp040 (2009).

45 Hill, R. Oxygen Evolved by Isolated Chloroplasts. *Nature* 139, 881-882, doi:10.1038/139881a0 (1937).

46 Britannica, T. E. o. E. *Photolysis*, <https://www.britannica.com/science/photolysis> (2018).

47 Thangaraj, B. *et al.* Efficient Light Harvesting in a Dark, Hot, Acidic Environment: The Structure and Function of PSI-LHCI from Galdieria sulphuraria. *Biophysical Journal* 100, 135-143, doi:https://doi.org/10.1016/j.bpj.2010.09.069 (2011).

48 Yang, C., Hua, Q. & Shimizu, K. Energetics and carbon metabolism during growth of microalgal cells under photoautotrophic, mixotrophic and cyclic light-autotrophic/dark-heterotrophic conditions. *Biochemical Engineering Journal* 6, 87-102, doi:https://doi.org/10.1016/S1369-703X(00)00080-2 (2000).

49 Bassham, J. A. & Calvin, M. in *Die CO2-Assimilation / The Assimilation of Carbon Dioxide: In 2 Teilen / 2 Parts* (ed André Pirson) 884-922 (Springer Berlin Heidelberg, 1960).

50 Raven, J. A. The Quantitative Role of 'Dark' Respiratory Processes in Heterotrophic and Photolithotrophic Plant Growth. *Annals of Botany* 40, 587-602 (1976).

51 Sujatha, B. in *Plant Biology and Biotechnology: Volume I: Plant Diversity, Organization, Function and Improvement* (eds Bir Bahadur, Manchikatla Venkat Rajam, Leela Sahijram, & K. V. Krishnamurthy) 569-591 (Springer India, 2015).

52 Eriksen, N. T. 5 Chapter heterotrophic production of phycocyanin in Galdieria sulphuraria. *Extremophiles: From Biology to Biotechnology*, 87 (2018).

53 Vanselow, C., Weber, A. P. M., Krause, K. & Fromme, P. Genetic analysis of the Photosystem I subunits from the red alga, Galdieria sulphuraria. *Biochimica et Biophysica Acta (BBA) - Bioenergetics* 1787, 46-59, doi:https://doi.org/10.1016/j.bbabio.2008.10.004 (2009).

54 Curien, G. *et al.* Mixotrophic growth of the extremophile galdieria sulphuraria reveals the flexibility of its carbon assimilation metabolism. *New Phytologist*, doi:10.1111/nph.17359 (2021).

55 Sakurai, T. *et al.* Profiling of lipid and glycogen accumulations under different growth conditions in the sulfothermophilic red alga Galdieria sulphuraria. *Bioresource Technology* 200, doi:10.1016/j.biortech.2015.11.014 (2015).

56 Kim, S., Park, J.-E., Cho, Y.-B. & Hwang, S.-J. Growth rate, organic carbon and nutrient removal rates of Chlorella sorokiniana in autotrophic, heterotrophic and mixotrophic conditions. *Bioresource technology* 144C, 8-13, doi:10.1016/j.biortech.2013.06.068 (2013).

57 Khan, M., Karmakar, R., Das, B., Diba, F. & Razu, M. 1-19 (2016).

58 Morales-Sánchez, D., Martinez-Rodriguez, O. A., Kyndt, J. & Martinez, A. Heterotrophic growth of microalgae: metabolic aspects. *World Journal of Microbiology and Biotechnology* 31, 1-9, doi:10.1007/s11274-014-1773-2 (2015).

59 Madigan, M., Martinko, J., Bender, K., Buckley, D. & Stahl, D. in *Brock Biology of Microorganisms* Vol. 14 105-121 (Pearson Education Limited, 2015).

60 Ternes, C.

61 Britannica, T. E. o. E. *Tricarboxylic acid Cycle*, <http://www.britannica.com/science/tricarboxylic-acid-cycle> (2013).

62 Li, T. *et al.* Evaluating differences in growth, photosynthetic efficiency, and transcriptome of Asterarcys sp. SCS-1881 under autotrophic, mixotrophic, and heterotrophic culturing conditions. *Algal Research* 45, 101753, doi:https://doi.org/10.1016/j.algal.2019.101753 (2020).

63 Perez-Garcia, O., Escalante, F. M. E., de-Bashan, L. E. & Bashan, Y. Heterotrophic cultures of microalgae: Metabolism and potential products. *Water Research* 45, 11-36, doi:https://doi.org/10.1016/j.watres.2010.08.037 (2011).

64 Yoon, H. S. *et al.* Establishment of endolithic populations of extremophilic Cyanidiales (Rhodophyta). *BMC Evolutionary Biology* 6, 78 (2006).

65 Oesterhelt, C., Schnarrenberger, C. & Gross, W. Characterization of a sugar/polyol uptake system in the red alga Galdieria sulphuraria. *European journal of Phycology* 34, 271-277 (1999).

66 Oesterhelt, C. & Gross, W. Different Sugar Kinases Are Involved in the Sugar Sensing ofGaldieria sulphuraria. *Plant physiology* 128, 291-299 (2002).

67 Schmidt, R. A., Wiebe, M. G. & Eriksen, N. T. Heterotrophic high cell-density fed-batch cultures of the phycocyanin-producing red alga Galdieria sulphuraria. *Biotechnology and Bioengineering* 90, 77-84, doi:https://doi.org/10.1002/bit.20417 (2005).

68 Khan, M. I., Shin, J. H. & Kim, J. D. The promising future of microalgae: current status, challenges, and optimization of a sustainable and renewable industry for biofuels, feed,

and other products. *Microb Cell Fact* 17, 36-36, doi:10.1186/s12934-018-0879-x (2018).

69 Li, T., Zheng, Y., Yu, L. & Chen, S. Mixotrophic cultivation of a Chlorella sorokiniana strain for enhanced biomass and lipid production. *Biomass and Bioenergy* 66, 204-213, doi:https://doi.org/10.1016/j.biombioe.2014.04.010 (2014).

70 Zhang, Z. *et al.* The synergistic energy and carbon metabolism under mixotrophic cultivation reveals the coordination between photosynthesis and aerobic respiration in Chlorella zofingiensis. *Algal Research* 25, 109-116, doi:https://doi.org/10.1016/j.algal.2017.05.007 (2017).

71 Baer, S., Heining, M., Schwerna, P., Buchholz, R. & Hübner, H. Optimization of spectral light quality for growth and product formation in different microalgae using a continuous photobioreactor. *Algal Research* 14, 109-115, doi:https://doi.org/10.1016/j.algal.2016.01.011 (2016).

72 Eyster, C. in *Algae and Man* (ed Springer) (1964).

73 Oswald, J. B. a. W. Final report to the US Department of Energy. USA patent (1996).

74 Daliry, S., Hallajisani, A., Mohammadi Roshandeh, J., Nouri, H. & Golzary, A. Investigation Of Optimal Condition For Chlorella Vulgaris Microalgae Growth (Review Paper). *Global Journal Of Environmental Science And Management* 3, - (2017).

75 Martinez-Garcia, M. & van der Maarel, M. J. E. C. Floridoside production by the red microalga Galdieria sulphuraria under different conditions of growth and osmotic stress. *AMB Express* 6, 71, doi:10.1186/s13568-016-0244-6 (2016).

76 Shimonaga, T. *et al.* Variation in Storage α-Glucans of the Porphyridiales (Rhodophyta). *Plant and Cell Physiology* 49, 103-116, doi:10.1093/pcp/pcm172 (2008).

77 Rocha Leão, M. H. M. in *Encyclopedia of Food Sciences and Nutrition (Second Edition)* (ed Benjamin Caballero) 2930-2937 (Academic Press, 2003).

78 Sakurai, T. *et al.* Profiling of lipid and glycogen accumulations under different growth conditions in the sulfothermophilic red alga Galdieria sulphuraria. *Bioresource Technology* 200, 861-866, doi:https://doi.org/10.1016/j.biortech.2015.11.014 (2016).

79 Qiu, R., Gao, S., Lopez, P. A. & Ogden, K. L. Effects of pH on cell growth, lipid production and CO2 addition of microalgae Chlorella sorokiniana. *Algal Research* 28, 192-199, doi:https://doi.org/10.1016/j.algal.2017.11.004 (2017).

80 Chen, C. Y. & Durbin, E. Effects of pH on the growth and carbon uptake of marine phytoplankton. *Marine Ecology-progress Series - MAR ECOL-PROGR SER* 109, 83-94, doi:10.3354/meps109083 (1994).

81 Russell, J. B. Effect of extracellular pH on growth and proton motive force of Bacteroides succinogenes, a cellulolytic ruminal bacterium. *Applied and Environmental Microbiology* 53, 2379-2383, doi:doi:10.1128/aem.53.10.2379-2383.1987 (1987).

82 Maltsev, Y., Maltseva, K., Kulikovskiy, M. & Maltseva, S. Influence of Light Conditions on Microalgae Growth and Content of Lipids, Carotenoids, and Fatty Acid Composition. *Biology (Basel)* 10, 1060, doi:10.3390/biology10101060 (2021).

83 Baker, N. R. in *Light as an Energy Source and Information Carrier in Plant Physiology* (eds Robert C. Jennings, Giuseppe Zucchelli, Francesco Ghetti, & Giuliano Colombetti) 89-97 (Springer US, 1996).

84 González-Camejo, J. *et al.* Wastewater nutrient removal in a mixed microalgae–bacteria culture: effect of light and temperature on the microalgae–bacteria competition. *Environmental Technology* 39, 503-515, doi:10.1080/09593330.2017.1305001 (2018).

85 Rossoni, A. W. *et al.* Cold Acclimation of the Thermoacidophilic Red Alga Galdieria sulphuraria: Changes in Gene Expression and Involvement of Horizontally Acquired Genes. *Plant and Cell Physiology* 60, 702-712, doi:10.1093/pcp/pcy240 (2018).

86 Ras, M., Steyer, J.-P. & Bernard, O. Temperature effect on microalgae: a crucial factor for outdoor production. *Reviews in Environmental Science and Bio/Technology* 12, 153-164, doi:10.1007/s11157-013-9310-6 (2013).

87 Ahlgren, G. Temperature Functions in Biology and Their Application to Algal Growth Constants. *Oikos* 49, 177-190, doi:10.2307/3566025 (1987).

88 Varshney, P., Mikulic, P., Vonshak, A., Beardall, J. & Wangikar, P. P. Extremophilic micro-algae and their potential contribution in biotechnology. *Bioresource Technology* 184, 363-372, doi:https://doi.org/10.1016/j.biortech.2014.11.040 (2015).

89 Eriksen, N. T. Production of phycocyanin—a pigment with applications in biology, biotechnology, foods and medicine. *Applied Microbiology and Biotechnology* 80, 1-14, doi:10.1007/s00253-008-1542-y (2008).

90 Graverholt, O. S. & Eriksen, N. T. Heterotrophic high-cell-density fed-batch and continuous-flow cultures of Galdieria sulphuraria and production of phycocyanin.

Applied Microbiology and Biotechnology 77, 69-75, doi:10.1007/s00253-007-1150-2 (2007).

91 Benemann, J. R., Tillett, D. M. & Weissman, J. C. Microalgae biotechnology. *Trends in biotechnology* 5, 47-53 (1987).

92 Glazer, A. N. Phycobiliproteins—a family of valuable, widely used fluorophores. *Journal of Applied Phycology* 6, 105-112 (1994).

93 Sloth, J. K., Wiebe, M. G. & Eriksen, N. T. Accumulation of phycocyanin in heterotrophic and mixotrophic cultures of the acidophilic red alga Galdieria sulphuraria. *Enzyme and Microbial Technology* 38, 168-175 (2006).

94 Ingledew, W. M. M. & Lin, Y. H. in *Comprehensive Biotechnology (Second Edition)* (ed Murray Moo-Young) 37-49 (Academic Press, 2011).

95 Smith, H. L. & Waltman, P. *The Theory of the Chemostat: Dynamics of Microbial Competition*. (Cambridge University Press, 1995).

96 Wan, M. *et al.* A novel paradigm for the high-efficient production of phycocyanin from Galdieria sulphuraria. *Bioresource Technology* 218, 272-278, doi:https://doi.org/10.1016/j.biortech.2016.06.045 (2016).

97 Gross, W. & Schnarrenberger, C. Heterotrophic growth of two strains of the acido-thermophilic red alga galdieria sulphuraria. *Plant and cell physiology* 36, 633-638 (1995).

98 Gross, W. & Oesterhelt, C. Ecophysiological Studies on the Red Alga Galdieria sulphuraria Isolated from Southwest Iceland. *Plant Biology* 1, 694-700, doi:https://doi.org/10.1111/j.1438-8677.1999.tb00282.x (1999).

99 Carbone, D. A., Olivieri, G., Pollio, A. & Melkonian, M. Comparison of Galdieria growth and photosynthetic activity in different culture systems. *AMB Express* 10, 170-170, doi:10.1186/s13568-020-01110-7 (2020).

100 Gifuni, I., Pollio, A., Marzocchella, A. & Olivieri, G. New ultra-flat photobioreactor for intensive microalgal production: The effect of light irradiance. *Algal Research* 34, 134-142, doi:10.1016/j.algal.2018.07.014 (2018).

101 Henkanatte-Gedera, S. M. *et al.* Removal of dissolved organic carbon and nutrients from urban wastewaters by Galdieria sulphuraria: Laboratory to field scale demonstration. *Algal Research* 24, 450-456, doi:https://doi.org/10.1016/j.algal.2016.08.001 (2017).

102 Sloth, J. K., Wiebe, M. G. & Eriksen, N. T. Accumulation of phycocyanin in heterotrophic and mixotrophic cultures of the acidophilic red alga Galdieria

sulphuraria. *Enzyme and Microbial Technology* 38, 168-175, doi:https://doi.org/10.1016/j.enzmictec.2005.05.010 (2006).

103 Dunfield, P. F. *et al.* Methane oxidation by an extremely acidophilic bacterium of the phylum Verrucomicrobia. *Nature* 450, 879-882, doi:http://dx.doi.org/10.1038/nature06411 (2007).

104 Colsell, A. *Cultivation, isolation and characterisation of thermophilic and acidophili red algae, Cyanidiales* Master's Degree thesis, University of Canterbury, (2020).

105 Gross, W., Heilmann, I., Lenze, D. & Schnarrenberger, C. Biogeography of the Cyanidiaceae (Rhodophyta) based on 18S ribosomal RNA sequence data. *European Journal of Phycology* 36, 275-280 (2001).

106 Toplin, J., Norris, T., Lehr, C. & McDermott, T. Biogeographic and Phylogenetic Diversity of Thermoacidophilic Cyanidiales in Yellowstone National Park, Japan, and New Zealand. *Applied and environmental microbiology* 74, 2822-2833, doi:10.1128/AEM.02741-07 (2008).

107 Yoon, H. S., Hackett, J. D., Pinto, G. & Bhattacharya, D. The single, ancient origin of chromist plastids. *Proc Natl Acad Sci U S A* 99, 15507-15512, doi:10.1073/pnas.242379899 (2002).

108 Sánchez Rojas, F. & Cano Pavón, J. M. in *Encyclopedia of Analytical Science (Second Edition)* (eds Paul Worsfold, Alan Townshend, & Colin Poole) 366-372 (Elsevier, 2005).

109 LeGresley, M. & McDermott, G. Counting chamber methods for quantitative phytoplankton analysis—haemocytometer, Palmer-Maloney cell and Sedgewick-Rafter cell. *UNESCO (IOC manuals and guides)*, 25-30 (2010).

110 Smith, D. *Optimisation of Eicosapentaenoic Acid Production from New Zealand Microalga in a Tubular Photobioreactor* Doctor of Philosophy thesis, University of Canterbury, (2020).

111 Gregor, J. & Maršálek, B. A Simple In Vivo Fluorescence Method for the Selective Detection and Quantification of Freshwater Cyanobacteria and Eukaryotic Algae. *Acta hydrochimica et hydrobiologica* 33, 142-148, doi:https://doi.org/10.1002/aheh.200400558 (2005).

112 Ebeling, M. E. The Dumas Method for Nitrogen in Feeds. *Journal of Association of Official Analytical Chemists* 51, 766-770, doi:10.1093/jaoac/51.4.766 (2020).

113 Thiex, N., Novotny, L. & Crawford, A. Determination of Ash in Animal Feed: AOAC Official Method 942.05 Revisited. *Journal of AOAC INTERNATIONAL* 95, 1392-1397, doi:10.5740/jaoacint.12-129 (2019).

114 Ahn, J. Y., Kil, D. Y., Kong, C. & Kim, B. G. Comparison of Oven-drying Methods for Determination of Moisture Content in Feed Ingredients. *Asian-Australas J Anim Sci* 27, 1615-1622, doi:10.5713/ajas.2014.14305 (2014).

115 Lunder, T. L. Simplified Procedure for Determining Fat and Total Solids by Mojonnier Method. *Journal of Dairy Science* 54, 737-739, doi:https://doi.org/10.3168/jds.S0022-0302(71)85917-9 (1971).

116 Gopalakrishnan, K. *Isolation, characterisation amd screening of New Zealand alphine algae for the production of secondary metabolites in photobioreactors* Ph.D, Thesis thesis, The University of Canterbury, (2015).

117 Mazumda, N. *"Algal blushing": CHracterization and optimization of culture conditions of a novel alphine Haematococcur species from New Zealand for astaxanthin production* Ph.D, Thesis thesis, The University of Canterbury, (2018).

118 Kamjunke, N., Koehler, B., Wannicke, N. & Tittel, J. Algae as competitors for glucose with heterotrophic bacteria. *Journal of Phycology* 44, 616-623, doi:10.1111/j.1529-8817.2008.00520.x (2008).

119 Toplin, J. A., Norris, T. B., Lehr, C. R., McDermott, T. R. & Castenholz, R. W. Biogeographic and Phylogenetic Diversity of Thermoacidophilic Cyanidiales in Yellowstone National Park, Japan, and New Zealand. *Applied and Environmental Microbiology* 74, 2822-2833, doi:doi:10.1128/AEM.02741-07 (2008).

120 Karavaiko, G. I. *et al.* Reclassification of 'Sulfobacillus thermosulfidooxidans subsp. thermotolerans' strain K1 as Alicyclobacillus tolerans sp. nov. and Sulfobacillus disulfidooxidans Dufresne et al. 1996 as Alicyclobacillus disulfidooxidans comb. nov., and emended description of the genus Alicyclobacillus. *International Journal of Systematic and Evolutionary Microbiology* 55, 941-947, doi:https://doi.org/10.1099/ijs.0.63300-0 (2005).

121 Kim, M. G., Lee, J.-C., Park, D.-J., Li, W.-J. & Kim, C.-J. Alicyclobacillus tengchongensis sp. nov., a thermo-acidophilic bacterium isolated from hot spring soil. *Journal of Microbiology* 52, 884-889, doi:10.1007/s12275-014-3625-z (2014).

122 Gilmour, D. J. in *Advances in Applied Microbiology* Vol. 109 (eds Geoffrey Michael Gadd & Sima Sariaslani) 1-30 (Academic Press, 2019).

123 Gomez, J. A., Höffner, K. & Barton, P. I. From sugars to biodiesel using microalgae and yeast. *Green Chemistry* 18, 461-475, doi:10.1039/c5gc01843a (2016).

124 Bailey, J. E. & Ollis, D. F. *Biochemical engineering fundamentals: [By] James E. Bailey [and] David F. Ollis*. (McGraw-Hill, 1977).

125 Monod, J. *Recherches sur la croissance des cultures bacteriennes*. (1942).

126 Doran, P. M. *Bioprocess engineering principles / Pauline M. Doran*. (London ; San Diego : Academic Press, [1995] ©1995, 1995).

127 Ramanan, R., Kim, B.-H., Cho, D.-H., Oh, H.-M. & Kim, H.-S. Algae–bacteria interactions: Evolution, ecology and emerging applications. *Biotechnology Advances* 34, 14-29, doi:https://doi.org/10.1016/j.biotechadv.2015.12.003 (2016).

128 Lee, J. *et al.* Microalgae-associated bacteria play a key role in the flocculation of Chlorella vulgaris. *Bioresource Technology* 131, 195-201, doi:https://doi.org/10.1016/j.biortech.2012.11.130 (2013).

129 Lea, P. J. in *Techniques in Bioproductivity and Photosynthesis (Second Edition)* (eds J. Coombs, D. O. Hall, S. P. Long, & J. M. O. Scurlock) 173-187 (Pergamon, 1985).

130 Khanna, A. R. & Williams, Z. M. Genes that give our brains their rhythms. *Nature Neuroscience*, doi:10.1038/s41593-021-00805-9 (2021).

131 Martinez-Garcia, M., Kormpa, A. & van der Maarel, M. J. The glycogen of Galdieria sulphuraria as alternative to starch for the production of slowly digestible and resistant glucose polymers. *Carbohydrate polymers* 169, 75-82 (2017).

132 Graziani, G. *et al.* Microalgae as human food: chemical and nutritional characteristics of the thermo-acidophilic microalga Galdieria sulphuraria. *Food & Function* 4, 144-152, doi:10.1039/C2FO30198A (2013).

133 Stadnichuk, I., Semenova, L., Smirnova, G. & Usov, A. A highly branched storage polyglucan in the thermoacidophilic red microalga Galdieria maxima cells. *Prikladnaia biokhimiia i mikrobiologiia* 43, 88-93, doi:10.1134/S0003683807010140 (2007).

134 Zhang, H., Wang, W., Li, Y., Yang, W. & Shen, G. Mixotrophic cultivation of Botryococcus braunii. *Biomass and Bioenergy* 35, 1710-1715, doi:https://doi.org/10.1016/j.biombioe.2011.01.002 (2011).

135 Pagnanelli, F., Altimari, P., Trabucco, F. & Toro, L. Mixotrophic growth of Chlorella vulgaris and Nannochloropsis oculata: interaction between glucose and nitrate. *Journal of Chemical Technology & Biotechnology* 89, 652-661, doi:https://doi.org/10.1002/jctb.4179 (2014).

136 Pruvost, J., Cornet, J.-F. & Pilon, L. in *Algae biotechnology* 41-66 (Springer, 2016).

137 Carruthers, T. J. B., Longstaff, B. J., Dennison, W. C., Abal, E. G. & Aioi, K. in *Global Seagrass Research Methods* (eds Frederick T. Short & Robert G. Coles) 369-392 (Elsevier Science, 2001).

138 Huisman, J. *et al.* Principles of the light-limited chemostat: theory and ecological applications. *Antonie Van Leeuwenhoek* 81, 117-133, doi:10.1023/a:1020537928216 (2002).

139 Kreis, C. T., Le Blay, M., Linne, C., Makowski, M. M. & Bäumchen, O. Adhesion of Chlamydomonas microalgae to surfaces is switchable by light. *Nature Physics* 14, 45-49, doi:10.1038/nphys4258 (2018).

Appendix A: Nomenclature

Acronym/ Abbreviation	Full Term
CH_2O	Formaldehyde
CH_2OH	Hydroxymethyl
CH_4	Methane
CO_2	Carbon Dioxide
H^+	Proton
HCOOH	Formic Acid
NAD^+	Nicotinamide adenine dinucleotide
NADH	Nicotinamide adenine dinucleotide (Reduced)
O_2	Molecular Oxygen
PQQ	Methoxatin (Pyrroloquinoline quinone)
$PQQH_2$	Methoxatin (Pyrroloquinoline quinone) (Reduced)
MOB	Methane Oxidizing Bacteria
ATP	Adenosine triphosphate
ADP	Adenosine diphosphate
PSI	Photosystem 1
PSII	Photosystem 2
$C_6H_{12}O_6$	Glucose
RPM	Revolutions per Minute
18s rRNA	18s Ribosomal RNA
rbcL	ribulose-1, 5-bisphosphate carboxylase/oxygenase large subunit
psaA	photosystem I P700 chlorophyll-α apoprotein A1
psbA	photosystem II reaction centre protein D1
16s rRNA	18s Ribosomal RNA
HPLC	High Pressure Liquid Chromatography

Appendix B: Data Analysis

Statistical analysis for the results was completed in GraphPad Prism (version 9.3.1) using data analysis functions. Results were considered to be statistically significant at 95% confidence levels using two-tailed unpaired t-tests and ANOVA, $p \leq 0.05$. Uncertainty was measured by standard deviation, by completing each measurement as either biologically or technical triplicates, as stated.

Uncertainty in results was estimated by completing each measurement or experiment in triplicates. Uncertainty in calculations was completed using the error formulae below:

$$q = ax + b$$
$$q = ax - b$$

$$\boldsymbol{Resultant\ error\ calculation}: \boldsymbol{\Delta q = ax}$$

$$q = x + y$$
$$q = x - y$$

$$\boldsymbol{Resultant\ error\ calculation}: \boldsymbol{(\Delta q)^2 = (\Delta x^2) + (\Delta y)^2}$$

$$q = cxy$$
$$q = \frac{cy}{x}$$

$$\boldsymbol{Resultant\ error\ calculation}: \boldsymbol{\left(\frac{\Delta q}{q}\right)^2 = \left(\frac{\Delta x}{x}\right)^2 + \left(\frac{\Delta y}{y}\right)^2}$$

$$q = \frac{cy}{x}$$
$$q = \frac{a}{x}$$

$$\boldsymbol{Resultant\ error\ calculation}: \boldsymbol{\left(\frac{\Delta q}{q}\right)^2 = \left(\frac{\Delta x}{x}\right)^2}$$

Appendix C: V4 Mineral Salt Growth Media Recipe

The mineral salt media contains 0.04 g of NH_4CI, 0.05 g of KH_2PO_4, 0.02 g of $MgSO_47H_2O$, 0.01 g of $CaCI_26H_2O$, 0.2 mL of 1 mM $Ce(SO_4)_2$, 0.02 mL of 1 mM $La_2(SO_4)_3$, 3 mL of FeEDTA solution, 3 mL of trace element solution 1 and 1 mL of trace element solution 2. The solution was then made up to 1 L with double distilled water (ddH_2O).

The FeEDTA solution contains [90]:

- 1.54 g/L $FeSO_4.7H_2O$
- 2.06 g/L Na_2EDTA

Trace element solution 1 contains [90]:

- 0.44 g $ZnSO_4.7H_2O$
- 0.06 g $Na_2MoO_4.2H_2O$
- 0.19 g $MnCI.4H_2O$
- 0.20 g $CuSO_4.5H_2O$
- 0.10 g H_3BO_3
- 0.08 g $CoCI_2.6H_2O$

The solution was then made up to 1 L using ddH_2O.

Trace element solution 2 contained [90]:

- 1.5 g nitrilotriacetic acid
- 0.2 g $Fe(NH_4)_2(SO_4)_2.6H_2O$
- 0.44 g $Na_2SeO_4.10H_2O$
- 0.1 g $CoCI_2.6H_2O$
- 0.12 g $MnSO_4.4H_2O$
- 0.1 g $Na_2MoO_4.2H_2O$
- 0.1 g $NaWO_4.2H_2O$
- 0.1 g $ZnSO_4.7H_2O$
- 0.04 g $AlCI_3.6H_2O$
- 0.025 g $NiCI_2.6H_2O$
- 0.1 g H_3BO_3
- 0.1 g $CuSO_4.5H_2O$

The solution was then made up to 1 L using ddH_2O.

Appendix D: Solid Media Preparation

Solid media for plating methods was made using double concentrated V4 media and combined with 15 g L^{-1} phytagel solution. Phytagel was dissolved in warm deionized water. To avoid clumping, a magnetic stirrer was used to generate a large vortex and then the phytagel powder was slowly added. Solutions were autoclaved separately and then combined immediately to ensure solidification did not occur until after the plates were poured. Plates were poured immediately after the solutions were combined and then let cool inside a laminar flow biohood.

Appendix E: HPLC Carbon Substrate Calibration Curves

The calibration curve for HPLC analysis is shown below in Figure E. The calibration curves were obtained using known concentrations of the standard and the average peak area was measured either using UV-visible spectrophotometer at a set wavelength of 210 nm or refraction index. Figure E. A shows the calibration curve for sorbitol concentration determination, where the average peak area was determined using the refraction index. Figure E. B shows the calibration curve for Galactose concentration determination, where the average peak area was determined using the refraction index. Figure E. C shows the calibration curve for Glucose concentration determination, where the average peak area was determined using the refraction index. Figure E. D shows the calibration curve for Succinate concentration determination, where the average peak area was determined using UV-visible spectrophotometer. Figure E. E shows the calibration curve for Acetate concentration determination, where the average peak area was determined using UV-visible spectrophotometer. The detection limit for all carbon substrates was 0.75 mM, excluding succinate which had a detection limit of 3 mM.

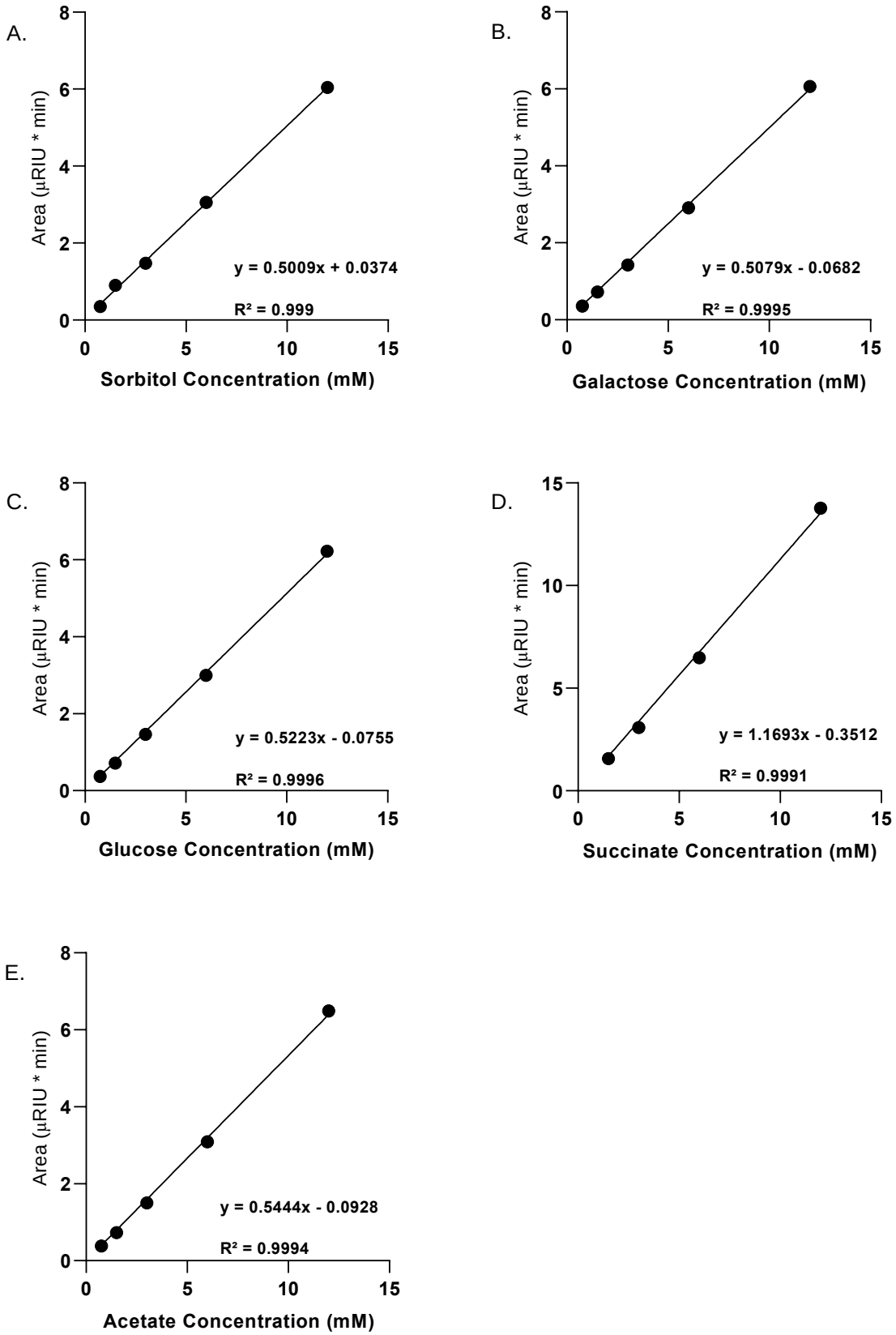

Figure E: HPLC Calibration curves for carbon substrate concentration determination based on the measured peak area. Data points represent known concentration stock solutions made through serial dilution, a linear regression line was then added. The linear relationship of the curve was used to determine the concentration, as expressed in the provided equations. A represents Sorbitol, B represents Galactose, C represents Glucose, D represents Succinate and E presents acetate.

Appendix F: Ammonia Concentration Calibration Curve

The calibration curve for ammonia concentration analysis is shown below in Figure F. The calibration curves were obtained using serial dilutions concentrations of the ammonia by diluting with V4 media containing no ammonia chloride. The potential difference was measured using an ammonia electrode, and the concentration of ammonia was determined. The limit to ammonia detection was 0.05 g L^{-1} ammonia chloride.

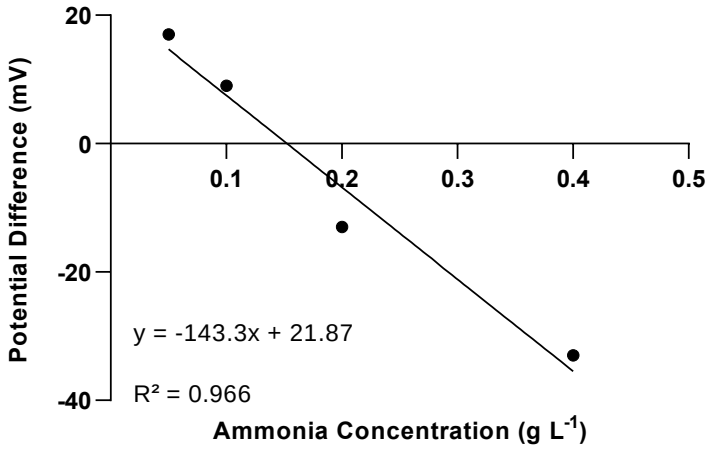

Figure F: Ammonia concentration calibration curve for determining the concentration of ammonia. Data points represent known concentration stock solutions made through serial dilution, a linear regression line was then added. The linear relationship of the curve was used to determine the concentration, as expressed in the provided equation.

Appendix G: Quantum Flux Correlation Curve

All light intensities were measured using an MQ-610 extended range Photon Flux density meter and then correlated to calibrated measurements taken using a spherical quantum sensor. Figure G below shows the correlation plot used to determine the light intensities measured throughout this research.

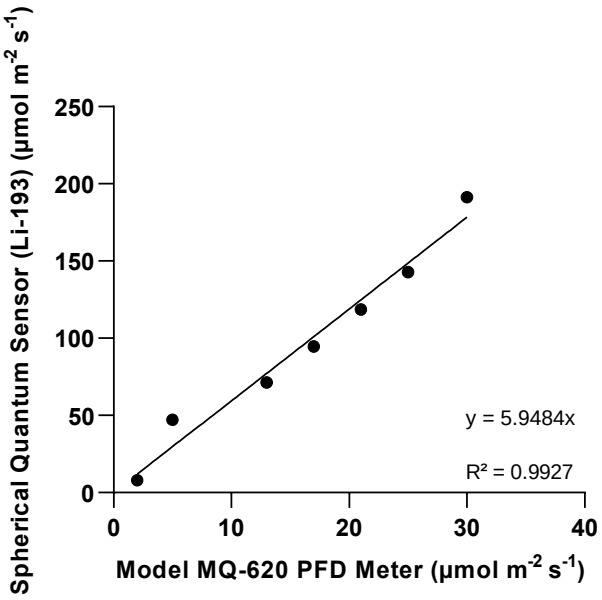

Figure G: Light intensity correlation plot. Data points represent measured light intensities using an MQ-610 extended range photon flux density meter, and correlating these to known light intensities measured using a spherical quantum sensor through a linear regression line. The linear relationship of the curve was used to determine the light intensity, as expressed in the provided equation.

Appendix H: UV Spectrophotometer and Plate Reader Discrepancy Calibration Curve

Due to the discrepancy between the OD_{600nm} measured using the UV spectrophotometer and the imaging reader, a discrepancy plot was made as shown in Figure H. All optical density measurements reported in this research are based on the UV-visible spectrophotometer (Ultrospec 2100 pro, Amersham Biosciences, UK).

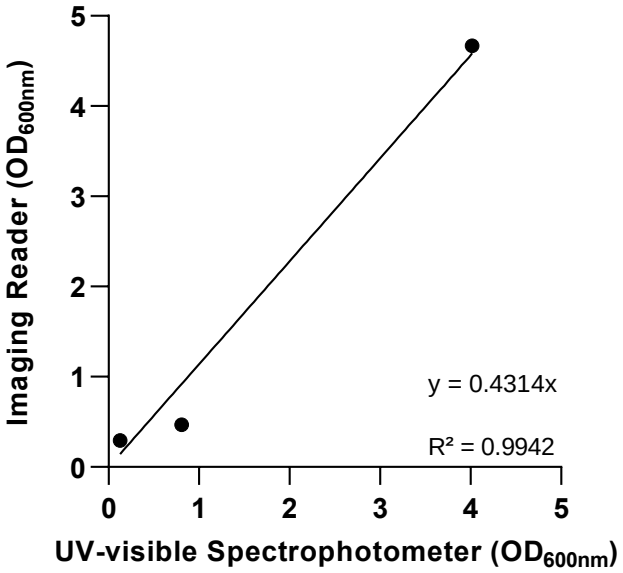

Figure H: Discrepancy plot between the UV-visible spectrophotometer and the imaging reader. All optical density measurements reported in this research are correlated to measurements taken on the UV-visible spectrophotometer. Data points represent optical density measurements correlated with a linear regression line. The linear relationship was defined by the equation provided.

Appendix I: Pump Calibration Curves

The calibration curve for peristaltic pumps used for continuous cultivation is shown below in Figure I. Figure I. A is for pump 5240 and Figure I. B is for pump 5242.

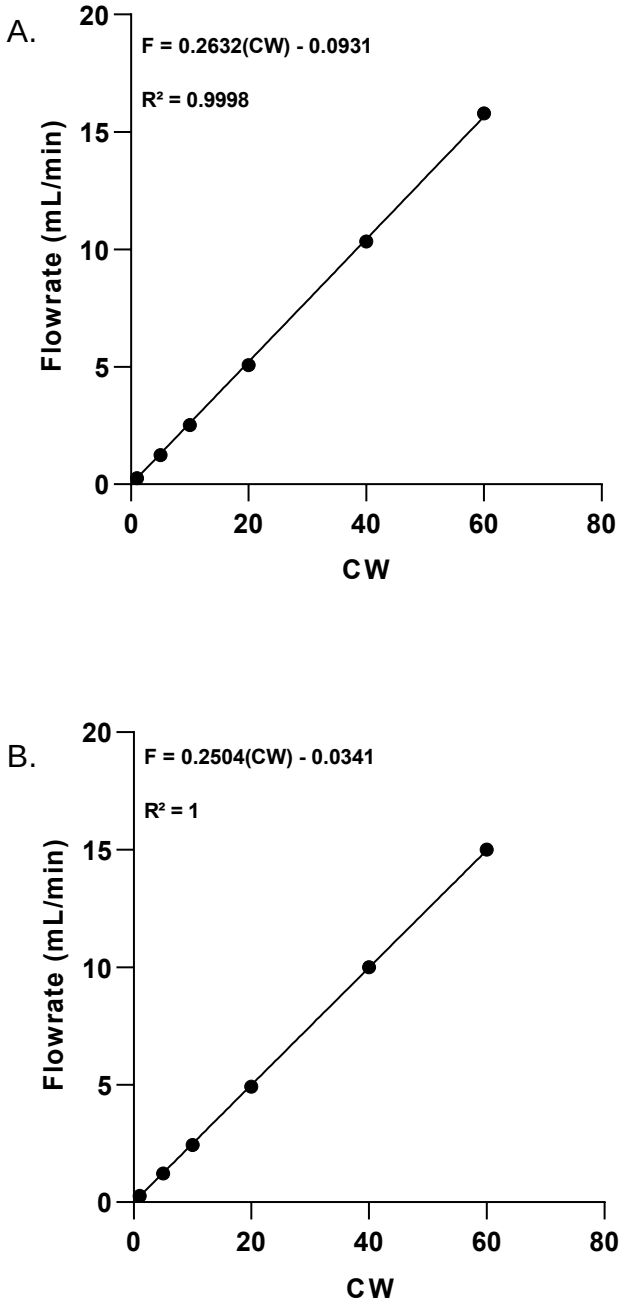

Figure I: Calibration curve for the peristaltic pump used during continuous cultivation. The linear relationship was defined by the equation provided.

Appendix J: Genomic Sequences for *18s rRNA*, *psaA* and *rbcL* genes of *Galdieria* sp. RTK37.1

DNA sequence for *18s rRNA* gene:

TCCTCGTTCATAAATACAGTTACAGTATTCAATCCCAAGCACGATGCAAGT
TCAAAGATTACCCAAGTCCTCTAGGAATAGGTAAATGAAAACTCTTTGAGTGCAT
CAGTGTAGCCCGCGTGCAGCCCAGGACATCAAAGGGCATCACAGACCTGTTATT
GCCTACAACTTCCATCCGTGAAAAACGAATAGTACCTCAAAGAAGTAAATATCG
TGCGAAAATACACACAATAYTACTACTTGGCAGGAAAAGGTCTCGTTCGTTAAC
GGAATTAACCAGACAAATCACTCCACCAACTAAGAACGGCCATGCACCACCACC
CATTCAATCAAGAAAGAGCTATCAATCTGTCAATCATAAAAATGTCCGGACCTG
GTAAGTTGCCCCGTGTTGAGTCAAATTAAGCCGCAGGCTCCACTCCTGGTGGTGC
CCTTCCGTCAATTCCTTTAAGTTCCAATCTTGCGACCATACTCCCCCCAGAACCCA
AAAACTTTGGTTTCCCGGAAAAAAAGGGTGTACGATATTTTCTCAGTACACCATC
TTTTAGATGGCATAGTTTATGGTTAAGACTACGACGGTATCTAATCGTCTTCGATC
CCCTAACTTTCGTCCTTGATCAATGGGGATATCCTTGCCAAACSCTTTCCCAACM
GKGKGTCTTCCAWAAATCC

DNA sequence for *psaA*:

TACAAATTCTTTAGAAGAATATCCCGTAAAATTTTTAGCGCTCATTTTGGT
CAATTAGCGATAATTTTTATATGGTTGAGTGGAATGTACTTTCATGGTGCTAAATT
TTCTAATTATGTGGCTTGGTTAAATAATCCTATTAACATCAAACCCAGCGCACAA
GTAGTTTGGCCGATTATAGGTCAAGAAATTTTAAATGCTGATGTTGGTGGAGGCT
TCCAAGGAATTCAAATTACTTCTGGATTATTCCAATTATGGAGAGCTTCAGGAAT
TACTAATGAAATGCAACTATATGTAACTGCAATAGGTGGCTTGTTTATGGCCAGT
TTAATGCTTTTTGCAGGTTGGTTTCATTATCACAAAGCGGCCCCTAAATTGGAAT
GGTTTCAAAACGTTGAATCAATGTTAAATCACCATTTAGCAGGCTTATTAGGCTT
AGGTTCACTGGGTTGGACAGGACACTTGATCCATGTTTCTTTACCAATTAATAAA
TTACTTGATTCTGGTATTTCGCCAGCTCAAATACCGCTACCTCATGAATTTATTTT
GAACCGTAATTTAATGTCAGAATTGTATCCAAGCTTTAGTAAGGGTTTATTACCT
TTCTTTAATTTAAATTGGAATGAATATAATGATTTTTTAACCTTTAAAGGAGGTTT
AAATCCTGTAACCGGAGGCTTATGGTTAACAGACATTGCCCATCATCACTTAGCT
ATAGCAGTGATTTTTATAATCGCTGGTCATATGTATAGAACTAACTGGAACATTG

GACATAGTTTAAAGGAGATCTTAGATGCTCACAAAGGACCTTTTACAGGTGAAG
GGCATAAAGGATTATTTGAAATACTTACAACTTCTTGGCATGCGCAACTTGCAAT
TAATTTAGCAATGTTAGGATCATTAAGTATAATAGTGGCACATCATATGTATGCT
ATGCCACCTTATCCATATTTAGCTACAGACTATCCAACTCAGCTATCTCTTTTTAC
ACATCATATGTGGATTGGTGGATTCTGTATTGTTGGAGCAGGTGCTCACGCGGCT
ATATTTATGGTAAGAGACTATAGTCCTGCACAAAATTATAATAATTTATTAGATA
GGGTAATAAGACATAGAGATGCAATAATTTCTCATCTAAACTGGGTCTGTATTTT
TCTAGGTTTTCATAGTTTTGGCTTATATATACATAATGATACTATGAGAGCATTAG
GAAGACCACAAGACATGTTTTCAGATGTAGCTATTCAACTGCAACCTATTTTTGC
ACAATGGATACAAAATTCTCATTCACTTGCACCAGGTAATACAGCTCCAAATGTT
CTAGCTACAACTAGCTATGTTTTCGGGGGAGACATTGTGTCAGTAGGAGGGAAA
ATCGGTCTCATGCCTATTTCTCTTGGAACAGCAGATTTTATGGTACATCATATTCA
TGCTTTTACAATTCATGTAACAGCTTTAATTTTATTAAAAGGAGTTTATTGCTCCG
TATCTAGATAATACCAG

DNA sequence for *rbcL*:

TGGAGAGAAAGATATTTGTTTGTAATGGAAGCAGTTAACAAGGCAGCAGC
TGCAACAGGAGAAGTTAAAGGACATTACTTAAATGTAACAGCTGCAACTATGGA
AGAAATGTATGCACGTGCTCAGTTAGCCAAAGAATTAGGTAGTGTAATTATAATG
ATTGATCTTGTTATAGGTTATACTGCTATTCAAACTATGGCAAAATGGGCTAGAG
ATAATGATATGATCCTACATCTACACAGAGCAGGAAATTCTACTTATTCAAGACA
AAAAAACCATGGTATGAATTTTAGAGTAATTTGTAAATGGATGAGAATGGCAGG
CGTAGACCATATTCATGCCGGAACTGTTGTTGGTAAACTAGAAGGAGATCCTATT
ATTACAAGAGGATTTTATAAAACTCTTCTTTTACCTAAACTAGAACGTAATTTAC
AAGAAGGTTTATTCTTCGATATGGACTGGGCCTCACTTAGAAAAGTAATGCCAGT
AGCTTCTG

Appendix K: Genomic Sequences for *16s rRNA* genes for *Alicyclobacillus* sp. EB1

DNA sequence for *16s rRNA*:

GCTGGCCCCTTTCGGGTTACCCCACCGACTTCGGGTGTTGCCAACTCTCGT
GGTGTGACGGGCGGTGTGTACAAGGCCCGGGAACGGATTCACCGCGGCATGCTG
ATCCGCGATTACTAGCAATTCCGGCTTCATGCAGGCGAGTTGCAGCCTGCAATCC
GAACTACGAGCGGTTTTCAGGGGTTCGCTCCAGATCGCTCTCTCGCTTCCCGTTG
TGCCGCCCATTGTAGCACGTGTGTCGCCCAGGACATCAGGGGCATGATGATTTGA
CGTCATCCCCGCCTTCCTCCGACTTGCGCCGGCAGTCACCTGTGAGTCCCCACCT
CTACGTGCTGGTAACACAGGTCAAGGGTTGCGCTCGTTGCGGGACTTAACCCAAC
ATCTCACGACACGAGCTGACGACAACCATGCACCACCTGTCTCCTCTGCCCCGAA
GGGACCTACCATCTCTGGTAGCGTCAGAGGGATGTCAAGCCCTGGTAAGGTTCTT
CGCGTTGCTTCGAATTAAACCACATGCTCCACTGCTTGTGCGGGCCCCCGTCAAT
TCCTTTGAGTTTCAGTCTTGCGACCGTACTCCCCAGGCGGAGTGCTTATTGGGTTT
CCTTCGGCACTGAGGGTGGTACCCCCCAACACCTAGCACTCATCGTTTACGGCGT
GGACTACCAGGGTATCTAATCCTGTTTGCTCCCCACGCTTTCGTGCCTCAGCGTC
AGTCACTGTCCAGCAAGGCGCCTTCGCCACTGGTATTCCTCCACATCTCTACGCA
TTTCACCGCTACACGTGGAATTCCCCTTGCCTCTCCAGTACTCAAGTCCTACAGTT
TCCAAGGCATTCCCAAGGTTGAGCCCTGGCCTTTCACCCCAGACTTGCAGAACCG
CCTACGCACCCTTTACGCCCAGTGATTCCGGACAACGCTTGCCCCCTACGTATTA
CCGCGGCTGCTGGCACGTAGTTTGCCGGGGCTTCCTCTCGGGGTACCGTCTCGCA
AAGAGCATTCCCTCTCCTTGCCGCTCTTCCCCCTTGACTGAGCTTTACAACCCGAA
GGCCTTCCTCGCTCACGCGGCGTTGCTCCGTCAGGCTTGCGCCCATTGCGGAAGA
TTCCCTACTGCTGCCTCCCGTAGGAGTCTGGGCCGTGTCTCAGTCCCAGTGTGGC
CGGTCACCCTCTCAGGTCGGCTACGCATCGTCGCCTTGGTAGGCCTTTACCCTAC
CAACTAGCTAATGCGCCGCGGGGTCCTCTCTCAGCGATGCCTCAGCATCCTTTCC
CGCATCAGGCATGCGCCTCATGCGCCTATCCGGCCTTAGCACCCGTTTCCAGGCG
TTATTCCAGTCTGTTAGGCAGATTCCCCACGTGTTCCTCACCCGTCCGCCGCTGGT
ATCTTTCGATACCCGCTCGACTGCA

Appendix L: Accession Numbers for Genomic Sequences used in Characterisation Comparison

Details surrounding the species, strain, pair identity and accession number for all organisms used during the characterisation of *Galdieria* sp. RTK37.1 and the bacterial contaminate, *Alicyclobacillus* sp. EB1 is summarised in Tables L.1 – Table L.4.

Table L.1: Organism description, strain type, pair identity and accession number for all *16s rRNA* genomic sequences used in the characterisation of the bacterial contaminate.

Organism Description	Strain	Pair Identity	Accession Number
Alicyclobacillus tolerans	DSM 16297	99.50%	NR_112550.1
Alicyclobacillus tengchongensis	ACK006	99.43%	NR_146350.1
Alicyclobacillus contaminans	3-A191	93.68%	NR _041475.1
Alicyclobacillus pomorum	3A	93.60%	NR_024801.1
Alicyclobacillus sacchari	RB718	93.45%	NR_041475
Alicyclobacillus disulfidooxidans	DSM 12064	93.43%	NR_040944.1
Alicyclobacillus ferrooxydans	TC-34	93.39%	NR_044413.1
Alicyclobacillus disulfidooxidans	SD-11	93.34%	NR_040944
Alicyclobacillus hesperidum	FR-11	93.20%	NR_025313.1
Alicyclobacillus cycloheptanicus	DSM 4006	93.15%	NR_024754.1
Alicyclobacillus cycloheptanicus	NBRC 15310	92.99%	NR_113745
Alicyclobacillus cycloheptanicus	SCH	92.63%	NR_118875
Alicyclobacillus sacchari	RB718	92.54%	NR041470.1
Effusibacillus pohliae	MP4	89.42%	NR_042184
Effusibacillus consociatus	CCUG 53762	89.20%	NR_117612
Effusibacillus lacus	skLN1	88.46%	NR_125469
Tumebacillus ginsengisoli	Gsoil 1105	87.94%	NR_112564
Tumebacillus soli	CAU 1105	87.80%	NR_149286
Tumebacillus luteolus	UC13	87.34%	NR_145584
Escheichia coli	U 5/41	79.54%	NR_024570.1

Table L.2: Organism description, strain type, pair identity and accession number for all *18s rRNA* genomic sequences used in the characterisation of *Galdieria* sp. RTK37.1.

Organism Description	Strain	Pair Identity	Accession Number
Galdieria sulphuraria	Gs72-YNP	97.47%	KP167587
Cyanidium caldarium	182	92.08%	AF441374
Galdieria partita	500	91.99%	AF441368
Galdieria partita	K	91.53%	AF441372
Galdieria sulphuraria	J	91.12%	AF441373
Galdieria sulphuraria	AZ	91.05%	AF441360
Galdieria daedala	IPPASP508	90.94%	AB090839
Galdieria maxima	P507(IPPAS)	90.80%	AB090832
Galdieria sulphuraria	NIES-550	90.48%	LC504058
Galdieria sulphuraria	ISG	90.25%	AF441363
Galdieria sulphuraria	074W	89.70%	AF441369
Rhodella violacea	SAG 115.79	86.68%	EU861395
Cyanidium caldarium	61D	86.00%	AB090833
Cyanidioschyzon merolae	199	84.16%	AF441376
Cyanidioschyzon merolae	10D	82.57%	XR_002461616
Cyanidioschyzon merolae	MS1-YNP	82.57%	KP167585

Table L.3: Organism description, strain type, pair identity and accession number for all *psaA* genomic sequences used in the characterisation of *Galdieria* sp. RTK37.1.

Organism Description	Strain	Pair Identity	Accession Number
Galdieria sulphuraria	SAG 107.79	93.33%	MN518834
Galdieria sulphuraria	SAG 108.79	93.19%	AY119695
Galdieria sulphuraria	UTEX 2393	93.12%	AY541285
Galdieria sulphuraria	074W	92.96%	HM440925
Galdieria partita	THAL024	92.76%	MN699561
Galdieria partita	THAL023	92.63%	MN518827
Galdieria daedala	IPPAS(P508)	92.60%	AY541283
Galdieria partita	IPPAS(P500)	92.52%	AY541284
Batrachospermum campyloclonum	87	78.61%	KM055289
Batrachospermum naiadis	BHO:A-0076	78.41%	MF940789
Batrachospermum macrosporum	-	78.12%	MF940791
Rhodella violacea	SAG 115.79	78.08%	AY119706

Table L.4: Organism description, strain type, pair identity and accession number for all *rbcL* genomic sequences used in the characterisation of *Galdieria* sp. RTK37.1.

Organism Description	Strain	Pair Identity	Accession Number
Galdieria sp.	CCMEE 5719	100.00%	EF675175
Galdieria sp.	CCMEE 5707	99.80%	EF675181
Galdieria sulphuraria	Gs72-YNP	99.60%	KP167591
Cyanidiales sp. DJS-2012	CHJ-4	95.77%	JQ269635
Galdieria sp.	CCMEE 5573	95.77%	EF675171
Cyanidiales sp. DJS-2012	SFFL-5	95.56%	JQ269630
Galdieria daedala	IPPAS(P508)	93.35%	AY541302
Galdieria partita	THAL023	92.94%	MN545931
Galdieria sulphuraria	074W	92.34%	NC_024665
Galdieria phlegrea	ACUF788	88.10%	KY033447
Cyanidioschyzon merolae	MS1-YNP	78.61%	KP167589
Cyanidioschyzon merolae	10D	75.65%	NC_004799
Rhodella violacea	SAG 115.79	-	AY119706
Galdieria maxima	IPPAS(P507)	-	AY391370

Appendix M: Heterotrophic Batch Growth Curve and Consumption Profiles

Growth curves for *Galdieria* sp. RTK37.1 grown in heterotrophic conditions with sorbitol, succinate and acetate are shown in Figure M. The substrate consumption rate profiles are also shown. No growth and consumption were observed using these organic carbon substrates. Figure M. A shows the growth curve and carbon substrate concentration for *Galdieria* sp. RTK37.1 grown in heterotrophic conditions with 10 mM of succinate. Figure M. B shows the growth curve and carbon substrate concentration for *Galdieria* sp. RTK37.1 grown in heterotrophic conditions with 10 mM of sorbitol. Figure M. C shows the growth curve and carbon substrate concentration for *Galdieria* sp. RTK37.1 grown in heterotrophic conditions with 10 mM of acetate.

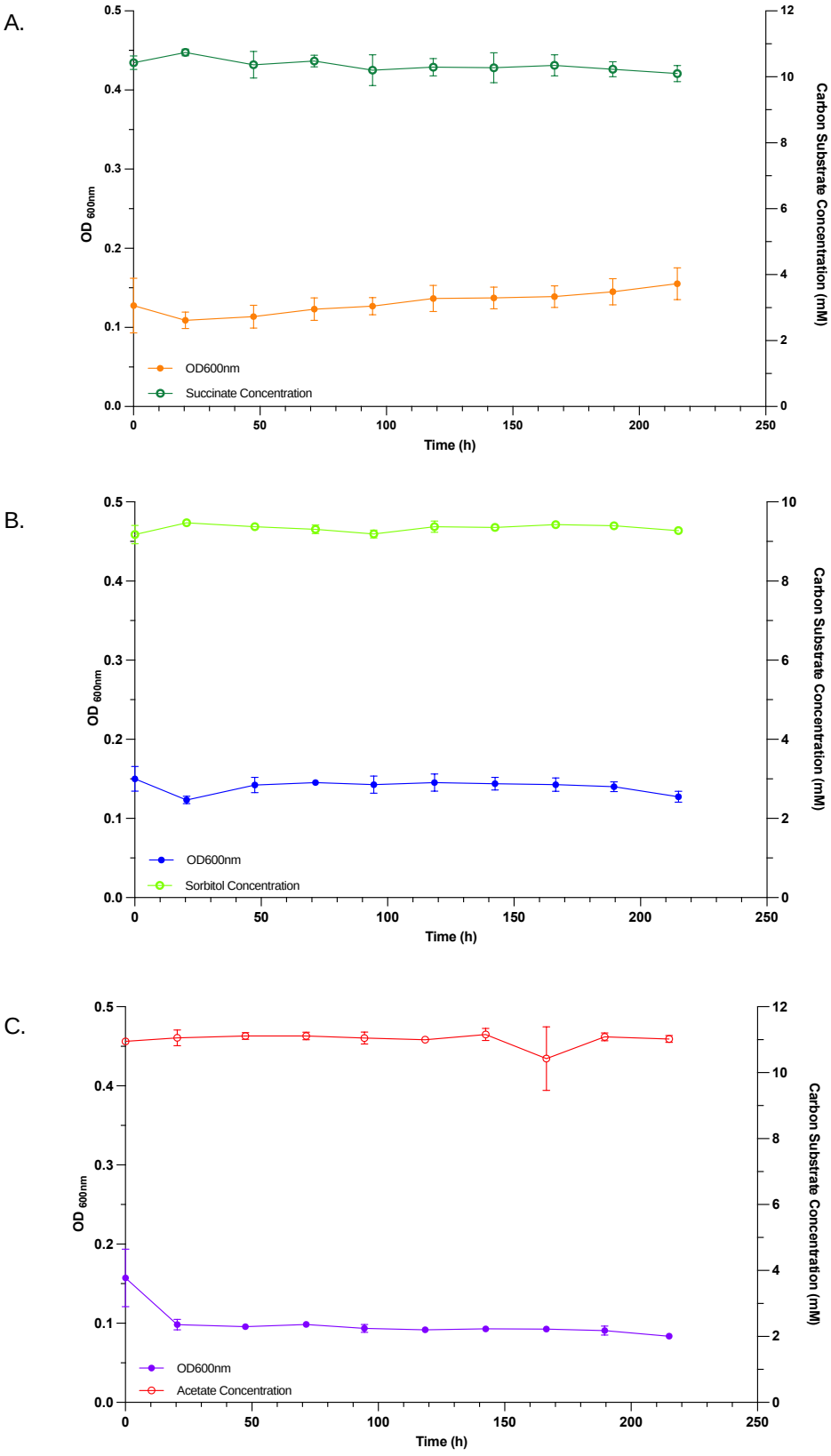

Figure M: Growth curves outlining the optical density and biomass yield of *Galdieria* sp. RTK37.1 grown in heterotrophic growth conditions. *Galdieria* sp. RTK37.1 cells were grown at a pH 2.5, 45°C in 160 mL serum bottle supplied with 50 mL of V4 medium. A represents Succinate, B represents Sorbitol and C represents Acetate. Error bars denote standard deviation.

Appendix N: Dry Cell Weight and Optical Density Correlation Curve for Batch Growth

The correlation curve for dry cell weight and optical density during batch growth is shown below in Figure N. The calibration curve was obtained using the known steady state optical density and correlating this to the dry cell weight for each trophic condition *Galdieria* sp. RTK37.1 was cultivated in.

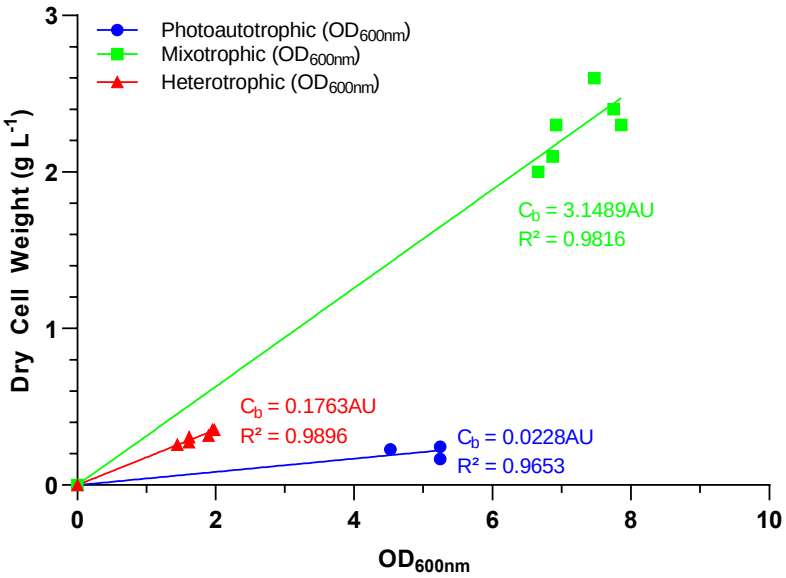

Figure N: Calibration curve for the optical density and dry cell weight in the different trophic growth conditions used during batch cultivation. The linear relationship was defined by the equation provided. *Galdieria* sp. RTK37.1 cells were grown at a pH 2.5, 45°C in 160 mL serum bottle supplied with 50 mL of V4 medium. During photoautotrophic and mixotrophic growth cells were illuminated under warm white LED lighting at 94.6 µmol m^{-2} s^{-1} and sparged with 3% (v/v) CO_2. During mixotrophic and heterotrophic growth, 10 mM of glucose to V4 medium.

Appendix O: pH Growth Curve for Photoautotrophic grown *Galdieria sp. RTK37.1*

Growth curves for photoautotrophic grown *Galdieria* sp. RTK37.1 under various initial pH conditions is shown in Figure O.

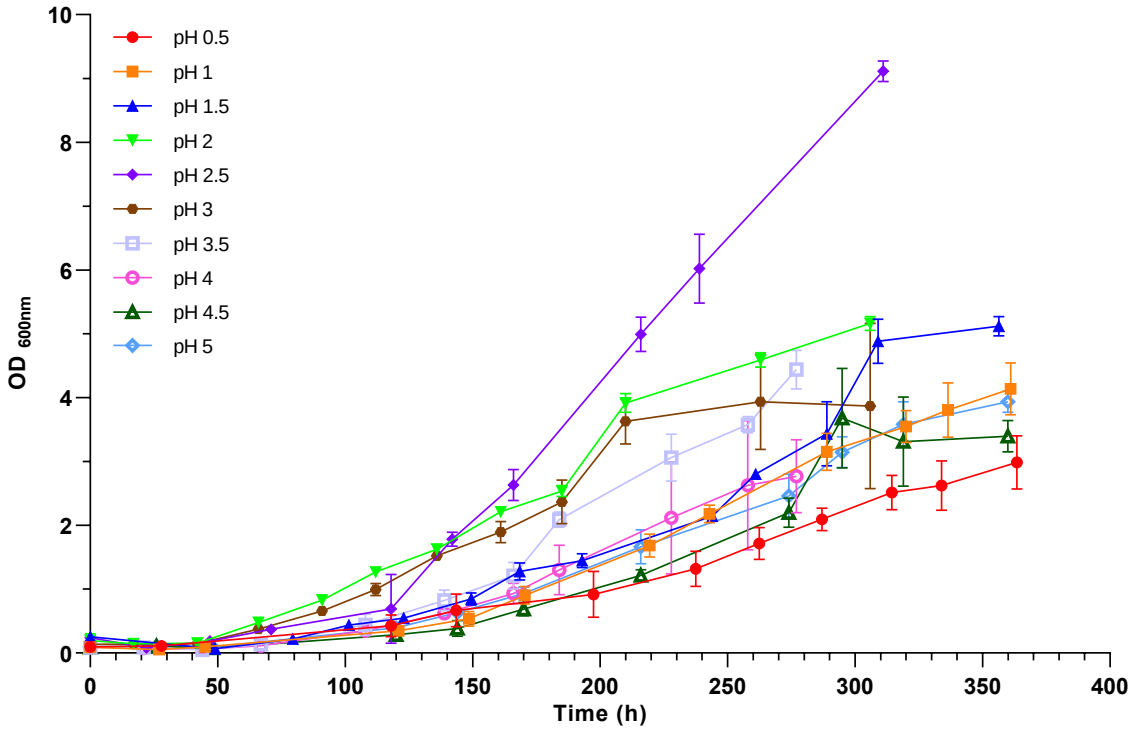

Figure O: Growth curve outlining the photoautotrophic growth of *Galdieria* sp. RTK37.1 under different pH conditions. *Galdieria* sp. RTK37.1 cells were grown at 45°C in 250 mL shake flasks supplied with 100 mL of V4 medium. Cells were provided with 3% (v/v) CO_2, under 170 µmol m^{-2} s^{-1} warm white LED lighting. Error bars denote standard deviation.

Appendix P: Oscillating Growth Curve for *Galdieria sp. RTK37.1*

Initially xenic cultures of *Galdieria* sp. RTK37.1 were cultivated to investigate the ability to achieve stable growth during photoautotrophic growth conditions. Both reactors were operated identically, initially in batch conditions with gas sparging set at 1000 mL min^{-1} (3% w/w CO_2), controlled at 500 mL min^{-1} in both reactors by rotameters. Cells were illuminated by warm white LED lighting set at 191.3 µmol m^{-2} s^{-1}. Initially, it was aimed to achieve a steady state OD value of 1 to reduce the error imposed by dilution. Both reactors were switched to chemostat operation, using a dilution rate of 0.38 day^{-1}. The light intensity was then reduced to 94.6 µmol m^{-2} s^{-1} in pursuit of achieving an OD of 1. A dilution rate of 0.3 d^{-1} was used during chemostat operation. Due to significant amounts of flocculation on the reactor walls, gas sparging was increased to 2000 mL min^{-1} (3% v/v CO_2), controlled at 1000 mL min^{-1} in both reactors by rotameters. The growth curve for xenic cultures *Galdieria* sp. RTK37.1, contaminated with *alicyclobacillus* sp. EB1 grown in photoautotrophic growth conditions is shown in Figure P.

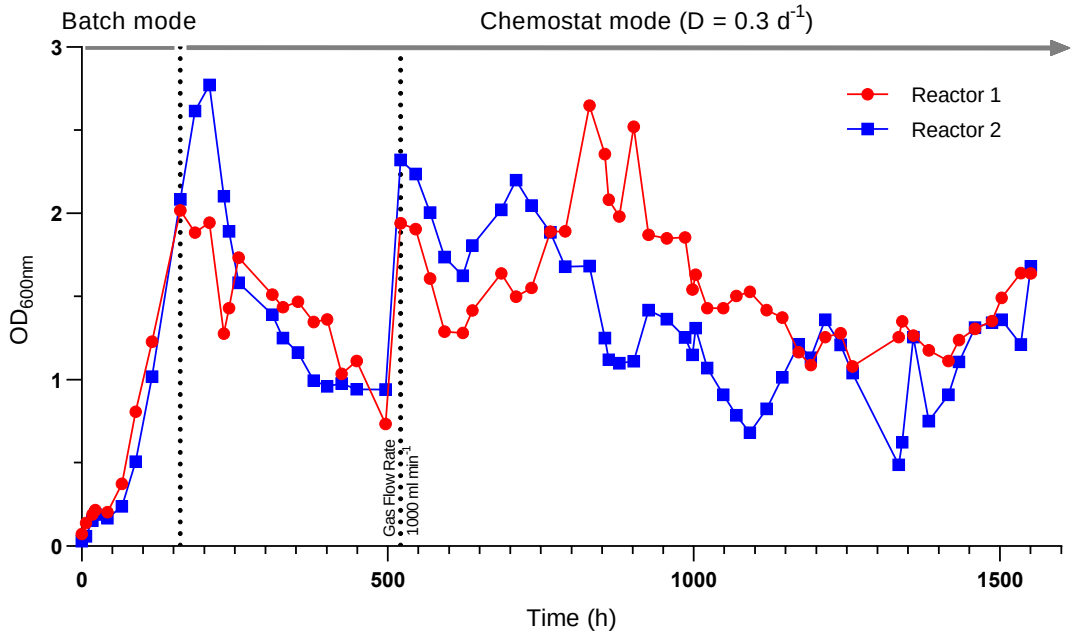

Figure P: Growth curve outlining xenic cultures of *Galdieria* sp. RTK37.1, contaminated with *Alicylcobacbillus* sp. EB1 grown in chemostat reactors at a pH 2.5, 45°C with a dilution rate of 0.3 d^{-1}. Cells were illuminated under warm white LED lighting at 94.6 µmol m^{-2} s^{-1} and sparged with 3% (v/v) CO_2. Gas flow rate was increased after 500 hours to 1000 mL min^{-1} in each reactor.

After analysing the growth of *Galdieria* sp. RTK37.1 during batch cultivation in the reactors, it was determined that the maximum growth rate was near the operating dilution rate. As discussed in Section 5.2.2, operating at a dilution rate that is equal or greater than the maximum growth rate has only one achievable steady state where the concentration of cell growth equals zero. This condition is called washout. Although, as seen in the growth profile in Figure P, washout was not observed. Due to the significant amount of biomass on the reactor walls, it was theorised that the cells were sticking to the reactor wall as a survival strategy due to the presence of bacteria and the dilution rate. The biomass on the wall was not diluted out of the reactor as fast as the cells within the bulk liquid solution. This allowed cells to be retained in the reactor despite the dilution rate being near the calculated exponential growth rate. This is likely the reason an oscillating effect was observed in the cell growth after the increase in total gas flow rate. The cell growth would increase as a result of non-sterile feed from the side of the reactor, while the decrease in cell growth would have been due to the washout effect. These results suggest that to obtain stable growth, the dilution rate must be reduced, which had a consequence of an increased hydraulic retention time.

Due to the presence of the bacterial contamination, *alicyclobacillus* sp. EB1, and the excess biofilm accumulation, the reactors were shut off and restarted after the generation of axenic cultures.

Appendix Q: Growth Curve for Ammonia Limited Photoautotrophic grown *Galdieria* sp. RTK37.1

Figure Q outlines the growth curves for photoautotrophic grown *Galdieria* sp. RTK37.1, where Reactor 1 was limited in Ammonia and Reactor 2 was not ammonia-limited.

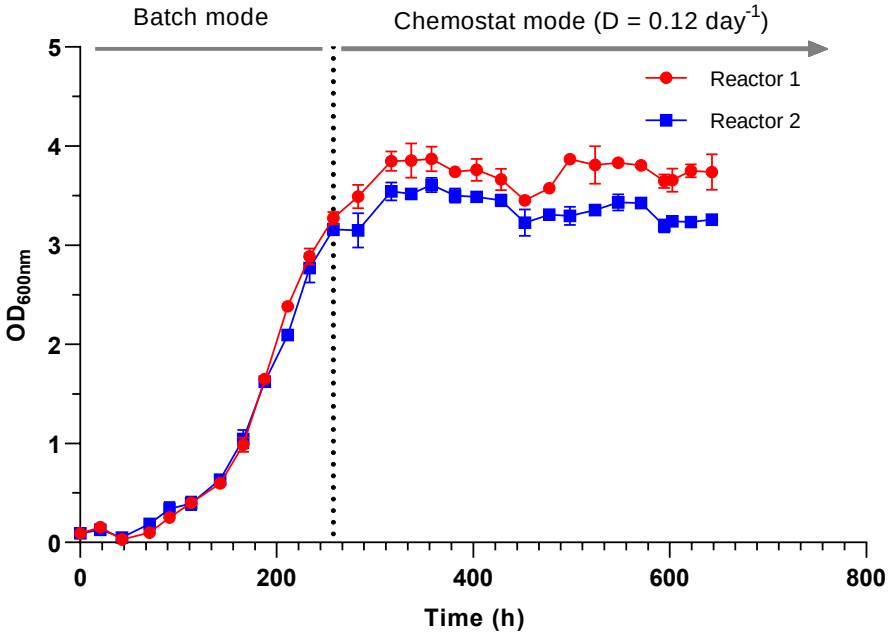

Figure Q: Growth curve outlining axenic cultures of *Galdieria* sp. RTK37.1, grown in chemostat reactors at a pH 2.5, 45°C with a dilution rate of 0.12 d^{-1}. Cells were illuminated under warm white LED lighting at 94.6 µmol m^{-2} s^{-1} and sparged with 3% (v/v) CO_2. Reactor 1 was ammonia-limited (0.2 g L^{-1}), Reactor 2 was not ammonia-limited (0.4 g L^{-1}).

Appendix R: Dry Cell Weight and Optical Density Correlation Curve for Chemostat Growth

The correlation curve for dry cell weight and optical density is shown below in Figure R. The calibration curve was obtained using the known steady state optical density and correlating this to the dry cell weight for each trophic condition *Galdieria* sp. RTK37.1 was cultivated in.

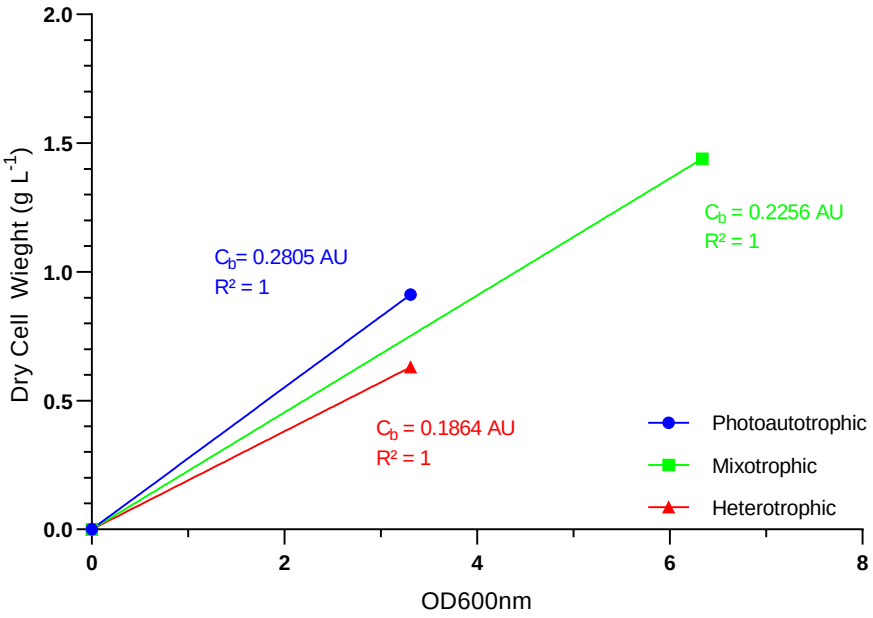

Figure R: Calibration curve for the optical density and dry cell weight in the different trophic growth conditions used during continuous cultivation. The linear relationship was defined by the equation provided. *Galdieria* sp. RTK37.1 was grown at a pH 2.5, 45°C in 1.5 L chemostat with a dilution rate of 0.12 d^{-1}. During photoautotrophic and mixotrophic growth cells were illuminated under warm white LED lighting at 94.6 µmol m^{-2} s^{-1} and sparged with 3% (v/v) CO_2. During mixotrophic and heterotrophic growth, 10 mM of glucose was added to inlet V4 Media.

Appendix S: Cell Count and Optical Density Correlation Curve

The correlation curve for cell counts and optical density is shown below in Figure S. The calibration curve was obtained using the known steady state optical density and correlating this to the cell count for each trophic condition *Galdieria* sp. RTK37.1 was cultivated in.

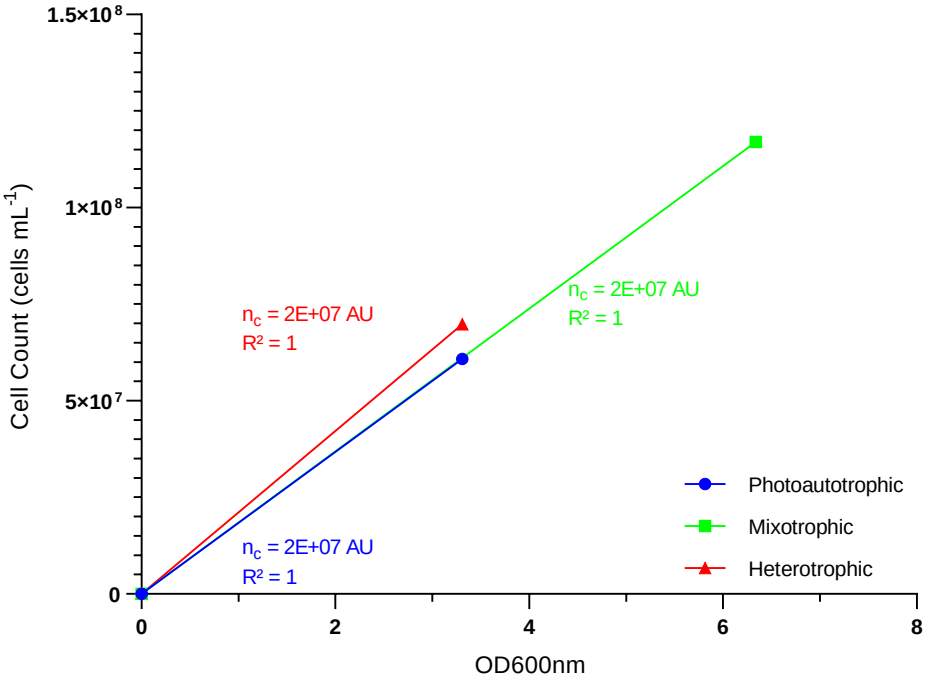

Figure S: Calibration curve for the optical density and cell counts in the different trophic growth conditions used during continuous cultivation. The linear relationship was defined by the equation provided. *Galdieria* sp. RTK37.1 was grown at a pH 2.5, 45˚C in a 1.5 L chemostat with a dilution rate of 0.12 d^{-1}. During photoautotrophic and mixotrophic growth cells were illuminated under warm white LED lighting at 94.6 μmol m^{-2} s^{-1} and sparged with 3% (v/v) CO_2. During mixotrophic and heterotrophic growth, 10 mM of glucose was added to inlet V4 Media.